Delivery of therapeutic antisense oligonucleotides for exon skipping in epidermolysis bullosa.

Author	Rindert Venema
Student number	3662802
Master	Biomedical Sciences (Biology of Cancer and Immune System)
Examiner	Prof. Dr. Jon D. Laman
Project supervisor	Dr. Jeroen Bremer
Location	University Medical Center Groningen Department of Dermatology
Start and end dates	January 9, 2023 – June 5, 2023

Abstract

Dystrophic epidermolysis bullosa (DEB) is caused by mutations in the *COL7A1* gene, encoding collagen type VII (C7). C7 is the major component of anchoring fibrils that form the structural connection between the basement membrane zone and the papillary dermis. In DEB, the absence of C7 leads to severe blistering of skin and mucosa. Currently, there is no cure for DEB, however, a promising therapy, antisense oligonucleotide (AON) mediated exon skipping, has shown to restore C7 expression *in vivo* and *in vitro*.

Therefore, we investigated and optimized delivery of a fluorescently labelled fab-conjugated AON construct (flAON-Fab conjugate) for exon skipping in DEB to gain insights in its cellular uptake, distribution and effectiveness. Second, we sought the most potent AON sequence by optimizing transfection of naked AONs in primary keratinocytes, and subsequently performing an 'Oligowalk' in which we transfected 102 unique AON constructs, specifically targeting exon 105 of the *COL7A1* gene. Lastly, we optimized a 3D skin model of human fibroblasts, keratinocytes and a collagen mix, to resemble the human skin as closely as possible that can potentially serve as a null-model or replacement model for human skin in EB.

We found that our flAON-Fab conjugate binds, internalizes and distributes intracellularly in differentiated primary keratinocytes. Moreover, the 'Oligowalk' showed for several of the 102 unique AON sequences clear exon skipping on agarose gel. Furthermore, hanging inserts did better regarding desmoglein-1 (DSG1) and desmoglein-3 (DSG3) expression, whereas standing inserts did better regarding C7 expression. Standing and hanging models have comparable collagen type 4 (C4) expression. Additionally, fungizone and antibiotics seems to have a negative impact on our skin models as indicated by the overall C4, C7, DSG-1 and DSG-3 expression. Moreover, waiting 3 days before seeding keratinocytes to the fibroblast containing collagen dermal scaffold is favorable to waiting 1 day. Lastly, we observed that the PET membrane outperformed the PC membrane in the hanging skin models.

In future experiments, we will perform a functional assay to investigate if our Fab-conjugated AON construct induces exon skipping and if so, quantify exon skipping by RT-qPCR. A RT-qPCR on the Oligowalk should also identify the most potent AON sequence by quantifying which AON sequence induces the highest amount of exon skipping. Lastly, we will improve our 3D human skin models by building on the data presented in this report and implement the model in future research.

Keywords: AON, DEB, exon skipping, flAON-Fab conjugate, Oligowalk, 3D human skin model.

Contents

List of abbreviations

AON	Antisense oligonucleotide
C4	Collagen type 4
C7	Collagen type 7
DSG	Desmoglein
DEB	Dystrophic Epidermolysis bullosa
DMPK	Myotonic dystrophy protein kinase
EB	Epidermolysis bullosa
EBS	Epidermolysis bullosa simplex
flAON	fluorescent antisense oligonucleotide
HBSS	Hanks' Balanced Salt Solution
IF	immunofluorescent
JEB	Junctional epidermolysis bullosa
KS	Kindler syndrome
LF	Lipofectamine
MXD3	MYC-associated factor X dimerization protein 3
OVA	Ovalbumin
PEI	Polyethyleneimine
PCR	Polymerase chain reaction
PreB ALL	precursor B-cell acute lymphoblastic leukemia
TBE	Tris/Borate/EDTA
TNS	Trypsin neutralizing solution
2-MEA	2-Mercaptoethylamine-HCl
2’-O-MOE	2’-O-methoxyethyl-

1. Introduction

EB is a group of heterogenous hereditary diseases characterized by fragility and easy blistering of the skin (Has et al., 2020). Its underlying etiology is mutations in a variety of genes that are important for the structural hierarchy of the skin. These genes encode for proteins that are mainly involved in adhesion of cells or providing a connection between the epidermis, the cutaneous basement membrane zone and the dermis (Has et al., 2019; Bardhan et al., 2020). When mutated, minimal mechanical trauma causes disruption at the dermal-epidermal junction resulting in blistering of the skin (Has et al., 2020). Based on the plane of cleavage, EB has been classified in four major groups; EB simplex (EBS), junctional EB (JEB), dystrophic EB (DEB) and Kindler syndrome (KS). However, over 30 subtypes have been recognized, with 16 distinct genes containing pathological mutations (Bardhan et al., 2020). One of these genes is *COL7A1*, encoding for the protein collagen type VII (C7). C7 is produced primarily by epidermal keratinocytes, however also dermal fibroblasts produce C7 (Watanabe et al., 2018). Mutations in C7 are implicated in the relatively severe form of EB, DEB. Biallelic or monoallelic mutations in C7 lead to absence, fluctuations or truncated forms of C7, disrupting its abundance and tertiary and quaternary structure (Tang et al., 2021). In total, the C7 gene exists out of 118 exons, that together code for an 8,835 bp long pro-α1 procollagen polypeptide [fig. 1.1] (Cristiano et al., 1994).

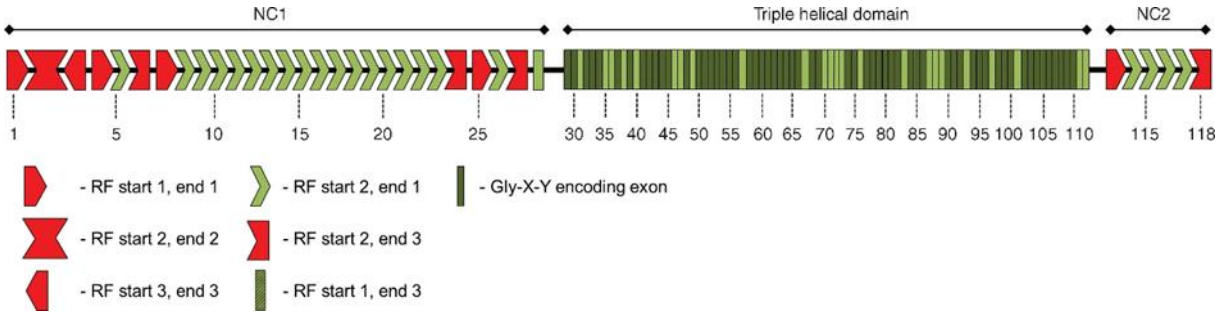

Fig. 1.1 All exons of the C7 protein including their reading phases. Visualization of all exons of the *COL7A1* gene and their reading phases. Green boxes indicate exon amenable AON-mediated exon skipping therapy. Squared boxes indicate exons that start and end with a complete codon. Arrow shaped boxes indicate exons that start and end with a partial codon. Dark green boxes indicate an exon that only encodes glycine-X-Y repeats. Red boxes indicate non-skippable exons. *(Figure reproduced from: Bremer et al., 2016)*

Post-translational modification organizes C7 in triple helical structures that form anti-parallel heterotrimers when secreted (Dieringer et al., 1985). Multiple anti-parallel dimer structures assemble into the main component of the anchoring fibrils at the dermal-epidermal junction, connecting the papillary dermis to the lamina densa of the basal lamina (Chen et al., 2001). Here, C7 binds through its non-collagenous NC1-domain to both laminin-332 and collagen type 4 (C4) that are located in the lamina densa [fig. 1.2] (Rousselle et al., 1997; Chen et al., 1997). The NC1-domain is important for C7 to retain the triple helical conformation of its collagenous domain, which is rich in glycine-X-Y-repeats (Chen et al., 1997). Another part of

the C7 structure includes the non-collagenous NC2 domain, which stabilizes the C7 dimer when partially cleaved (Colombo et al., 2003).

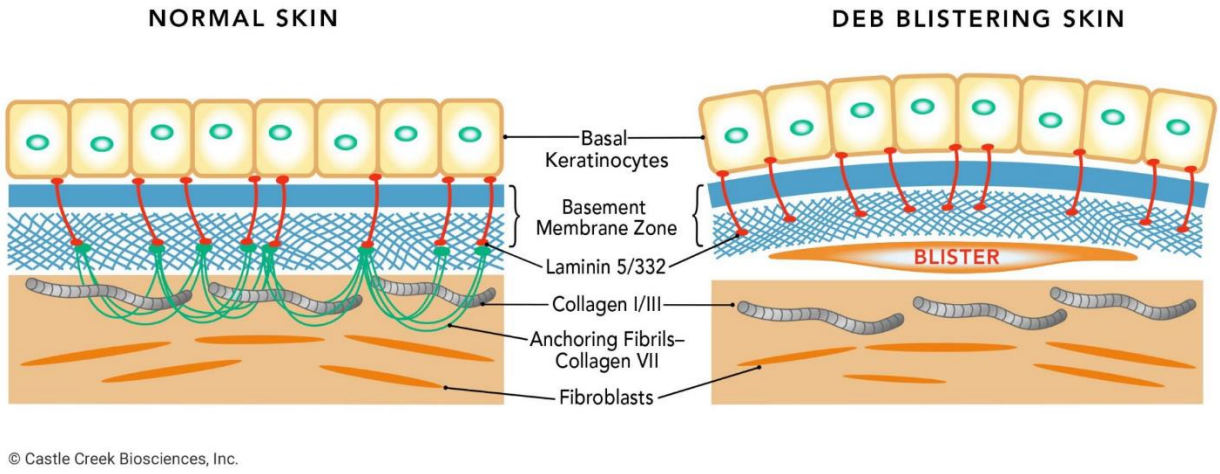

Figure 1.2: Simplified representation of healthy skin and DEB blistering skin. In normal skin C7 forms anchoring fibrils that connect the papillary dermis with proteins in the basement membrane zone as laminin 5/332 and C4. In DEB blistering skin there is an absence of C7 and therefore anchoring fibrils, making the skin loose its structural integrity, giving rise to blister formation at the location of the anchoring fibrils in healthy skin. *(figure reproduced from: Castle Creek Biosciences, Inc. 2022, June 29).*

Currently, there is no cure for DEB, however, a promising therapy, antisense oligonucleotide (AON) mediated exon skipping, has shown to restore C7 expression *in vivo* and *in vitro* (Bremer et al., 2016; Turczynski et al., 2016). One of the reasons exon skipping therapy is promising is that 107 of the 118 exon of C7 are in-frame exons, including exon 105, which is targeted in the experiments included in this report as well. Exon 105 is part of the 84 exons encoding the collagenous triple helix domain. In this collagenous triple helix domain, the open reading frame of all exons included starts at position 1 and ends at position 3 [fig 1.1]. Therefore, skipping in this collagenous triple helix domain will not result in an ammino acid change at the skipping junction, leaving the glycine-X-Y repeat structure unchanged. Moreover, it has been shown that the glycine x-y-repeat structure is crucial for triple helix formation and not the length of the domain (Bornert et al., 2016).

AONs are small single-stranded RNA molecules of about 15-25 nucleotides long. They are designed to bind to mRNA. AONs can have several modes of actions. One is interfering with the pre-mRNA splicing process by affecting small nuclear ribonucleoproteins through steric hindrance. This type of AONs is also used in the experiments that are described in this report. Another mode of action is by binding to the mRNA and degrading it via RNase-H mediated degradation (Vermeer et al., 2021). In EB, exon-skipping therapy aims to mask the exon containing the pathogenic variant from the splicing machinery. In this way, the exon is removed, producing a slightly shorter, however, functional alternatively spliced product (Bornert et al., 2016). In example, targeting a mutated exon 105 containing a nonsense mutation, normally resulting in a premature termination codon, should with the use of AON

therapy result in the production of a slightly shorter in-frame functional product, hopefully improving the pathogenic phenotype caused by the pathogenic variant (Bremer et al., 2016). However, several important factors have to be considered regarding AON therapy. These include the method of delivery, the specific AON sequence and the composition of the chemical backbone including its nucleotide modifications (Vermeer et al., 2021). At the moment, a total 18 AONs have been approved and proven successful for disorders of similar etiology to DEB like Duchenne muscular atrophy (Egli & Manoharan., 2023). In Duchenne muscular dystrophy AON-mediated exon skipping therapy makes use of the same mechanism of action as in the experiments conducted on AON-mediated exon skipping therapy in DEB in this report (Dzierlega & Yokota., 2020). A visualization of the mechanism of exon of AON-mediated exon skipping therapy in Duchenne muscular dystrophy can be observed in figure 1.3.

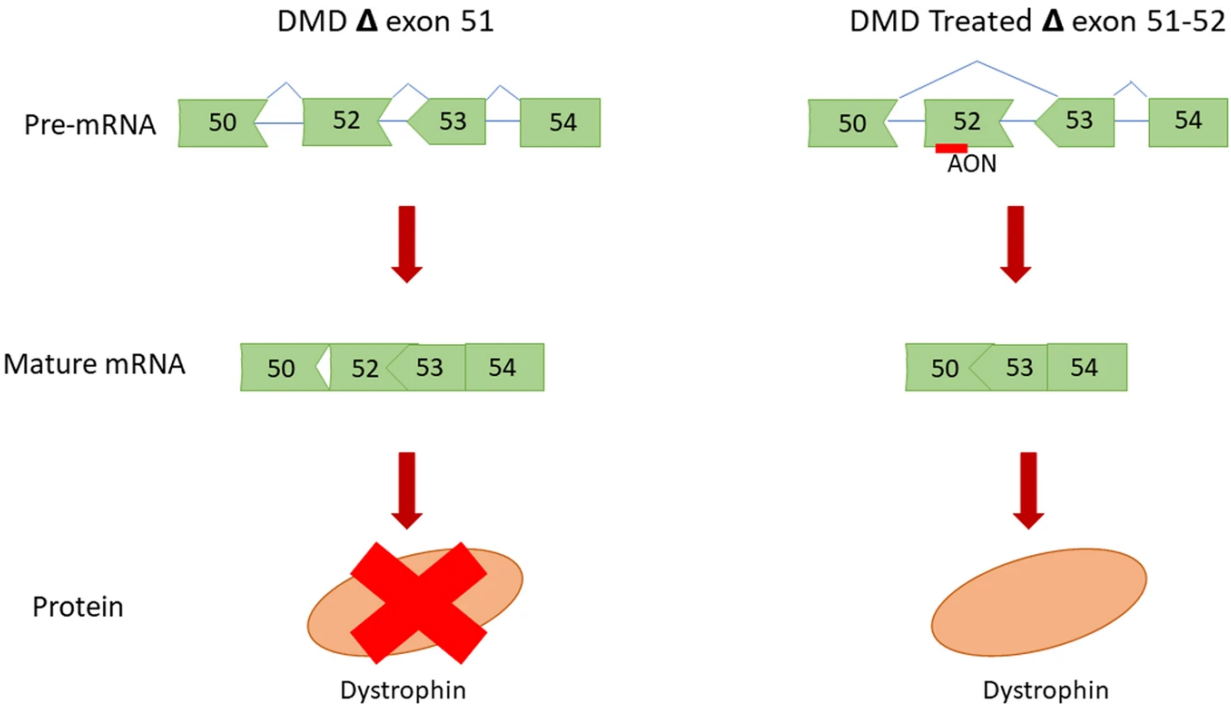

Figure 1.3: Example of AON-mediated exon skipping therapy in Duchenne muscular dystrophy. On the left; a deletion mutation in exon 51 results in a premature termination codon, leading to no expression of the dystrophin protein. On the right; an AON targets exon 52 causing exon 52 to be removed from the dystrophin mRNA as well, restoring the open reading frame. This results in the end in a slightly shortened, however functional dystrophin protein. *(Figure reproduced from: Dzierlega & Yokota., 2020)*

In this report, one part specifically focusses on optimizing the specific AON sequence and to a lesser extent on investigating a new method of delivery for AONs. The other part is on creating a 3D skin model. The need for 3D skin models is becoming more urgent. The increasing attention on ethical issues regarding animal experimentation and the three R's (Replacement, Reduction and Refinement) over the past years has led to guidelines becoming more strict and most probably become even stricter in the future. This in combination with the limited availability of human skin will make a human skin model

closely resembling the biology and physiology of the human skin crucial for studying skin biology in health as well as in disease (Niehues et al., 2018). In EB such a skin model could be useful by serving as a null-model or replacement model for human skin.

Objective: First, investigate and optimize delivery of a flAON-Fab conjugate for exon skipping in EB to gain insights in its cellular uptake, distribution and effectiveness. Second, identify the most potent AON sequence by optimizing transfection of single AONs in keratinocytes, and subsequently perform an 'Oligowalk' in which we will transfect 102 unique AON constructs, specifically targeting exon 105 of the *COL7A1* gene. Last, optimize a 3D skin model of human fibroblasts, keratinocytes and a collagen mix, to resemble the human skin as closely as possible that can serve as a null-model or replacement model for human skin in EB.

2. Materials and Methods

2.1 Cell culture

Control keratinocytes were isolated from leftover skin material obtained from healthy skin donors after informed consent.

Before thawing keratinocytes, CnT-PR (CELLnTEC Advanced Cell Systems AG, Bern, Switzerland) was preheated in a water bath heated to 37 °C and afterwards, 4 ml of medium was added to a T25 Nunc EasyFlasks 25 cm^2 (Thermo Scientific). Next, the vial of keratinocytes was heated in the water bath until one-third to half of the vial had thawed. Before moving the vial to the hood, the vial was disinfected with 70% ethanol. A little bit of CnT-PR was added to the vial, followed by resuspending and transferring the cells to the T25 flask with the previously added 4 ml of medium. Lastly, the vial was rinsed with 1 ml of CnT-PR, which was also added to the T25 flask (total ~5 ml). The medium was refreshed after 1 day.

From this point on, medium was refreshed every 2-3 days with 5 ml of CnT-PR. Cells were harvested when reaching 70-90% confluency. To harvest one T25 culturing flask, first 3 ml of Trypsin Neutralizing Solution (TNS) was added to 15 ml tube. TNS was a mixture of Hanks' Balanced Salt Solution (HBSS) (Gibco™) and 1 % fetal calf serum (FCS) (Invitrogen). Next, Trypsin-EDTA Solution (10x); 0.5% Trypsin and 5.3 mM EDTA*4Na (Gibco™) was thawed and diluted to 1X in HBSS. Afterwards, the medium was removed from the to be harvested T25 flask of keratinocytes and the cell were washed with 2 ml of HBSS. Next, 1 ml of 1X Trypsin-EDTA was added to the T25 flask to be subsequently incubated for 3-5 minutes at 37 °C 5% CO_2. Afterwards, the flask was tapped against a hard surface to loosen the cells from the flasks (confirmed by microscopy). Following this, 1 ml HBSS was added to the cells. The cells were resuspended and transferred to the 15 ml tube with 3 ml of TNS. The T25 flask was rinsed with 2 ml of HBSS, which was also transferred to the 15 ml tube. Subsequently, the cells were centrifuged for 10 minutes at 281 × *g*. Afterwards, the supernatant was removed and the cells were harvested, pooled and resuspended in 1-3 ml of CnT-PR. Cells were used for experiments or reseeded in new T25 culturing flasks.

2.2 Cell counting

Cells were counted using a Bürker counting chamber. 30 µl of the pooled cells was divided between the two counting chambers. Next, 25 of the 0.2 mm x 0.2mm squares were counted and multiplied by 10.000. This gives the amount of keratinocytes per ml (25 x 0.2 x 0.2 x 0.1 (dept) = 0.1 mm^3 = 0.1 µl, 0.1 µl x 10.000 = 1 ml). After knowing the amount of cells per ml, the cells were diluted to the preferred seeding density to be used in experiments. Leftover cells were either reused and reseeded in new T25 culturing flasks or thrown away.

2.3 Keratinocyte differentiation for investigating the effect of varying Fab-2 reducing agent concentrations on AON distribution, uptake and effectivity in keratinocytes.

Keratinocytes were differentiated in a 24-well plate according to the following protocol: First, keratinocytes were seeded at a seeding density of 1.2 * 10^4 cells per well in 500 µl of CnT-PR medium. After 48 hours of incubation at 37 °C 5% CO_2, the medium was replaced with CnT-PR-D + ½ gentamycin (g)/fungizone (f). 24 hours later, the medium was replaced again with CnT-PR-D + Ca + ½ g/f (CnT-PR-D + Ca + ½ g/f = 10 ml CtP-2D + 100 µl $CaCl_2$ stock 100x (BioVision BV) + 50 µl fungizone = amphotericin B 250 ug/ml (Gibco) + 5 µl gentamicin 10 mg/ml (Gibco)) and the cells were incubated for another 72 hours. After 72 hours, the medium was replaced with 180 µl of CnT-PR-D + Ca + ½ g/f and 20 µl of treatment according to table 1. After 24 hours, wells containing the fluorescent AON conjugates were imaged using a Leica inverted fluorescence microscope and RNA was isolated according to section 2.6.1. Afterwards, cDNA conversion was performed according to section 2.6.2 and subsequent PCRs were performed according to 2.6.3. Example of Fab-2 reduction to Fab fragment with varying reducing agent concentrations can be seen in figure 2. The experimental setup can be seen in figure 1.

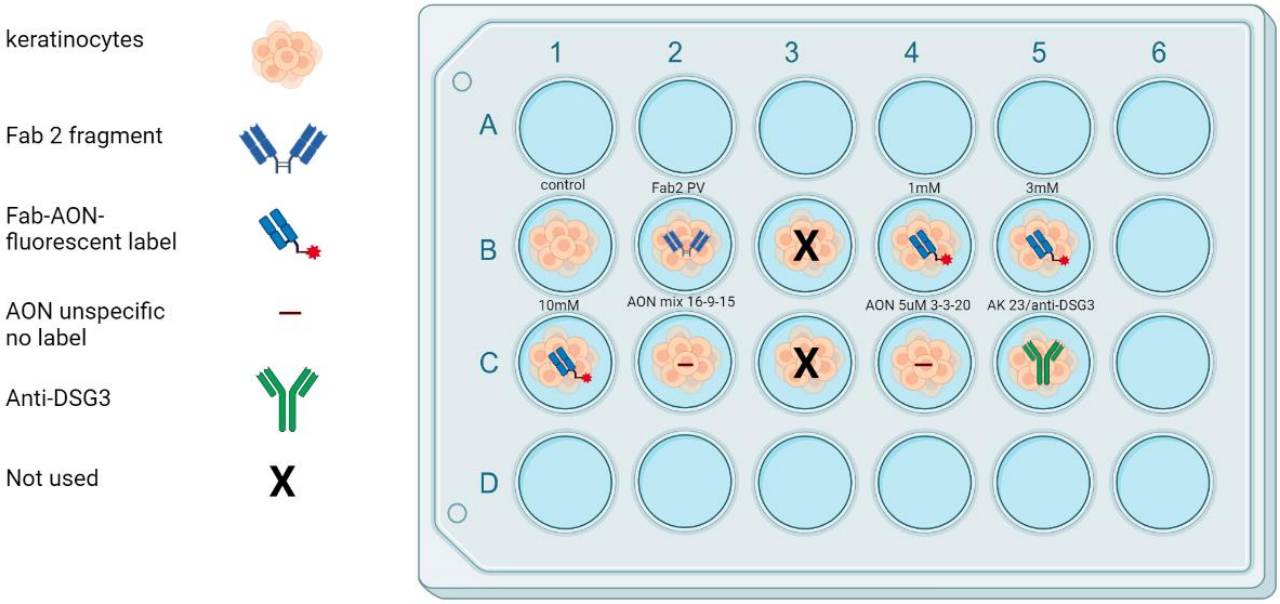

Figure 1. Experimental setup 1st experiment. The effect of varying Fab-2 reducing agent concentrations on AON distribution, uptake and effectivity in keratinocytes

Table 1. Treatment and its corresponding well 1st experiment.

	1	2	3	4	5
B	Keras + CT2D (control)	Fab2 PV 12-7-22 (control)	X	Fab-AON-fluorescent label 1mM 19-7-22	Fab-AON-fluorescent label 3mM 19-7-22
C	Fab-AON-fluorescent label 10mM 19-7-22	AON mix no label Aspecifiek 16-9-15 (control)	X	AON no label Aspecifiek 5µM werkoplossing 3-3-20 (control)	AK23/Anti-DSG3 (control)

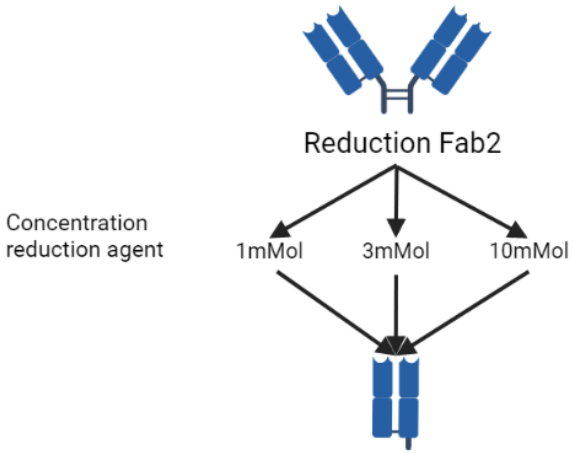

Figure 3. Example of Fab-2 reduction

2.4 *In vitro* transfection optimization of antisense oligonucleotides

In vitro keratinocyte cationic lipid transfection was optimized and performed in 96-well plates using polyethyleneimine (PEI) (MBI Fermentas, Life Technologies, Bleiswijk, the Netherlands) and Lipofectamine-2000 (LF) (Invitrogen). Lipid-AON complex formation was investigated for several weight:weight ratios for both PEI and LF (table 2). 24 hours before transfection, cells were harvested, pooled and subsequently dissolved in CnT-PR to be seeded in 200 µl at a seeding density of 2.5*10^4 cells per well (optimized). Prior to transfection cells were grown to 70-85% confluency, washed once with HBSS and 75 µl of OptiMEM (Gibco™) was added per well. Next, transfection mixtures were prepared and dissolved in OptiMEM. Before adding the transfection mixtures dropwise to the cells, the transfection mixtures were incubated for either 10 minutes using PEI or 20-30 minutes using LF at RT to allow Lipid-AON complex formation. The final concentration of the fluorescent AON was 250 nmol/L, whereas the concentrations of the transfection agents were varied (table 2). Cells were transfected for 5 hours at 37°C 5% CO_2 Afterwards, the medium was removed, cells were washed once with HBSS and cultured for 24 hours at 37 °C 5% CO_2 in 200 µl of CnT-PR. 30 minutes before analyses, cells were stained by 20 µl of bisbenzimide (Hoechst) at a dilution of 1:100.000 in CnT-PR. Lastly, cells were washed and 200 µl of CnT-

PR was added per well to be submitted for subsequent analysis by fluorescence microscopy using LEICA and LAS software version and Adobe Photoshop 2023.

Table 2. Transfection optimization scheme

Transfection mix 50 µl			seeding density 2,5*10^4 cells per well								
	OptiMEM	AON (12.5µM)	PEI	Total	AON/PEI		OptiMEM	AON (12.5µM)	PEI	Total	AON/PEI
A1	45	0	5	50	N.A.		45	0	5	50	N.A.
A2	47,5	2,5	0	50	N.A.		47,5	2,5	0	50	N.A.
A3	40	2,5	7,5	50	1/1,5		40	2,5	7,5	50	1/1,5
A4	41,25	2,5	6,25	50	1/1,25		41,25	2,5	6,25	50	1/1,25
A5	42,5	2,5	5	50	1,0/1,0		42,5	2,5	5	50	1,0/1,0
A6	43,75	2,5	3,75	50	1/0,75		43,75	2,5	3,75	50	1/0,75
A7	45	2,5	2,5	50	1/0,5		45	2,5	2,5	50	1/0,5
A8	46,25	2,5	1,25	50	1/0,25		46,25	2,5	1,25	50	1/0,25
A9	50	0	0	50	N.A.		50	0	0	50	N.A.
tot	401,25	17,5	31,25	450			401,25	17,5	31,25	450	
	OptiMEM	AON (12.5µM)	LPF2000	Total	AON/LPF2000		OptiMEM	AON (12.5µM)	LPF2000	Total	AON/LPF2
D1	46	0	4	50	N.A.		46	0	4	50	N.A.
D2	47,5	2,5	0	50	N.A.		47,5	2,5	0	50	N.A.
D3	41,5	2,5	6	50	1/1,5		41,5	2,5	6	50	1/1,5
D4	42,5	2,5	5	50	1/1,25		42,5	2,5	5	50	1/1,25
D5	43,5	2,5	4	50	1,0/1,0		43,5	2,5	4	50	1,0/1,0
D6	44,5	2,5	3	50	1/0,75		44,5	2,5	3	50	1/0,75
D7	45,5	2,5	2	50	1/0,5		45,5	2,5	2	50	1/0,5
D8	46,5	2,5	1	50	1/0,25		46,5	2,5	1	50	1/0,25
D9	50	0	0	50	N.A.		50	0	0	50	N.A.
tot	407,5	17,5	25	450			407,5	17,5	25	450	

2.5 *In vitro* transfection of antisense oligonucleotides Oligowalk

Keratinocytes were transfected in 96-well plates using LF cationic lipid transfections. Lipid-AON complex formation was optimized (section 2.4) to a weight:weight ratio of 1:1. Transfection was performed according to section 2.4, however 102 different AONs were used instead of one unspecific flAON. Moreover, no nuclei staining was performed as this possibly interferes with downstream applications. The AONs used are all specific for exon 105, however all of their sequences differ from each other. 24 hours after transfection, the medium was removed and cells were lysed using 200 µl of TRIzol (Invitrogen) and stored at -80 °C. The transfection scheme can be observed below (table 3) and was performed in triplicate.

Table 3. Oligowalk transfection scheme

	1	2	3	4	5	6	7	8	9	10	11	12
A	HBSS	1	9	17	25	33	41	49	c	HBSS		
B	HBSS	2	10	18	26	34	42	50	c	HBSS		
C	HBSS	3	11	19	27	35	43	51	c	HBSS		
D	HBSS	4	12	20	28	36	44	52	c	HBSS		
E	HBSS	5	13	21	29	37	45	53	c	HBSS		
F	HBSS	6	14	22	30	38	46	54	c	HBSS		
G	HBSS	7	15	23	31	39	47	55	c	HBSS		
H	HBSS	8	16	24	32	40	48	56	c	HBSS		

	1	2	3	4	5	6	7	8	9	10	11	12
A	HBSS	57	65	73	81	89	97	c	c flAON1	HBSS		
B	HBSS	58	66	74	82	90	98	c	c flAON2	HBSS		
C	HBSS	59	67	75	83	91	99	c	c flAON3	HBSS		
D	HBSS	60	68	76	84	92	100	c	c LF	HBSS		
E	HBSS	61	69	77	85	93	101	c	c	HBSS		
F	HBSS	62	70	78	86	94	102	c	HBSS			
G	HBSS	63	71	79	87	95	c LF	c	HBSS			
H	HBSS	64	72	80	88	96	c	c	HBSS			

2.6 *In vitro* RNA and protein analysis

2.6.1 RNA isolation Phasemaker Tubes

For the analysis of exon skipping on the RNA level, RNA isolation of the *in vitro* transfections was performed with Invitrogen™ Phasemaker™ Tubes according to the manufacturer's protocol. One sample (200 µl of lysate) was added per Phasemaker Tubes and incubated for 5 minutes to allow complete dissociation of the nucleoproteins complex. Next, the sample was shaken vigorously by hand (important note: don't shake too vigorously), to be subsequently centrifuged for 5 minutes at 14.100 × *g* at 4°C. Now, the polymer included in the Phasemaker Tubes, separates the mixture in phases based on its density: the lower red phenol-chloroform phase, and the interphase, and the upper colorless RNA containing aqueous phase. The aqueous phase was transferred to a new tube and the RNA was subsequently precipitated by incubating with isopropanol for 10 minutes, to be centrifuged for the next 10 minutes at 12.000 × *g* at 4 °C. Now, a gel-like pellet should occur at the bottom of the tube, however, from experience; the lysate from keratinocytes in 96-well plates was hardly visible and most of the times not visible at all (important note: the RNA is still present). Next, the pellet was resuspended in 75% ethanol and centrifuged for 5 minutes at 7.500 × *g* at 4 °C. Subsequently the supernatant was removed and the RNA pellet (generally not visible) was air dried for 5-10 minutes, after which the pellet was solubilized in 20 µl of RNase free water and incubated in a heat bath for 10-15 minutes at 55-60 °C. Lastly, The RNA was stored at -80 °C, prior cDNA conversion.

2.6.2 cDNA conversion

RevertAid H Minus First Strand cDNA Synthesis Kit (Thermo Scientific™) was used for cDNA conversion according to the manufacturer's protocol. First the template RNA (up to 11 µl) is mixed with 1 µl of Random Hexamer Primer and nuclease free water (depending on the amount of template RNA added). This volume of 12 µl was pre-heated to 85 °C to denature secondary structures and remove the AON from the RNA. To the total volume of 12 µl a mixture of four components is added in the following order: 4 µl of 5X Reaction Buffer, 1 µl of RiboLock RNase Inhibitor (20 U/µl), 2 µl of 10 mM dNTP Mix and 1 µl of RevertAid M-

MuLV RT (200 U/µl) giving a total volume of 20 µl. This mixture was incubated in a PCR machine for 5 minutes at 25 °C, followed by 60 minutes at 42 °C, and ended by incubating for 5 minutes at 70 °C. The cDNA originating from the optimization of the *in vitro* cationic transfection of keratinocytes, was used for two following PCR reactions. A primary and a nested PCR reaction.

2.6.3 Primary PCR and nested PCR

1 µl of the cDNA product per sample was used as a template for the primary PCR reaction. This 1 µl was added to a primary PCR reaction mixture of 24 µl containing the following: 12.5 µl of AmpliTaq Gold (Thermo Scientific™), 2.5 µl of 5 µM forward primer exon 105 skip large, 2.5 µl of 5 µM reverse primer exon 105 skip large and 6.5 µl of milli-Q water. This mixture was incubated in a PCR machine for 10 minutes at 95 °C, followed by a cycle of 35 of 30 seconds at 95 °C, 30 seconds at 69 °C (annealing temperature) and 30 seconds at 70 °C, after 35 cycles, the reaction was extended 10 minutes at 70 °C, and ended at 4 °C. The obtained product was used for a subsequent nested PCR reaction following the same protocol as the primary PCR reaction, only a different set of primers was used. For the nested PCR 2.5 µl of 1:20 forward primer exon 105 skip nested and 2.5 µl of reverse primer exon 105 skip nested were used. All primers were diluted in milli-Q water. The product of the nested PCR was used for gel electrophoresis. First a 1 % agar 0.5X TBE gel solution was made and 1 µl of Midori Green (NIPPON Genetics) per 60 ml of TBE was added. subsequently, the gel solution was casted in a casting tray, a well comb was put in and the gel was let to stiffen for 20-30 minutes. In the meantime, 6X TriTrack DNA Loading Dye (Thermo Scientific™) was diluted 1:6 in TBE and from this solution 5 µl was added to 10 µl of nested product per sample. The DNA ladder also contained 5 µl of the TriTrack solution and 1.5 µl of GeneRuler 1kb Plus DNA ladder. When the gel had stiffened, the gel was transferred to a gel electrophoresis machine. The comb was carefully taken out and the samples were loaded. Next, the samples ran, depending on the gel volume, for 30-50 minutes at 100 Volts. After running, gels were imaged using a Bio-Rad Gel Doc.

2.6.4 Gel extraction for exon skip confirmation

To ensure the bands represented forms of C7 or a skipped product of C7, the finished gel was placed on a UV light box. Bands were excised with a scalpel blade, captured in 1.5 ml Eppendorf tubes, to be processed with the GeneJET Gel Extraction Kit (Thermo Scientific™) according to the manufacturer's protocol. First a 1:1 volume:weight ratio of binding buffer was added per excised gel slice (e.g., add 100 µL of Binding Buffer for every 100 mg of agarose gel). Subsequently, the gel slice was dissolved by incubation for 10 minutes at 50-60 °C and vortexed briefly afterwards. If the band in the excised gel fragment was below 500 kb, also 1 volume of isopropanol was added. Next, the gel solution was transferred to a GeneJET purification column and centrifuged for 1 minute at 12.000 × *g*. Afterwards, the flow-through was discarded. Another 100 µl Binding Buffer was added to the spin column, centrifuged for 1 minute at 12.000 × *g* and the flow-through was discarded. Next, 700 µl of Wash buffer was added to the spin column, centrifuged for 1 minute at 12.000 × *g* and the flow-through was discarded. The spin column was centrifuged again for 1 minute a 12.000 × *g* to remove residual wash buffer. From this point, the spin column was transferred to a

clean 1.5 ml Eppendorf tube and eluted by adding 20 µl of Elution Buffer to the center of the purification column membrane and subsequently centrifuging for 1 minute at 12.000 × *g*. The concentration of the eluted DNA was measured on a Nanodrop machine and diluted to a concentration of 5 ng/µl. This diluted DNA was divided amongst two 1.5 ml Eppendorf tubes for each excised gel slice. One of the two tubes contained the forward primer of the nested skip for exon 105 and the other tube contained the reverse primer of the nested skip for exon 105. Lastly, the tubes were barcoded and send to GATC by mail for Sanger sequencing.

2.7 Skin cryosection protein analysis

Healthy skin was obtained from healthy skin donors after informed consent. From this skin, 6 mm biopsies were obtained by using a small drill. Next, biopsies were inserted in a 24-well plate in 1 ml of DMEM with 10% FCS and streptomycin/fungizone. Afterwards, treatment was added according to figure 4. A total of 15 µl was added for the flAON and the 1, 3 and 10 mm of flAON-Fab conjugate. A total of 10 µl was added of AK23 (mouse anti-human desmoglein-3). The biopsies were incubated for 48 hours at 37 °C 5 % CO_2. Afterwards, the biopsies were flash frozen using liquid nitrogen and transferred to a container that was stored at -80 °C for further analysis. To investigate internalization, distribution and expression of the flAON-Fab conjugates, 4 µm cryosections were cut on a Leica CM3050S cryostat after embedding the biopsies in Tissue-Tek (Sakura Finetek™). After cutting, the cryosections were attached to Polysine Adhesion Microscope Slides and circled with a hydrophobic PAP pen. Biopsies incubated with flAON-Fab conjugates were stained for 30 minutes with goat anti-human IgG Fab Alexa Fluor 488 diluted 1:100 in PBS/OVA and biopsies incubated with AK23 were stained for 30 minutes with goat anti-mouse IgG Alexa 488 diluted 1:60 in PBS/OVA. This was done by pipetting between 50-100 µl of diluted antibody inside the PAP ring that encloses the skin cryosection. Afterwards, the slides were washed for 30 minutes in PBS. Cell nuclei were stained for 5 minutes using Hoechst (Bisbenzimide) at a final dilution of 1:10.000 in PBS and to be subsequently washed for 5 minutes in PBS. After washing, the slides were wiped dry except for the PAP ring. Subsequently, the slides were embedded using Slowfade Gold (Invitrogen) and analyzed by a Leica DMRA fluorescence microscope.

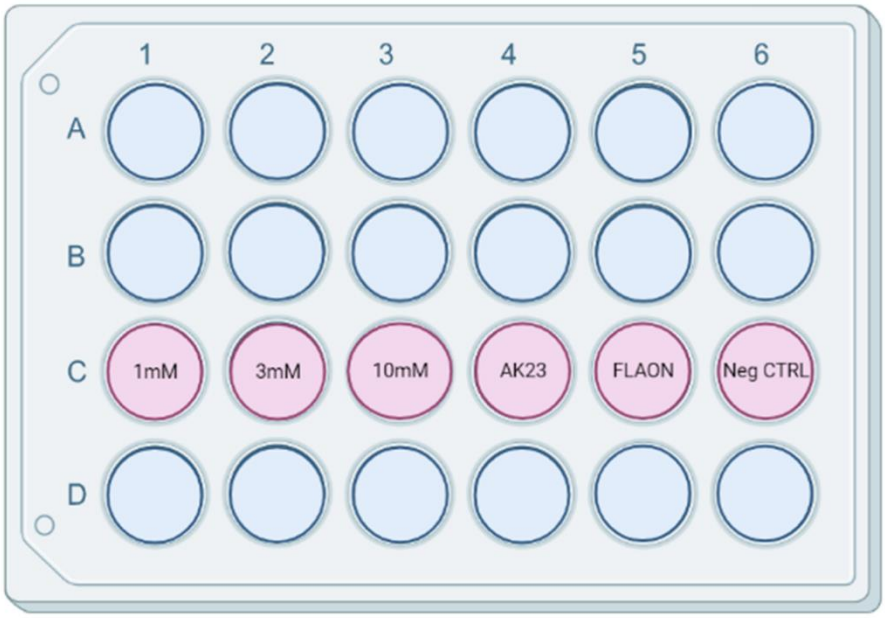

Figure 3. 24-well plate setup 6 mm biopsies: 48 hour incubation with flAON-Fab conjugates

2.8 3D Culture and protein analysis of a 3D skin model

Fibroblasts that were previously isolated form a healthy skin donor, were thawed and resuspended in CnT-PR-F and cultured in a T25 culturing flask. The medium was refreshed after 5 hours of culturing and from then on, every 2 days. One day after starting the fibroblast culture, keratinocytes were thawed and cultured according to section 2.1. The next day, the fibroblasts were harvested and equally divided over 3 T25 culturing flasks. Harvesting was performed according to section 2.1, however instead of 3 ml of TNS, 3 ml of CnT-PR-F was used and instead of HBSS, PBS was used. 3 days later, both the keratinocytes and 1/3 of the flasks of fibroblasts were harvested. Keratinocytes were cultured 1 to 2 and two times 1 to 4 in T25 culturing flasks. Fibroblasts were cultured 1 to 2. The next day, fibroblasts were harvested, pooled and counted. Afterwards, a collagen mix was prepared on ice for 8 inserts existing out of the following components: 6.4*10^5 fibroblasts resuspended in 160 µl of CnT-PR-F, 640 µl of 5X Reconstitution Buffer and 2.4 ml of collagen. Next, inserts were put in a 12-well plate and 300-400 µl of collagen mix was added per insert. Afterwards, the plate was incubated for 30 minutes at 37 °C 5% CO_2. After 30 minutes, 2-3 ml of FTAL or FTAL + fungizone was added to its corresponding well with insert, Af and B (Millicell 0.4 µm). The day after, keratinocytes cultured 1 in 2 were harvested and counted. Continuing, 2 tubes were prepared, each containing 2*10^5 keratinocytes to be subsequently centrifuged and resuspended in 300 µl of FTAL or 300 µl of FTAL + fungizone. The 300 µl of keratinocytes were pipetted into their corresponding inserts, Af and B, after which the 12-well plate was incubated at 37 °C 5% CO_2. 2 days later, the other inserts, Cf and D (Millicell 0.4 µm), and Ef (Brand 0.4 µm PC) and Ff (Brand 0.4 µm PET) were provided with 300 µl of 2*10^5 keratinocytes that were obtained from the two T25 flasks of keratinocytes that were cultured 1 to 4. Cf, Ef and Ff received keratinocytes resuspended in FTAL + fungizone and D received keratinocytes resuspended in FTAL. 2-3 ml of medium was added around the inserts in the corresponding well (D -> FTAL, Cf, Ef and Ff -> FTAL + fungizone)

and the 12-wells pate was incubated at 37 °C 5% CO_2. The day after, insert Af and B were airlifted by removing the medium from the wells and inserts, and adding 350 µl of their corresponding medium (Af -> FTAL + fungizone, Bf -> FTAL) to the well. 2 days later, the other inserts were airlifted as well. Cf and D received 350 µl of their corresponding medium and Ef and Ff received 1.8 ml of their corresponding medium. After the airlift, the skin models were cultured for a duration of 14 days at 37 °C 5% CO_2. The medium was refreshed every 2 days. Skin models were harvested by excising the 0.4 µm membranes with a small scalpel blade to subsequently paste the membrane with grown skin model in a small drop of Tissue-Tek (Sakura Finetek™) placed in the lit of a container. The container was closed and flash frozen in liquid nitrogen (lit down for 5 seconds). After obtaining all models, the skin models were transferred and stored at – 80 °C. For protein analysis, skin model cryosections were cut and prepared for IF staining according to section 2.7. Skin model cryosections were incubated for 30 minutes with one of the following primary antibodies; mouse anti-human COL7A diluted 1:25 in PBS/OVA, mouse anti-human COL4 diluted 1:500 PBS/OVA, mouse anti-human DSG1 diluted 1:10 in PBS/OVA or mouse anti-human DSG-3 diluted 1:30 in PBS/OVA. Afterwards, the cryosection slides were washed for 15 minutes in PBS to be subsequently stained with a secondary fluorescently labelled goat anti-mouse IgG Alexa 488 antibody diluted 1:600 in PBS/OVA. Cell nuclei staining, cryosection slide embedding and analysis was performed according to section 2.7.

3. Results

3.1 Differentiated keratinocytes incubated for 24 hours with flAON-Fab conjugates specific for exon 105

Primary keratinocytes from a healthy donor were cultured and differentiated. After reaching 80-90 % confluency, they were incubated for 24 hours with flAON-Fab conjugates reduced with varying reducing agent, 2-Mercaptoethylamine•HCl (2-MEA) concentrations. We observed that keratinocytes incubated with a flAON-Fab conjugates, reduced with a 2-MEA concentration of 1 mM, showed internalization, distribution and binding of the conjugated AON construct. These observations can also be seen for keratinocytes incubated with the conjugated AON construct reduced with a 2-MEA concentration of 3mM. However, when incubating keratinocytes with a conjugated AON construct reduced at a 2-MEA concentration of 10 mM, hardly any internalization, binding nor distribution can be seen, comparable to the negative control incubated with no construct at all [Fig. 3.1A].

After 24 hours of incubation, RNA was isolated from the wells and converted to cDNA. A subsequent nested PCR with primers covering exon 102-106 of C7, followed by gel electrophoresis of the nested PCR product, revealed no clear band at the predicted location of the exon skipped product.

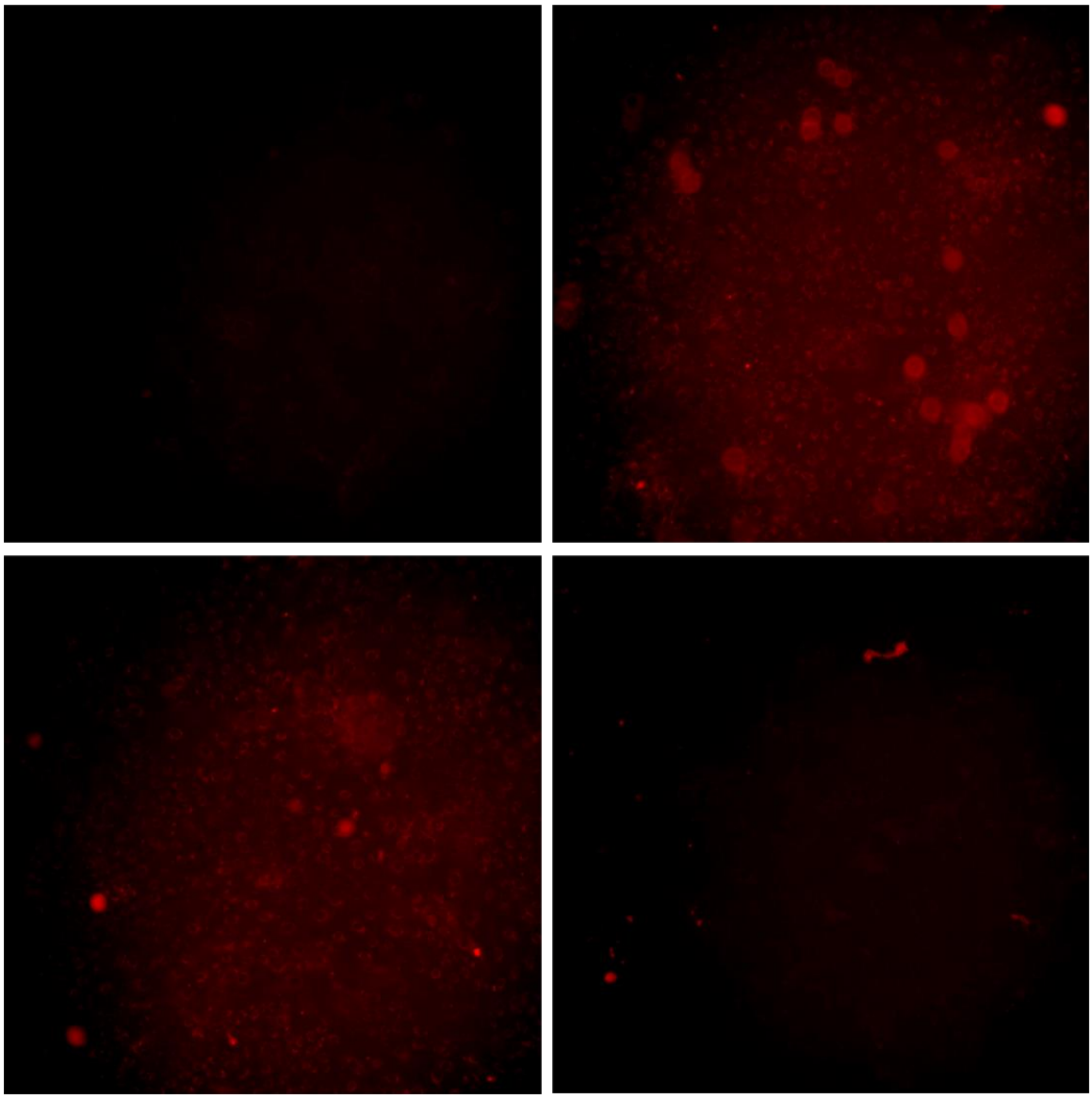

Figure 3.1A Differentiated keratinocytes incubated with flAON-Fab conjugates reduced at varying 2-MEA concentrations of 1, 3 and 10 mM. 20x fluorescent microscopy images of differentiated keratinocytes incubated for 24 hours with flAON-Fab conjugates specific for exon 105 reduced at varying 2-MEA concentrations of 1, 3 and 10 mM. Top left = negative control (no AON construct), top right = 1 mM, bottom left = 3 mM and bottom right = 10 mM

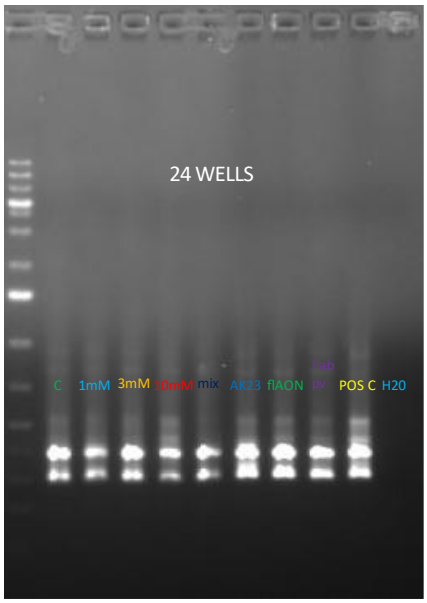

Figure 3.1B Gel electrophoresis of differentiated keratinocytes incubated with flAON-Fab conjugates at varying 2-MEA concentrations of 1, 3 and 10 mM. 1% agar TBE gel electrophoresis ran on the nested PCR product of differentiated keratinocytes incubated with flAON-Fab conjugates at varying 2-MEA concentrations of 1, 3 and 10 mM, at the optimal AON: transfection agent concentration. The first set of primers cover exon 100-108 (510bp) of the C7 gene. The nested primers cover exon 102-106 (289bp) of the C7 gene. C = keratinocytes incubated with nothing, 1 mM, 3 mM and 10 mM are keratinocytes incubated with flAON-Fab conjugates at 2-MEA concentrations of 1, 3 and 10 mM. Mix = keratinocytes incubated with a mix of multiple AONs, AK23 = keratinocytes incubated with anti-DSG3, flAON = keratinocytes incubated with a fluorescently labelled unspecific AON. Fab-PV = keratinocytes incubated with a Fab fragment, Pos C = control DNA, H_2O = negative control.

3.2 Skin cryosections of 6 mm biopsies incubated for 48 hours with our flAON-Fab conjugates reduced at varying 2-MEA concentrations

Heathy skin biopsies of 6 mm were incubated for 24 hours with flAON-Fab conjugates reduced with varying 2-MEA concentrations. We observed that only the conjugated AON construct, reduced at a 2-MEA concentration of 3 mM, showed signs of binding and internalization [Fig. 3.2B]. The fluorescent microscopy image at the bottom left of figure 3.2B shows a couple of cell nuclei in blue, that seem to express a fluorescently labelled AON indicated by the red signal in their respective nuclei. Interestingly, there seems to be no specific overlap between green and red signal in these nuclei, possibly indicating that the conjugated-Fab construct is lost before internalization in the nuclei. However, these observations should be taken with precaution since it is hard to tell whether there is any specific red fluorescent or green fluorescent signal at all. The cells possibly expressing red-fluorescent signal in their nuclei are located in the dermis. However, in the epidermis no specific red nor specific green fluorescent signal could be seen at all, indicating hardly to no internalization nor binding or distribution. Moreover, the dermis shows quite some nonspecific staining. This is true for every 6 mm biopsy incubated with a flAON-Fab conjugate and the negative control. Therefore, we

conclude that red signal we see in the respective nuclei in figure 3.2B is nonspecific. The 6 mm biopsy incubated with anti-DSG3 showed a regular intercellular staining pattern for DSG3 [fig 3.2D] .

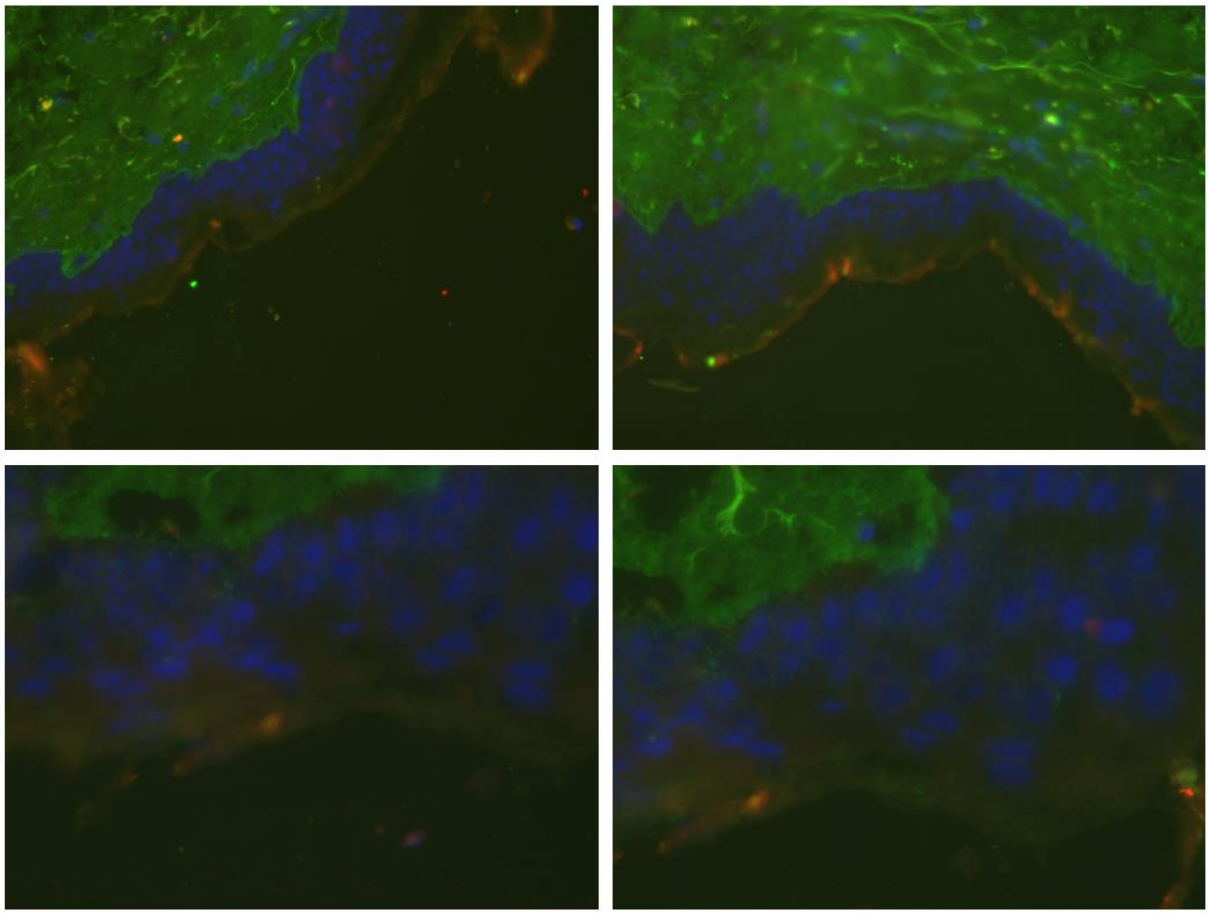

Figure 3.2A 4 µm skin cryosections of a 6 mm biopsy incubated with our flAON-Fab conjugate reduced at a 2-MEA concentration of 1 mM. Fluorescent microscopy images of skin cryosections made from a 6 mm biopsy that was incubated for 48 hours with our flAON-Fab conjugate reduced at a 2-MEA concentration of 1 mM. The two fluorescent images above show a 10x magnification of two locations of the 4 µm cryosection. The two images below show a 40x magnification. Blue = Bisbenzimide (Hoechst) nuclei staining, Red = flAON-Fab conjugate, Green = anti-Fab.

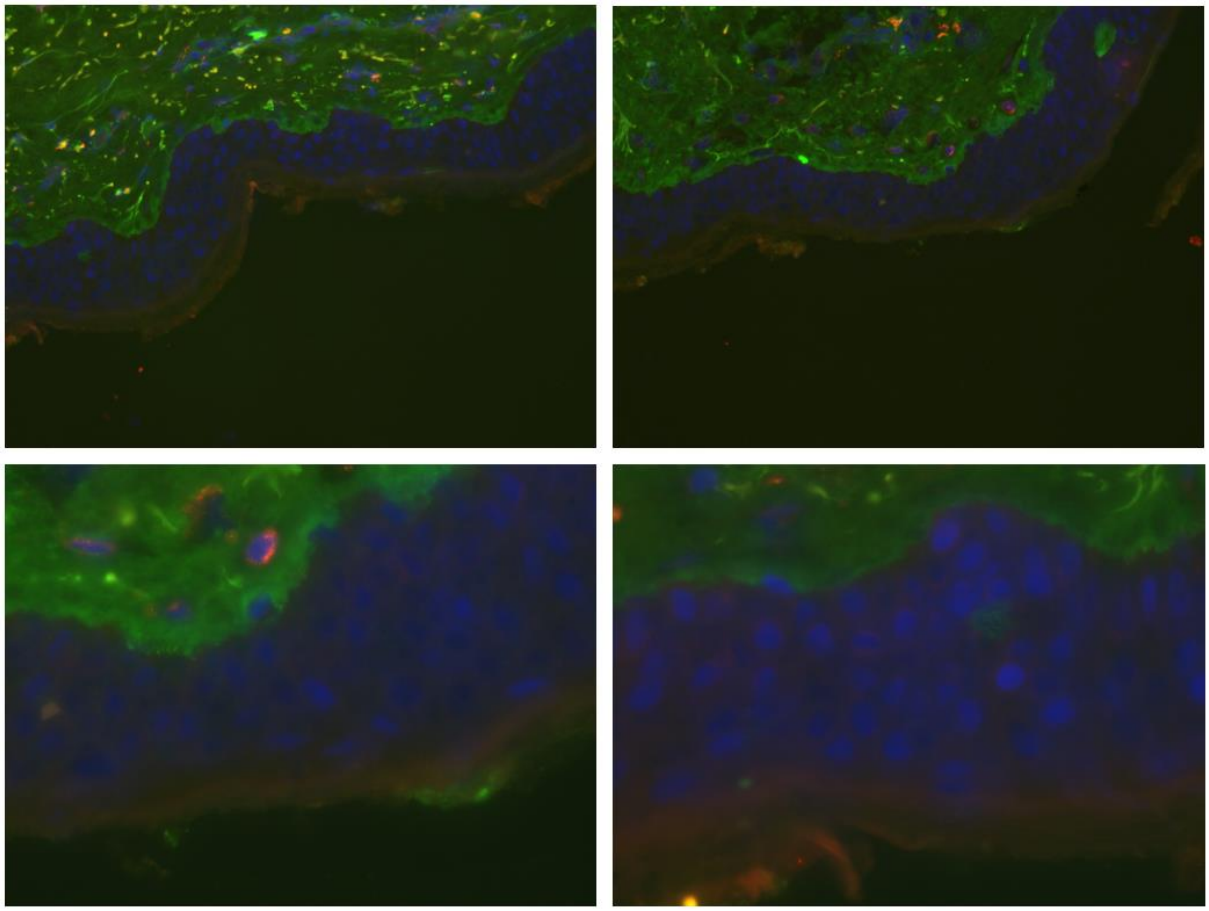

Figure 3.2B 4 µm skin cryosections of a 6 mm biopsy incubated with our flAON-Fab conjugate reduced at a 2-MEA concentration of 3 mM. Fluorescent microscopy images of skin cryosections made from a 6 mm biopsy that was incubated for 48 hours with our flAON-Fab conjugate reduced at a 2-MEA concentration of 3 mM. The two fluorescent images above show a 10x magnification of two locations of the 4 µm cryosection. The two images below show a 40x magnification. Blue = Bisbenzimide (Hoechst) nuclei staining, Red = flAON-Fab conjugate, Green = anti-Fab.

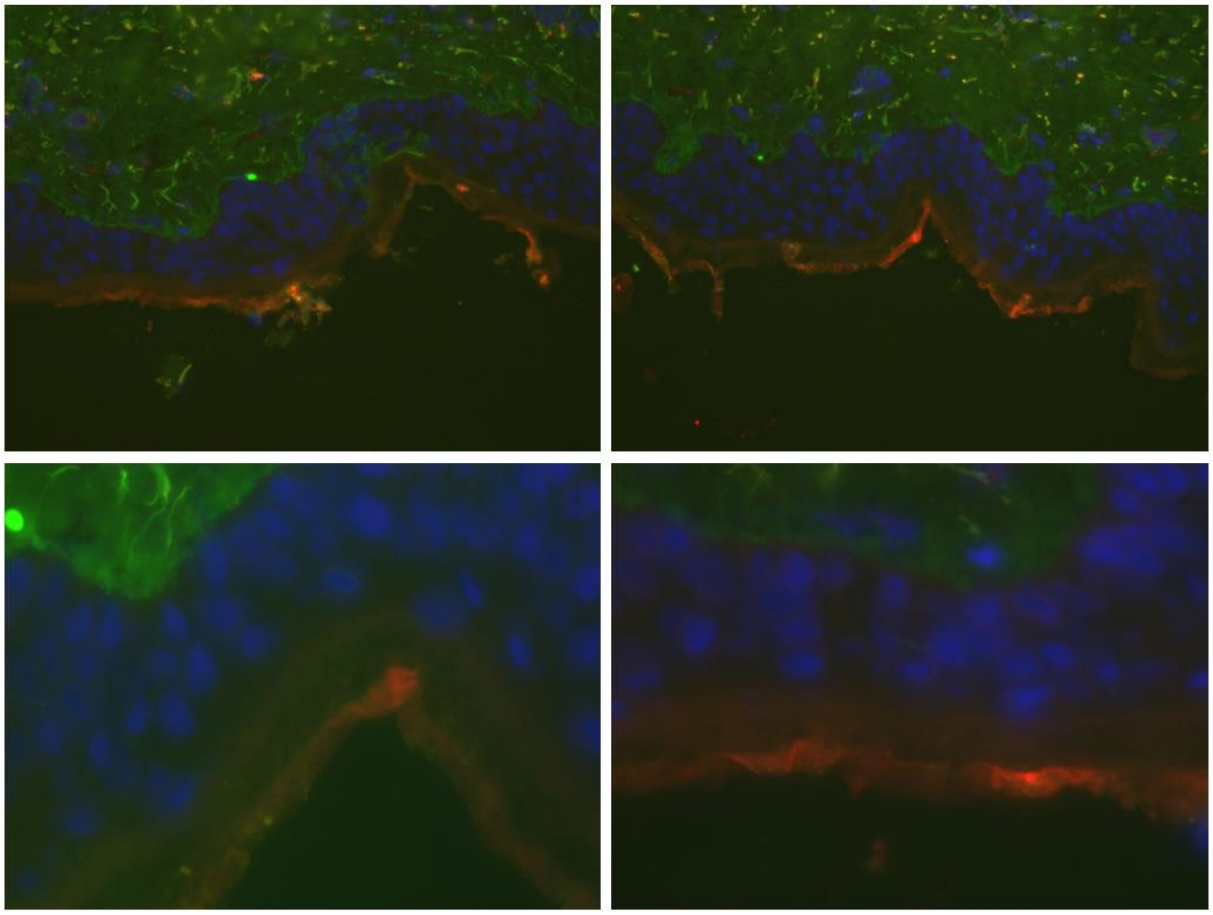

Figure 3.2C 4 µm skin cryosections of a 6 mm biopsy incubated with our flAON-Fab conjugate reduced at a 2-MEA concentration of 10 mM. Fluorescent microscopy images of skin cryosections made from a 6 mm biopsy that was incubated for 48 hours with our flAON-Fab conjugate reduced at a 2-MEA concentration of 10 mM. The two fluorescent images above show a 10x magnification of two locations of the 4 µm cryosection. The two images below show a 40x magnification. Blue = Bisbenzimide (Hoechst) nuclei staining, Red = flAON-Fab conjugate, Green = anti-Fab.

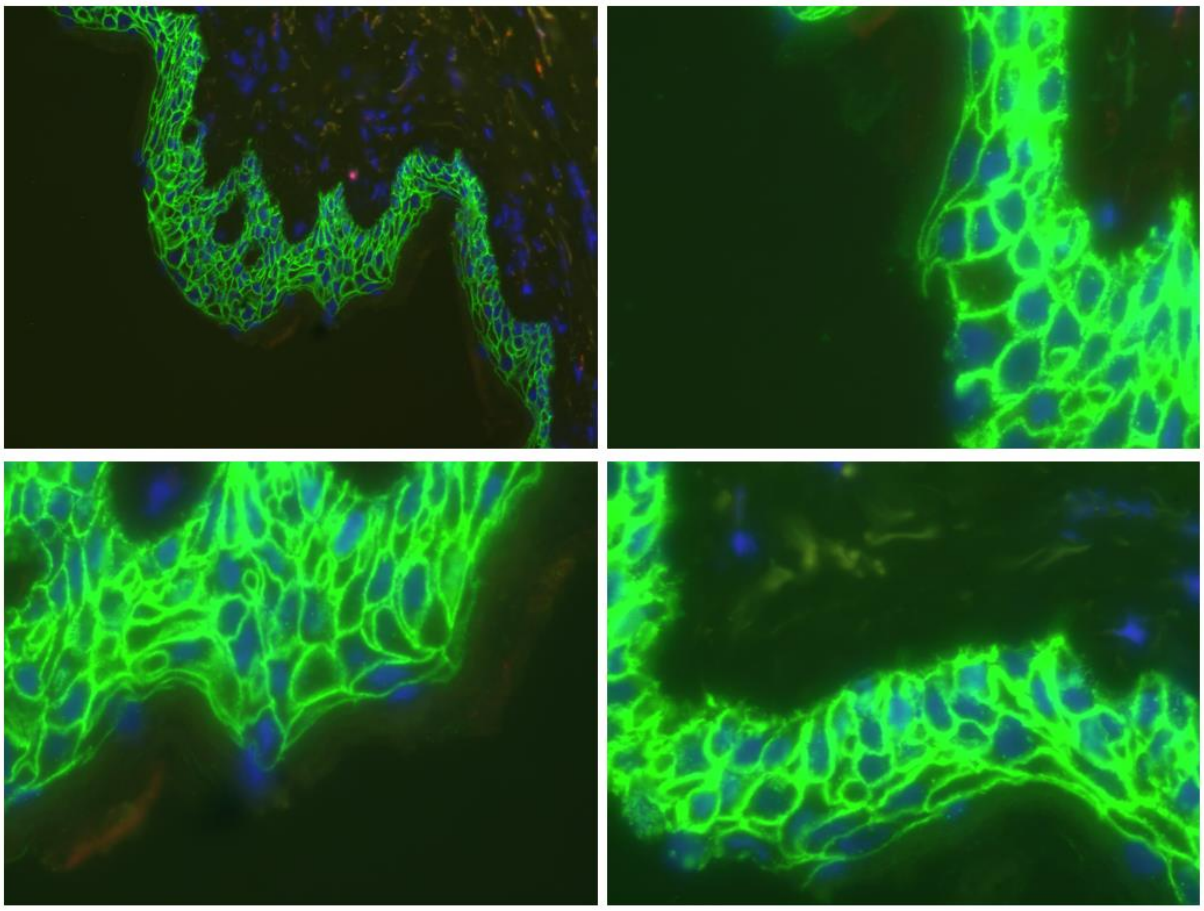

Figure 3.2D 4 µm skin cryosections of a 6 mm biopsy incubated with anti-DSG3 AK23. Fluorescent microscopy images of skin cryosections made from a 6 mm biopsy that was incubated for 48 hours with anti-DSG3 AK23. The two fluorescent images above show a 10x magnification of two locations of the 4 µm cryosection. The two images below show a 40x magnification. Blue = Bisbenzimide (Hoechst) nuclei staining, Red = flAON-Fab conjugate, Green = anti-DSG3.

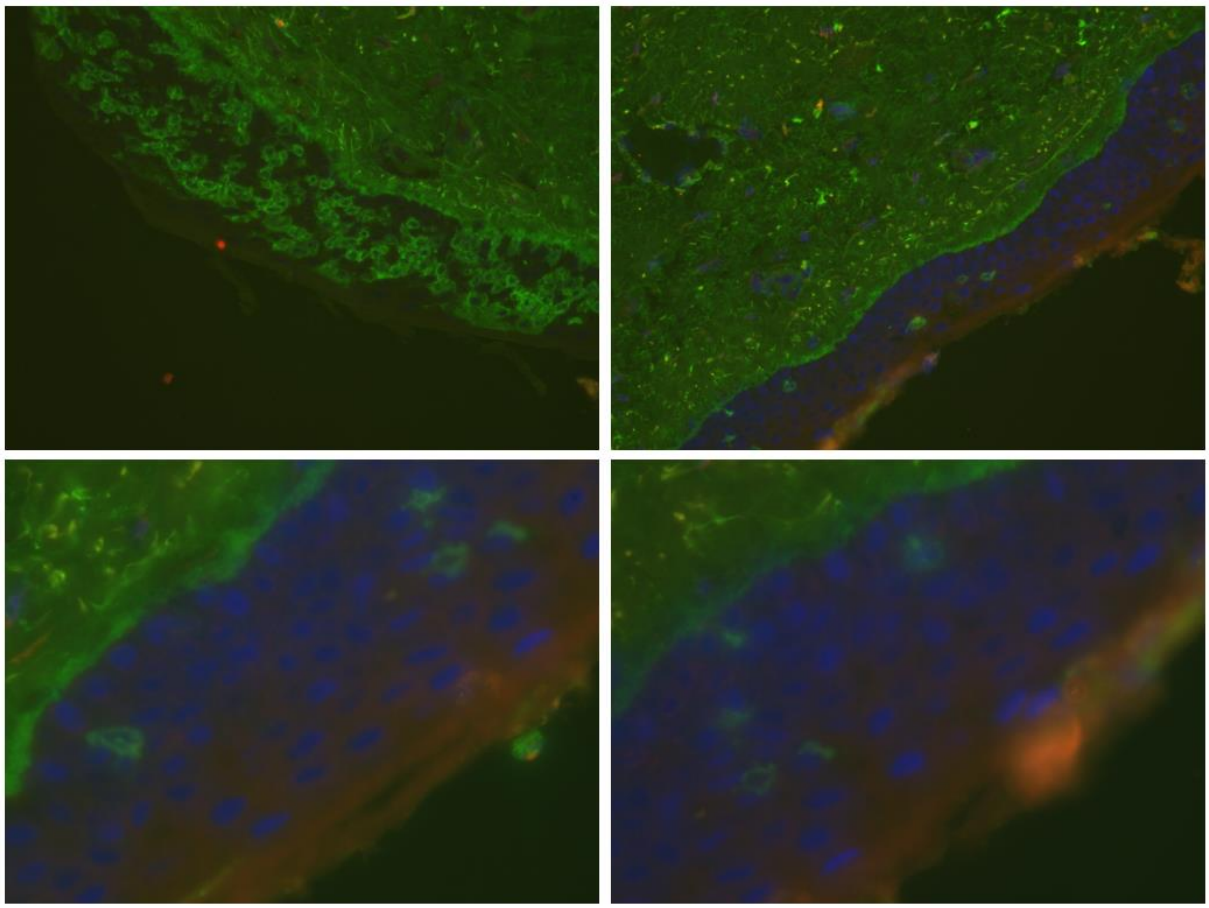

Figure 3.2E 4 µm skin cryosections of a 6 mm biopsy negative control. Fluorescent microscopy images of skin cryosections made from a 6 mm biopsy negative control that was incubated for 48 hours. The two fluorescent images above show a 10x magnification of two locations of the 4 µm cryosection. The two images below show a 40x magnification. Blue = Bisbenzimide (Hoechst) nuclei staining, Red = flAON-Fab conjugate, Green = anti-Fab.

3.3 Transfection optimization 1: keratinocytes transfected with a fluorescently labelled unspecific AON at varying AON: transfection agent concentrations.

Healthy keratinocytes were transfected with a fluorescently labelled AON at varying AON: lipofectamine2000 ratios and varying AON: PEI ratios. The concentration of the AON was kept constant at 250 nm/l, whereas the lipofectamine2000 and PEI concentrations had been varied. The specific AON: lipofectamine2000 ratios and AON: PEI can be observed in table 2 of the materials & methods section. We observed by brightfield microscopy that transfection of AONs with PEI was more cell friendly compared to transfection of AONs with lipofectamine (images not shown). However, when comparing the two transfection agents regarding transfection efficiency using fluorescent microscopy we observed that both transfection agents did relatively well at transfecting the fluorescently labelled AON into the cell. Especially for AON: transfection agents ratios of 1:1 and 1:0.75, the transfection efficiency seemed to be high, with cell morphology looking normal.

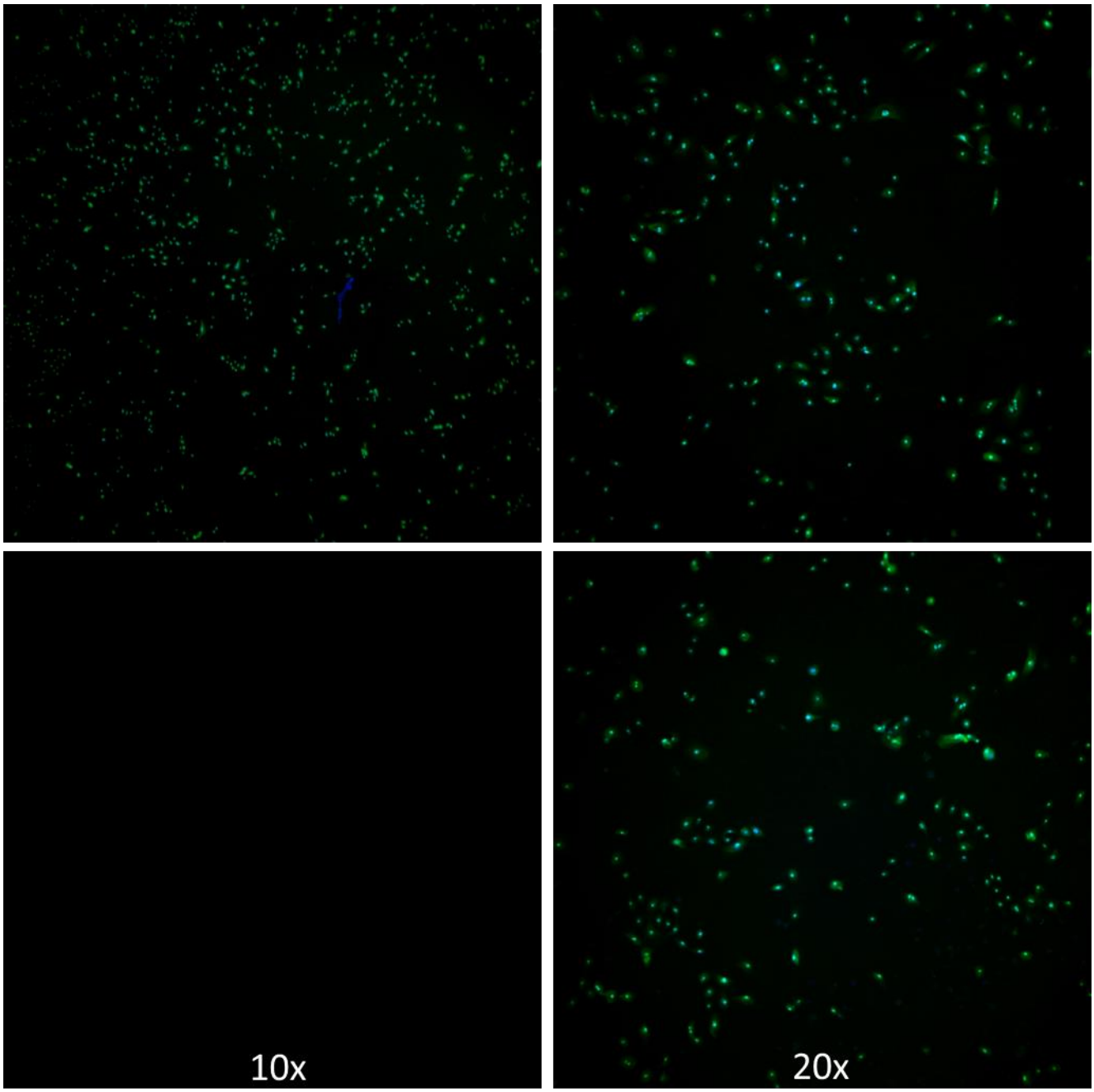

Figure 3.3A Keratinocytes transfected at an AON-PEI ratio of 1-1 in duplicate. 10x and 20x fluorescent microscopy image of keratinocytes transfected at an AON-PEI ration of 1-1. The 10x image of one of the two duplicates is missing. Green = fluorescently labelled unspecific AON, Blue = Bisbenzimide (Hoechst) nuclei staining.

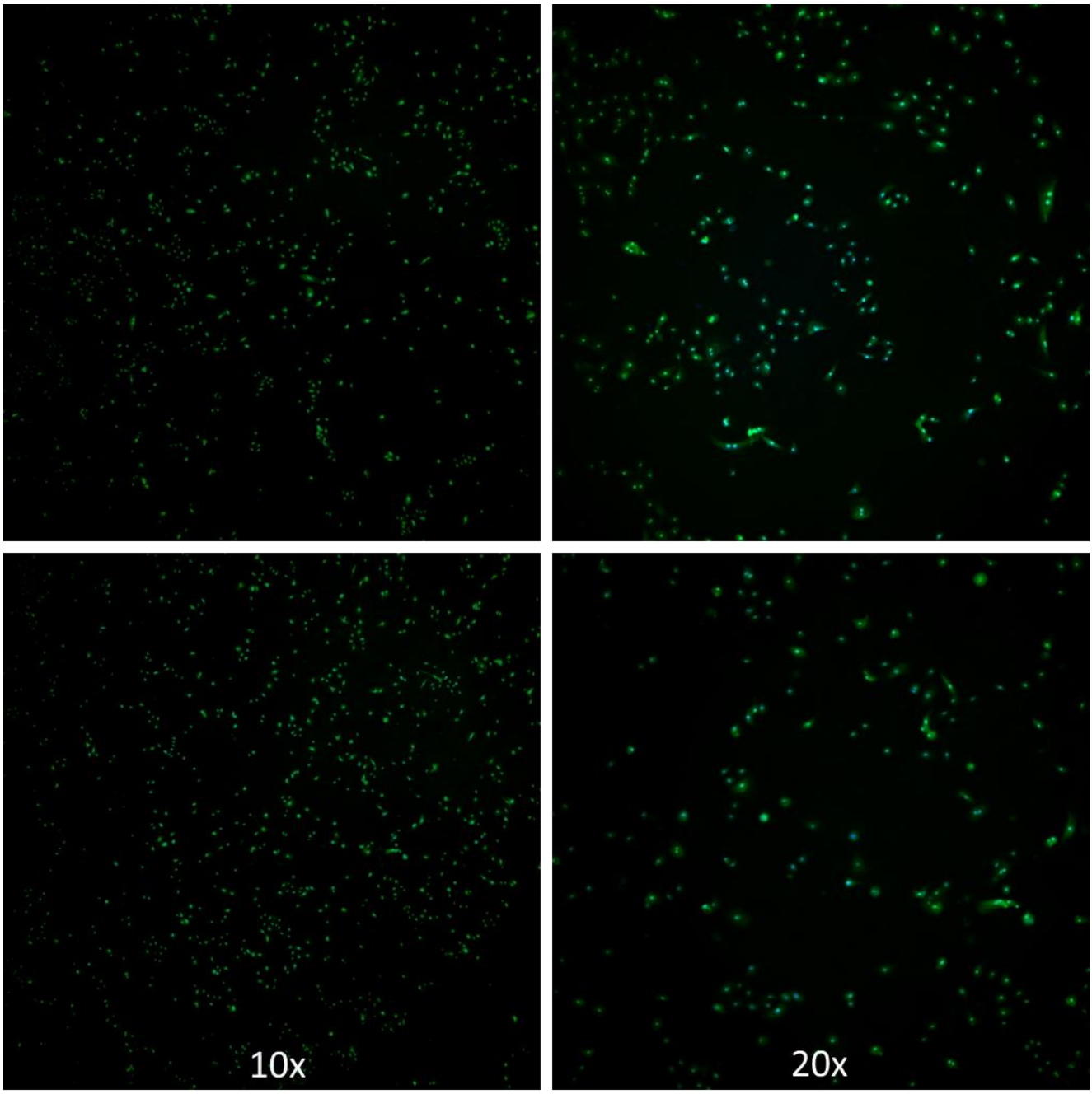

Figure 3.3B Keratinocytes transfected at an AON-PEI ratio of 1-0.75 in duplicate. 10x and 20x fluorescent microscopy image of keratinocytes transfected at an AON-PEI ration of 1-0.75. Green = fluorescently labelled AON, Blue = Bisbenzimide (Hoechst) nuclei staining.

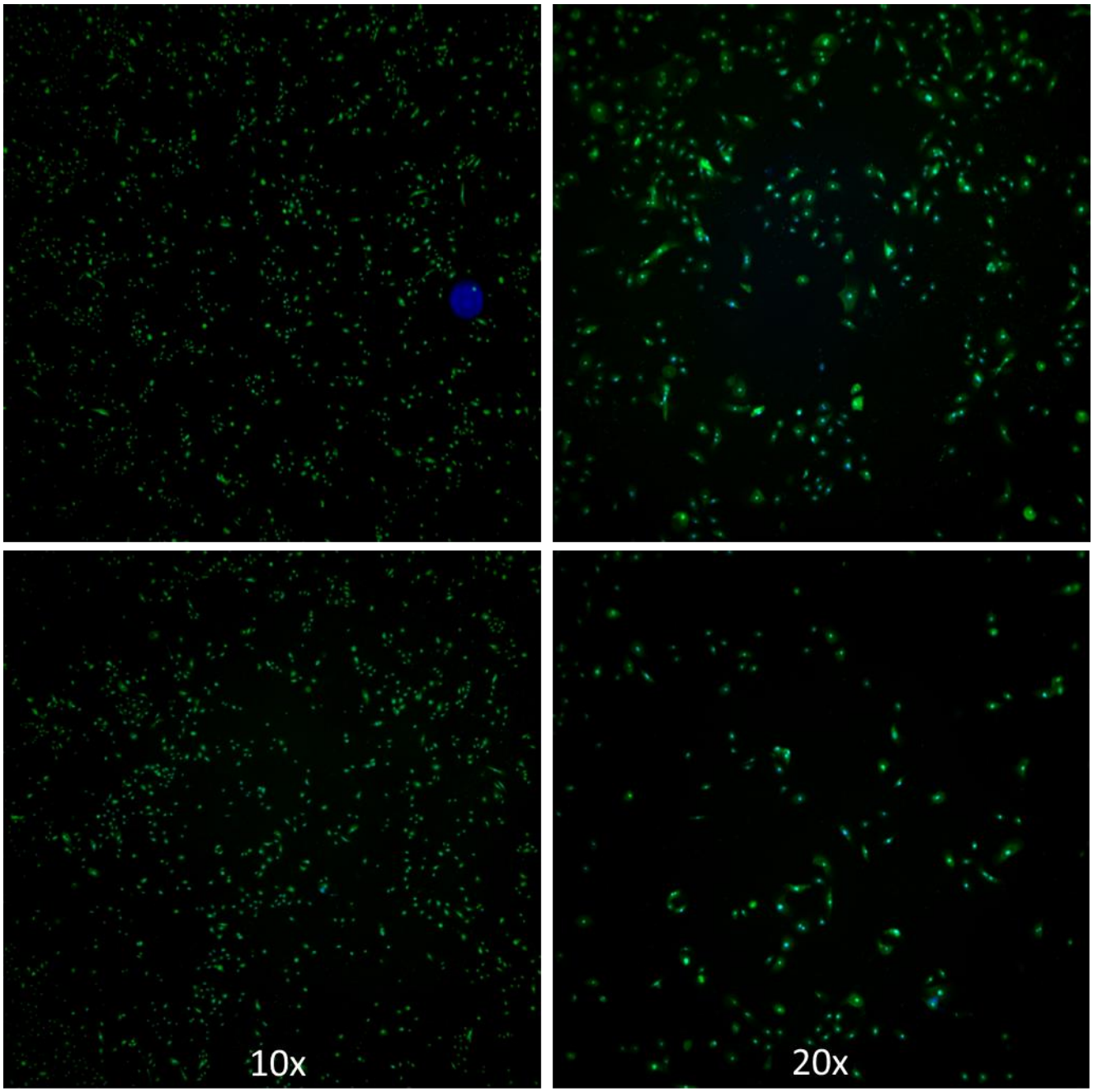

Figure 3.3C Keratinocytes transfected at an AON-Lipofectamine2000 ratio of 1-1 in duplicate. 10x and 20x fluorescent microscopy image of keratinocytes transfected at an AON-PEI ration of 1-1. Green = fluorescently labelled AON, Blue = Bisbenzimide (Hoechst) nuclei staining.

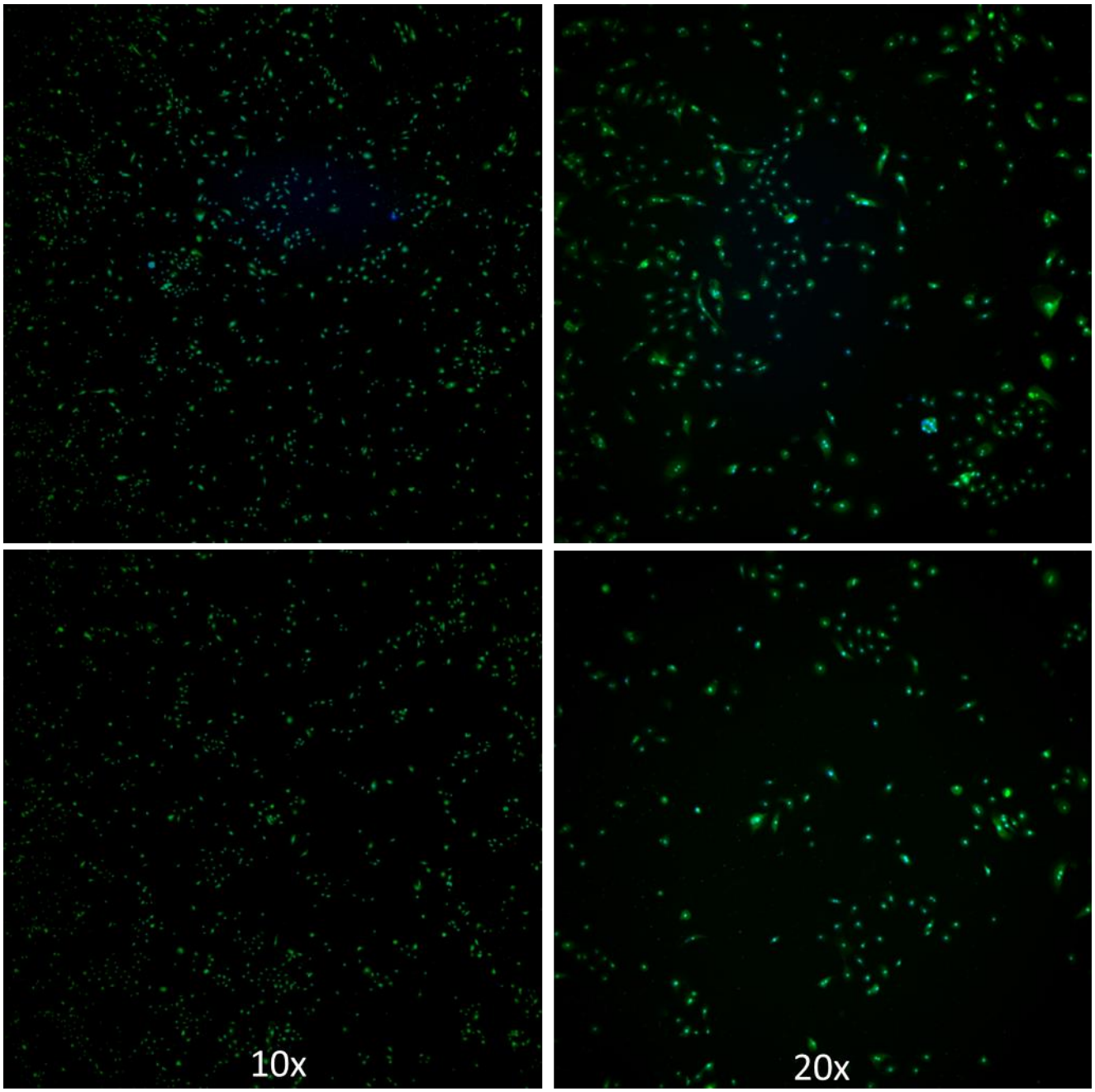

Figure 3.3C Keratinocytes transfected at an AON-Lipofectamine2000 ratio of 1-0.75 in duplicate. 10x and 20x fluorescent microscopy image of keratinocytes transfected at an AON-PEI ration of 1-0.75. Green = fluorescently labelled AON, Blue = Bisbenzimide (Hoechst) nuclei staining.

3.4 Transfection optimization 2: keratinocytes transfected with a combination of AONs specific for exon 105 at the optimized AON: transfection agent concentration.

Primary keratinocytes were transfected at the optimized AON: transfection agent ratios with a combination of two AONs specific for exon 105. Figure 3.4A shows the plating setup of transfection optimization 2. Table 3.4A shows the transfection mixtures that were added to the corresponding wells of the plating setup. Figure 3.4B and 3.4C both show successful transfection of an unspecific fluorescently labelled AON for both transfection agents at an AON: transfection agent concentration of 1:1. 24 hours after transfection, RNA was isolated from the wells and converted to cDNA. A subsequent nested PCR with primers covering exon 102-106 of C7, followed by gel electrophoresis of the nested PCR product, revealed a clear band at the predicted location of the exon skipped product for AON: Lipofectamine2000 ratios of 1:1 (figure 3.4D, LF1A & LF1B) and 1:0.75 (figure 3.4D, LF0.75A & LF0.75B). For keratinocytes transfected with PEI this was not the case, however, the AON: PEI ratio of 1:0.75 shows for 1 of the 2 PEI transfected keratinocytes (figure 3.4D, LF0.75A) a possible, slightly visible skipped product of the nested PCR on C7. Both the LFC as the PEI control show no clear exon skipping band, which is identical for keratinocytes transfected with the unspecific fluorescently labelled AON. Next, we performed a gel extraction on several bands of 1 lane containing a hypothesized exon skipped product (figure 3.4E, LF1A, indicated with a blue arrows), followed by subsequent subjection to Sanger sequencing. The sequencing result in figure 3.4F show the sequencing results of the lowest band indicated with a blue arrow. This band should contain the smallest and therefore hypothesized exon skipped product since smaller products migrate further across the gel. We observed exactly an 81 base-pair skip at the location of exon 105 when comparing the sequencing results of the lowest excised band to the wild-type mRNA sequence of C7, indicating exon 105 had been skipped out of the C7 protein successfully (Figure 3.4F). When comparing the sequencing results of the other excised bands, we observed for singular bands, two specific sequences being mixed up, indicating this excised band contained a heterogeneous product also called heteroduplex of two distinct products. One of these products being the larger wildtype C7 protein, and one of these products being the smaller C7 protein containing a skip for exon 105 (sequencing results not shown).

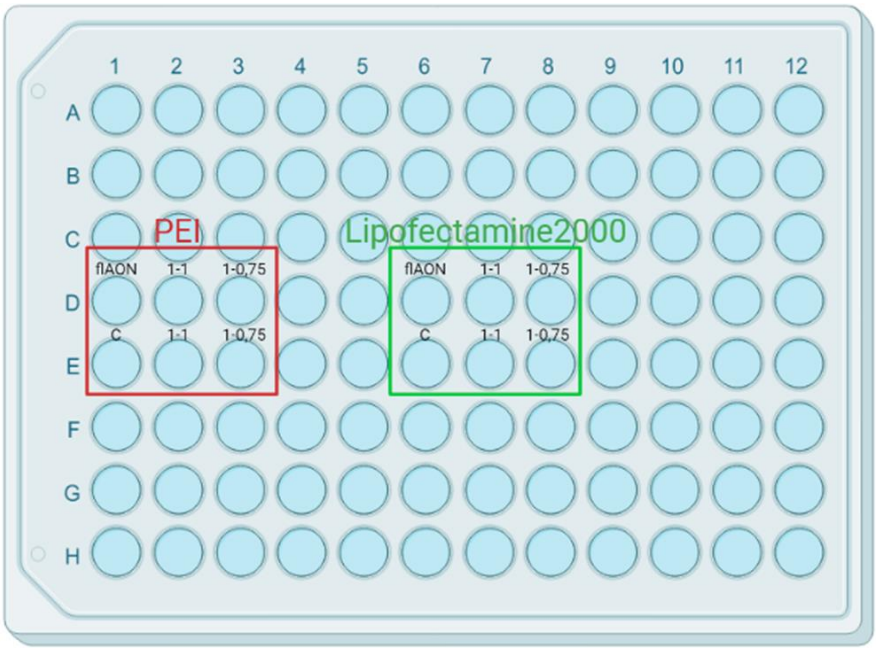

Figure 3.4A Plating setup transfection optimization 2. Plating setup of transfection optimization 2. Well transfected with PEI are encircled by a red box and wells transfected with Lipofectamine 2000 are encircled by a green box. flAON = fluorescently labelled unspecific AON, C = control, 1-1 and 1-0.75 are AON: transfection agent ratios for keratinocytes transfected with a mix of two AONs specific for exon 105.

Table 3.4A Transfection mixtures transfection optimization 2

Transfection mix 50 µl		seeding density 2.5*10^4 cells per well											
96		OptiMEM	AON (12.5	PEI	Total	AON/PEI			OptiMEM	AON (12.5µ	LPF20(	Total	AON/LPF2
flAON	D1	43,75	2,5	3,75	50	1,0/0,75	flAON	D6	44,5	2,5	3	50	1,0/0,75
mix AON	D2	42,5	2,5	5	50	1,0/1,0	mix AON	D7	43,5	2,5	4	50	1,0/1,0
mix AON	D3	43,75	2,5	3,75	50	1,0/0,75	mix AON	D8	44,5	2,5	3	50	1/0,75
control	E1	50	0	0	50	0/0	control	E6	44,5	2,5	3	50	1/0,75
mix AON	E2	42,5	2,5	5	50	1,0/1,0	mix AON	E7	43,5	2,5	4	50	1,0/1,0
mix AON	E3	43,75	2,5	3,75	50	1/0,75	mix AON	E8	44,5	2,5	3	50	1/0,75

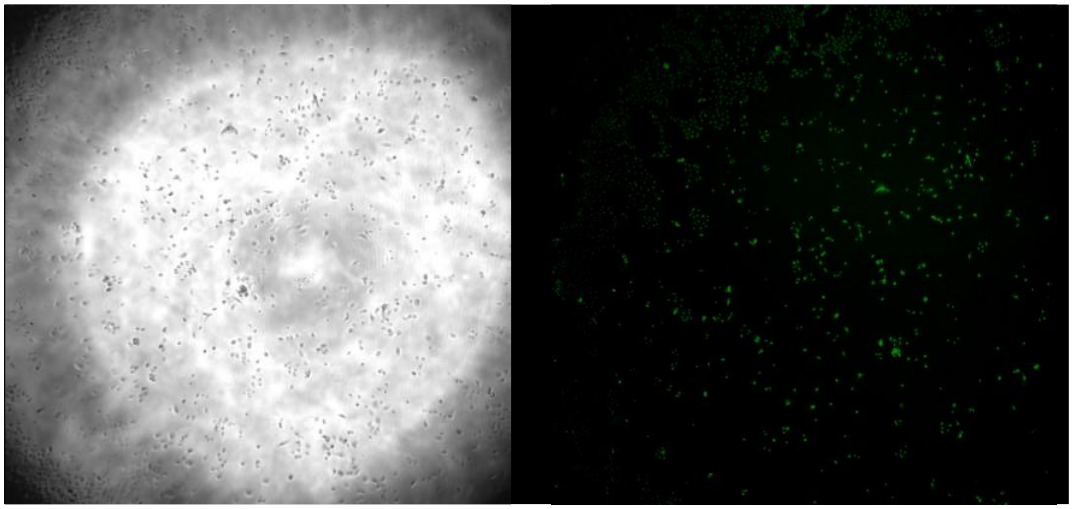

Figure 3.4B Keratinocytes transfected at an AON-PEI ratio of 1-1. 10x brightfield microscopy and 20x fluorescent microscopy image of keratinocytes transfected with an unspecific fluorescently labelled AON at an AON-PEI ration of 1-1. Green = fluorescently labelled AON

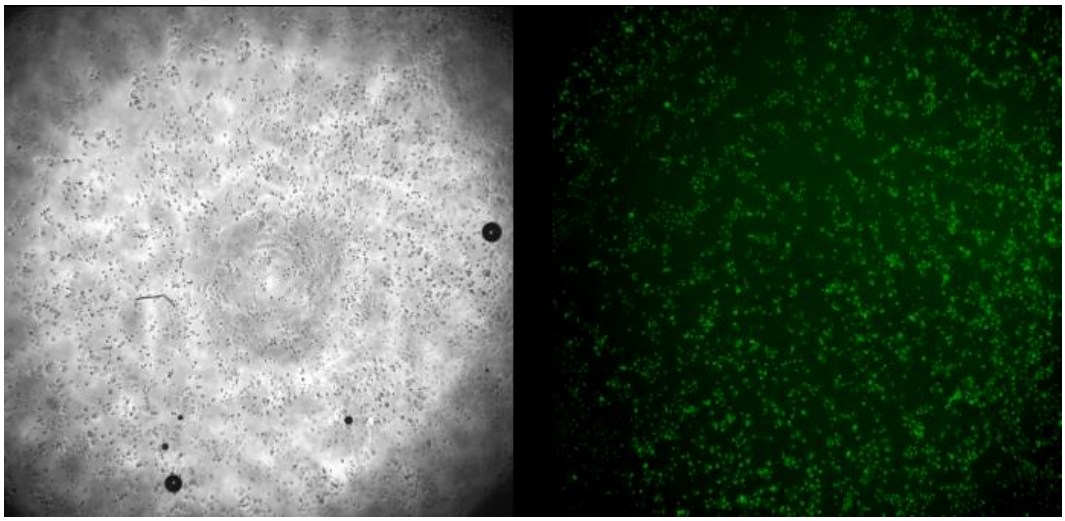

Figure 3.4C Keratinocytes transfected at an AON-Lipofectamine2000 ratio of 1-1. 10x brightfield microscopy and 20x fluorescent microscopy image of keratinocytes transfected with an unspecific fluorescently labelled AON at an AON-Lipofectamine ratio of 1-1. Green = fluorescently labelled AON

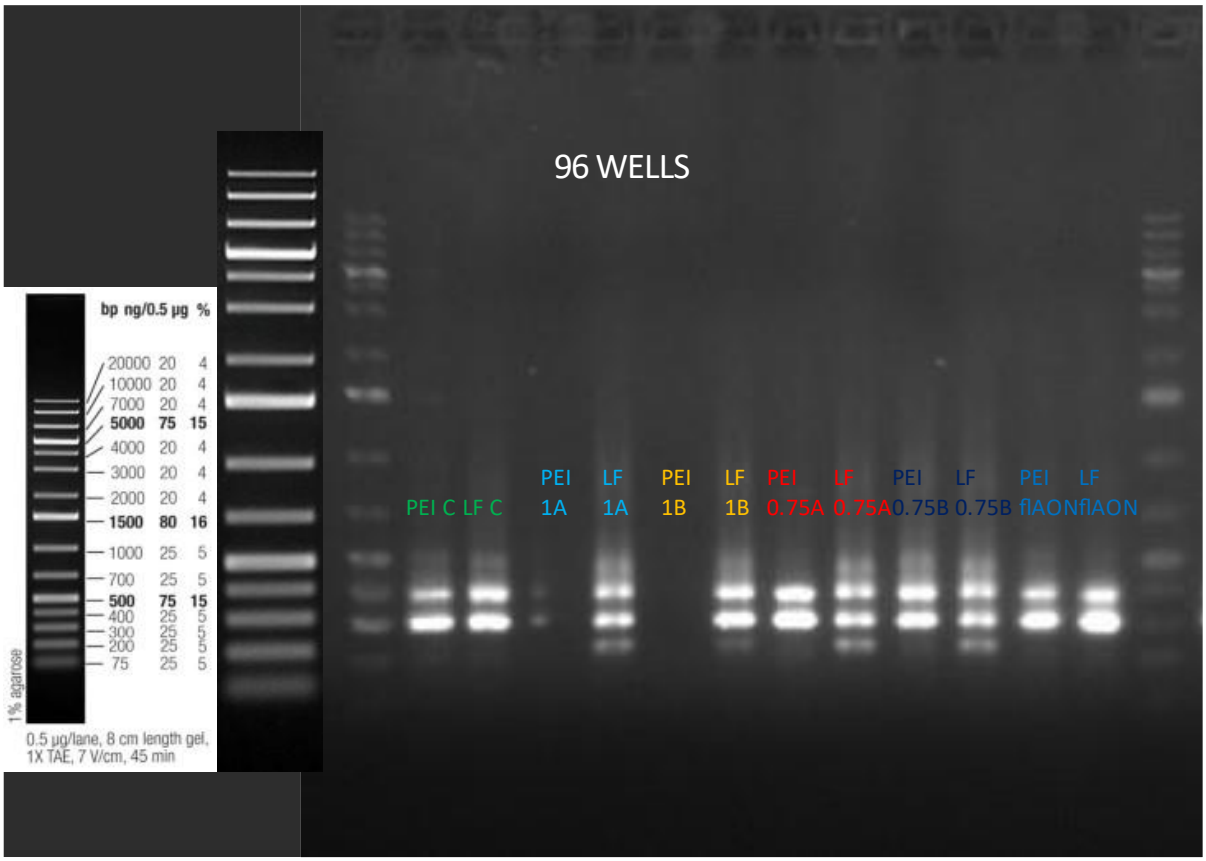

Figure 3.4D Gel electrophoresis of keratinocytes transfected with a mix of two AONs specific for exon 105 of the C7 gene. 1% agar TBE gel electrophoresis ran on the nested PCR product of keratinocytes transfected with a mix of two AONs specific for exon 105 (81 bp) at the optimal AON: transfection agent concentration. The first set of primers cover exon 100-108

(510bp) of the C7 gene. The nested primers cover exon 102-106 (289bp) of the C7 gene. LF = Lipofectamine2000, C = control and 1 or 0.75 = [AON]/[lipofectamine2000].

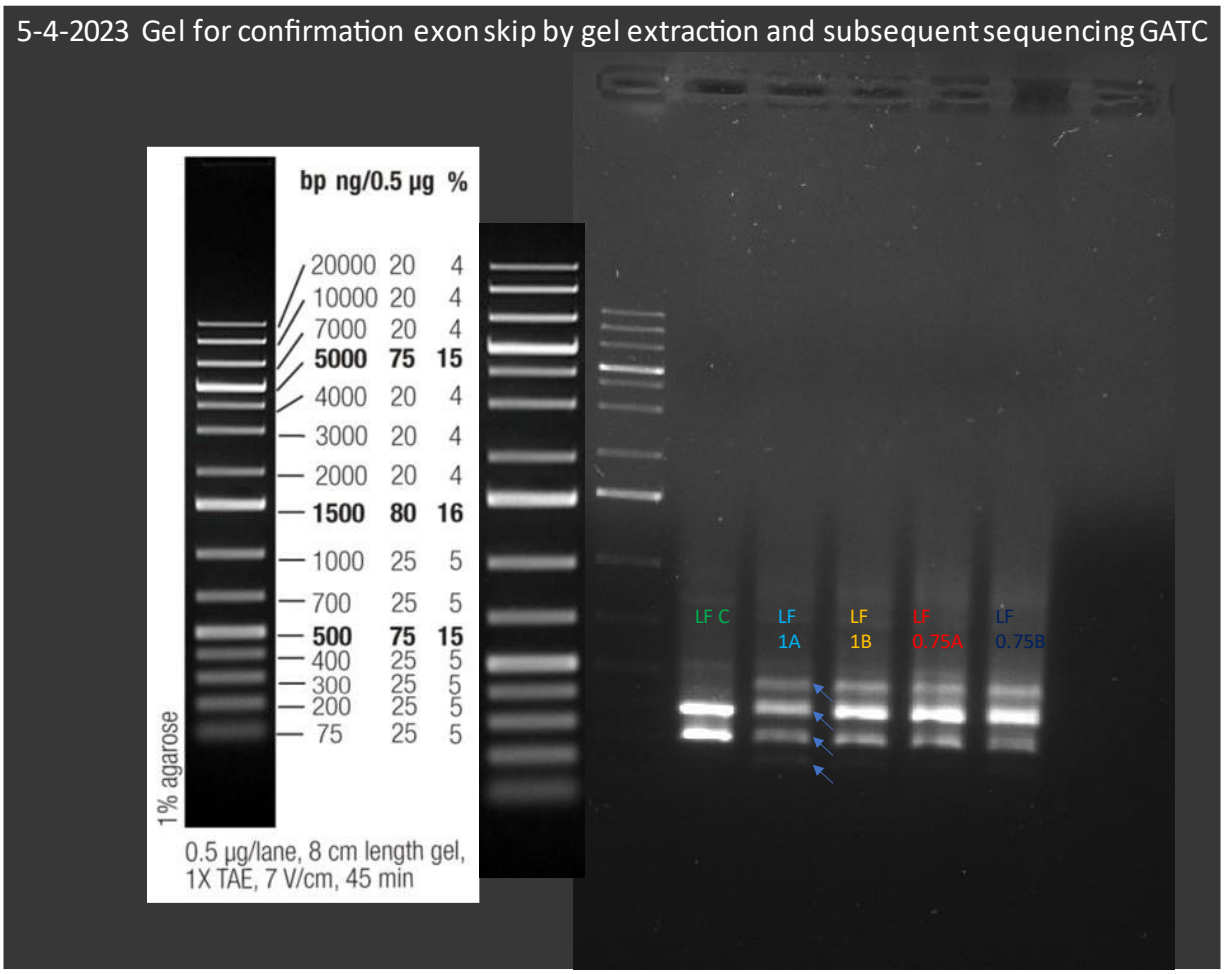

Figure 3.4E Gel electrophoresis of keratinocytes transfected with a mix of two AONs specific for exon 105 of the C7 gene. 1% agar TBE gel electrophoresis ran on the nested PCR product of keratinocytes transfected with a mix of two AONs specific for exon 105 (81 bp) at the optimal transfection agent: AON ratio. Bands indicated with an arrow have been subjected to gel extraction and subsequent Sanger sequencing. The first set of primers cover exon 100-108 (510bp) of the C7 gene. The nested primers cover exon 102-106 (289bp) of the C7 gene. LF = Lipofectamine2000, C = control and 1 or 0.75 = [AON]/[lipofectamine2000].

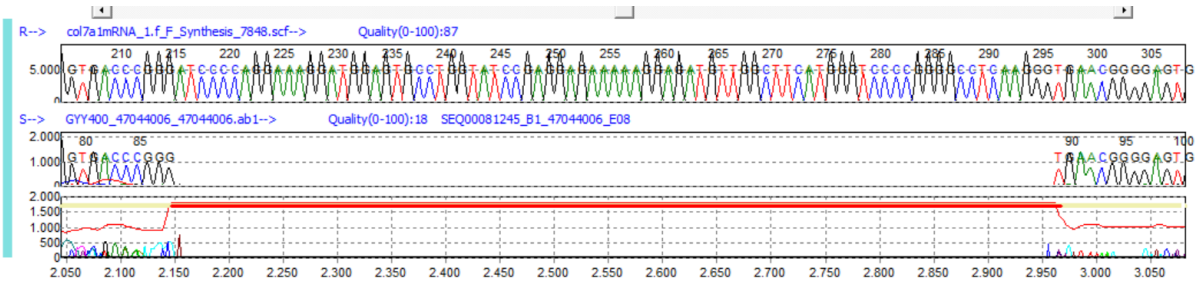

Figure 3.4F: Sanger sequencing of keratinocytes transfected with an AON specific for exon 105 of C7. Sanger sequencing of the band indicated in figure 2 by a red arrow, surrounded by

the red box. The upper sequence indicated by R--> shows an area surrounding exon 105 of the wildtype *COL7A1* mRNA sequence. The lower sequence indicated by S--> shows the same area of *COL7A1*, however here the gel extracted product of figure 2 was sequenced. The sequence indicated by S--> shows exactly a red line for the length of exon 105 in the *COL7A1* gene, indicating a skipped exon 105.

3.5 Oligowalk: keratinocytes transfected with 102 unique AONs targeting exon 105 of the C7 gene (n=3)

Primary keratinocytes of 3 distinct healthy donors were transfected with 102 unique AONs specific for exon 105 in our so called 'Oligowalk'. The principle of the Oligowalk has been visualized in figure 3.5A. This figure shows exon 105 and part of its flanking intronic sequences; intron 104 and intron 105. Across this whole sequence 20 nucleotides long 2'-O-MePS (2'-O-methyl phosphorothioate) AONs have been designed with each unique AON covering a different part of the sequence, by sliding across 1 nucleotide for every other unique AON sequence. An example of 5 of these consecutive AONs (18, 19, 20, 21, 22) is shown by the dark horizontal lines. 24 hours after transfection, RNA was isolated from the wells and converted to cDNA. A subsequent nested PCR with primers covering exon 102-106 of C7, followed by gel electrophoresis of the nested PCR product, revealed a clear band at the predicted location of the exon skipped product for several of the AONs transfected. An example of such clear bands can be observed in figure 3.5B Oligowalk 1 for keratinocytes transfected with AON 38, 39, 40, 41, 42. However, these exon skip bands only indicate some degree of exon skipping has occurred. The RT-PCR is not quantitative. Therefore, a RT-qPCR should be performed on the converted cDNA. This RT-qPCR will also capture any form of exon skipping masked by heteroduplex formation, quantifying exactly how much exon skipping every single unique AON induced.

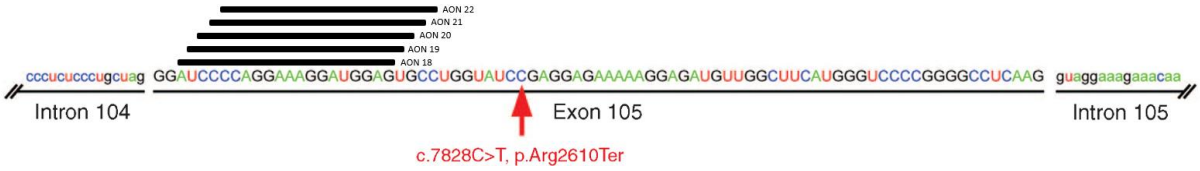

Figure 3.5A: C7 exon 105 and its flanking intronic sequences that are covered by the 102 unique AON sequences of the Oligowalk. Visualization of C7 exon 105 and its flanking intronic sequences, intron 104 and intron 105. The 102 unique AON sequences are directed against the sequence above, each covering a different part of the sequence, by sliding across 1 nucleotide for every other unique AON sequence. The red arrow indicates a known patient mutation.

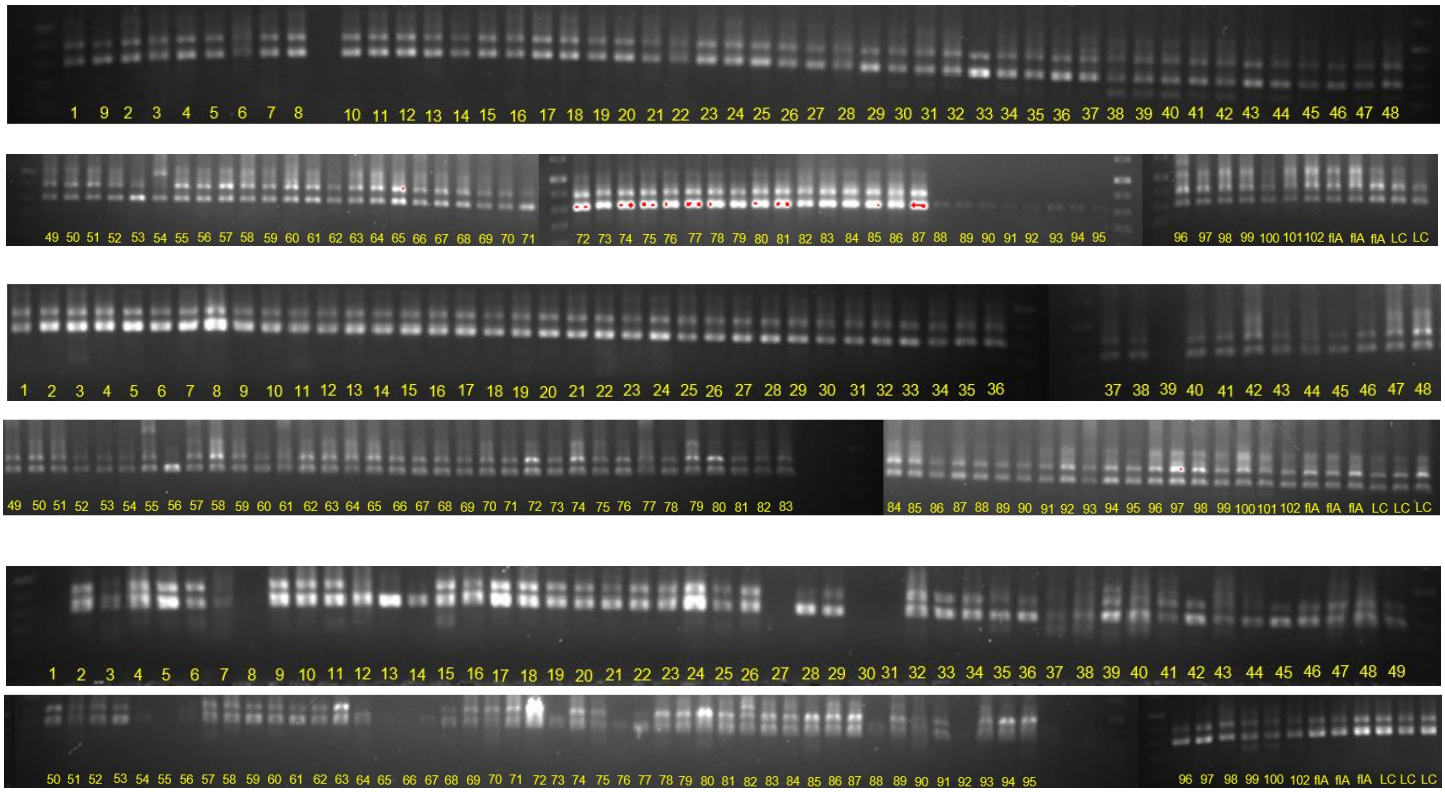

Figure 3.5B: Oligowalk: Multiple gel electrophoreses on keratinocytes transfected with 102 unique AONs targeting exon 105 of the C7 gene (n=3) Multiple 1 % agar TBE gel electrophoreses ran on the nested PCR product of keratinocytes transfected with 102 unique AON sequences specific for exon 105 of the C7 gene. The first set of primers cover exon 100-108 (510bp) of the C7 gene. The nested primers cover exon 102-106 (289bp) of the C7 gene. flA = unspecific fluorescently labelled AON, LC = lipofectamine control.

3.6 3D human skin models

3D skin models were cultured as described is section 2.8 of the materials and methods section. Fibroblasts were cultured in a standing or either hanging insert containing a membrane that allowed the passage of medium and nutrients, however cells could not pass through the membranes. Skin model Af + 1 [Fig. 3.6A] contained a standing insert with keratinocytes seeded one day after the fibroblasts and the culture medium contained fungizone. C4 staining in this model showed a linear pattern mimicking healthy human skin C4 expression, whereas C7 only showed a little granular pattern. DSG1 staining in this model is as good as absent, whereas DSG3 staining mimicked the intercellular pattern of healthy human skin. Skin model B + 1 [Fig. 3.6B] contained a standing insert with keratinocytes seeded one day after the fibroblasts, also the culture medium contained no anti-fungal product. C4 staining in this model showed a linear pattern mimicking healthy human skin C4 expression, whereas C7 only showed a little granular pattern. DSG1 staining in this model is as good as absent, whereas DSG3 staining mimicked the intercellular pattern of healthy human skin.

Skin model Cf + 3 [Fig. 3.6C] contained a standing insert with keratinocytes seeded three days after the fibroblasts and the culture medium contained fungizone. C4 staining in this model showed a mix between a granular and a linear staining pattern, whereas C7 staining only showed a granular staining pattern. DSG1 staining was hardly visible and DSG3 staining was mimicking healthy human skin, showing the regular intercellular deposition of DSG3. Skin model D + 3 [Fig 3.6D] contained a standing insert with keratinocytes seeded three days after the fibroblasts, also the culture medium contained no anti-fungal product. C4 and C7 staining in this model both showed a linear pattern lining the basement membrane, mimicking healthy human skin C4 and C7 expression. DSG1 staining in this model is hardy visible, whereas DSG3 staining mimicked the intercellular pattern of healthy human skin. Skin model Ef + 1 [Fig 3.6E] contained a hanging insert with keratinocytes seeded three days after the fibroblasts, culture medium containing fungizone and a PC membrane. The epidermis of this skin model completely ruptured during making cryosections of the model, therefore showing no good dermis epidermis connection. The staining for all proteins appeared to be present, however not mimicking healthy human skin, except for DSG3. DSG3 shows some resemblance to healthy human skin with its intercellular pattern. Skin model Ff + 1 [Fig 3.6F] contained a hanging insert with keratinocytes seeded three days after the fibroblasts, culture medium containing fungizone and a PET membrane. C4 staining in this model showed a mix between a granular and a linear staining pattern, whereas C7 staining only showed a granular staining pattern. DSG1 staining showed a faded, however recognizable pattern for DSG1, resembling healthy human skin. DSG3 staining showed a beautiful intercellular DSG3 deposition, mimicking healthy human skin.

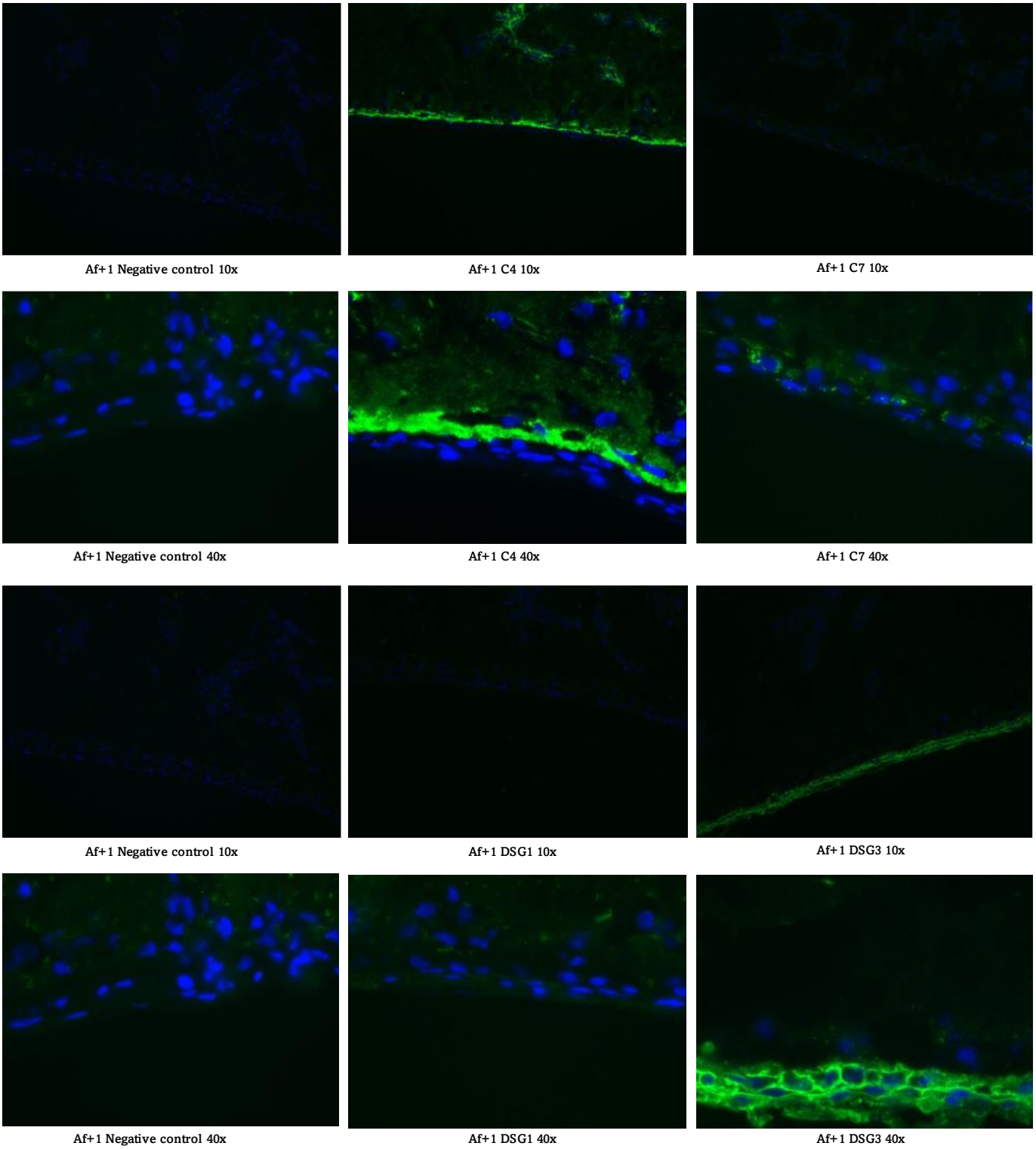

Figure 3.6A: Cryosections of standing skin model Af + 1 stained for C7, C4, DSG-3 and DSG-1. 10x and 40x fluorescent microscopy images of skin model Af + 1 cryosections stained for either C7, C4, DSG-3, or DSG-1 (green), all containing a bisbenzimide (Hoechst) nuclei staining (Blue). The f of Af = 1 indicates that the medium used for culturing the model contained fungizone. The + 1 indicates how many days after adding the collagen mix containing fibroblasts, keratinocytes were added to the insert.

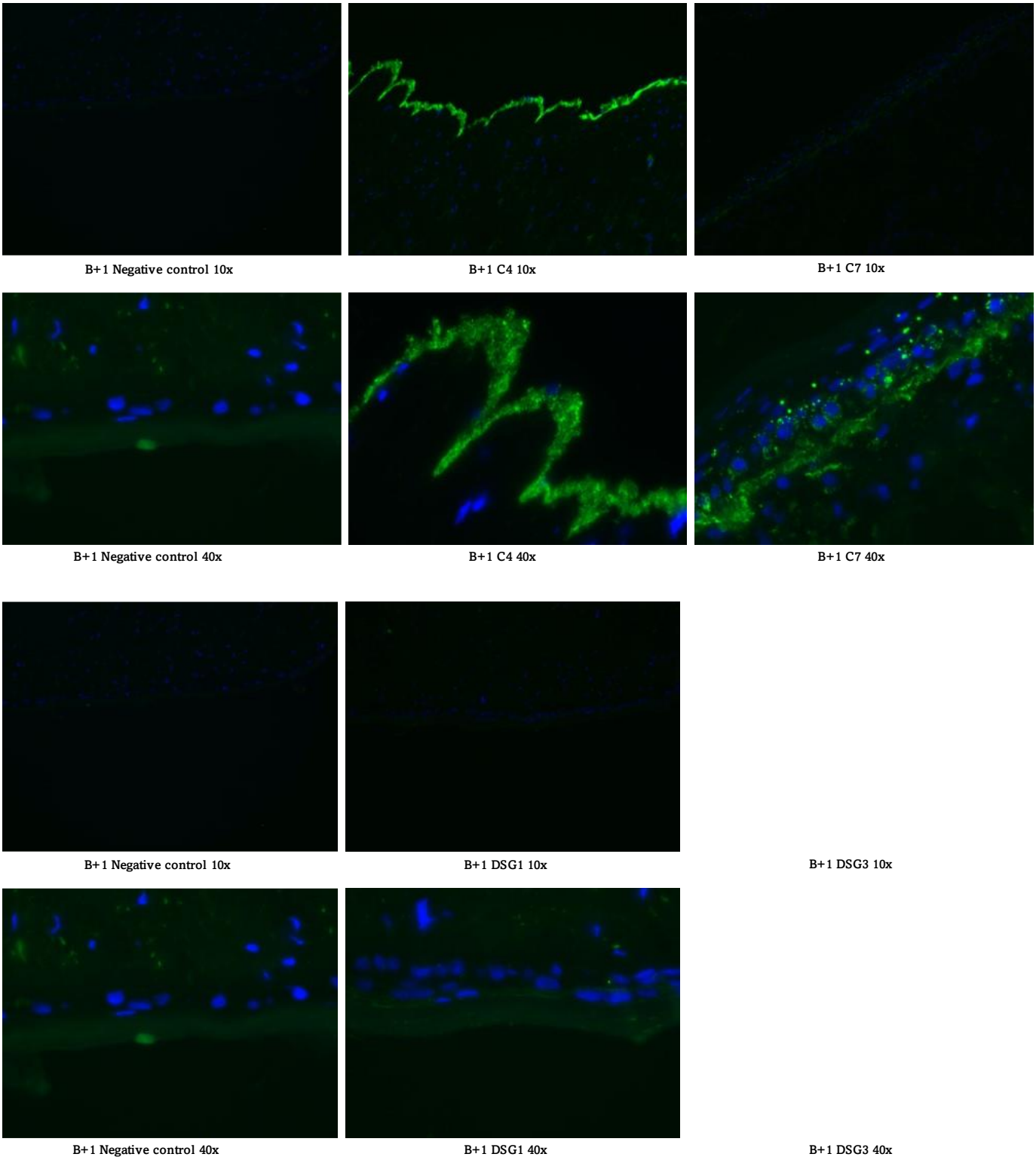

Figure 3.6B: Cryosections of standing skin model B + 1 stained for C7, C4 and DSG-1. 10x and 40x fluorescent microscopy images of skin model B + 1 cryosections stained for either C7, C4, or DSG-1 (green), all containing a bisbenzimide (Hoechst) nuclei staining (Blue). The + 1 indicates how many days after adding the collagen mix containing fibroblasts, keratinocytes were added to the insert.

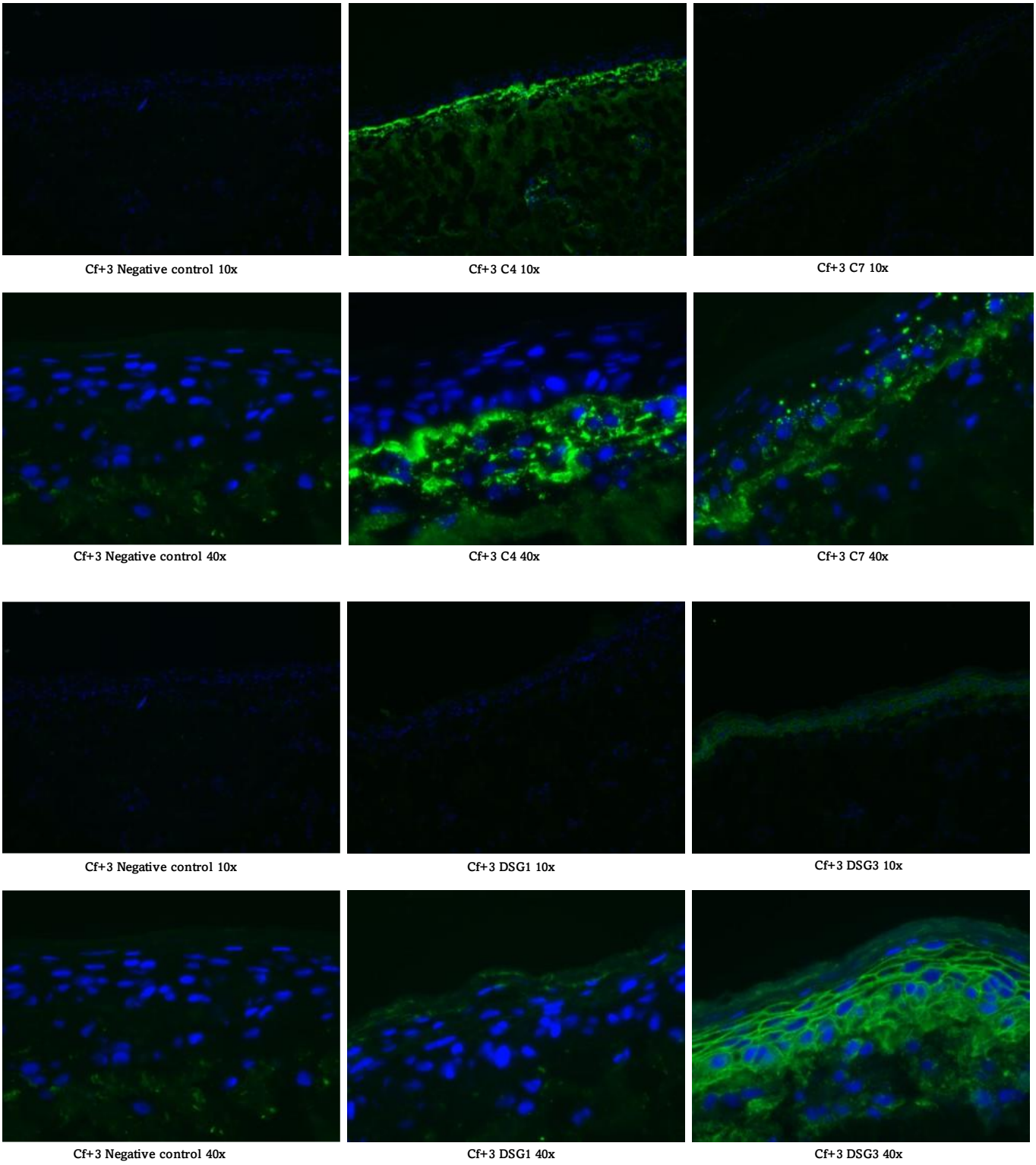

Figure 3.6C: Cryosections of standing skin model Cf + 3 stained for C7, C4, DSG-1 and DSG-3. 10x and 40x fluorescent microscopy images of skin model Cf + 3 cryosections stained for either C7, C4, DSG3 or DSG-1 (green), all containing a bisbenzimide (Hoechst) nuclei staining (Blue). The f of Cf indicates that the medium used for culturing the model contained fungizone. The + 3 indicates how many days after adding the collagen mix containing fibroblasts, keratinocytes were added to the insert.

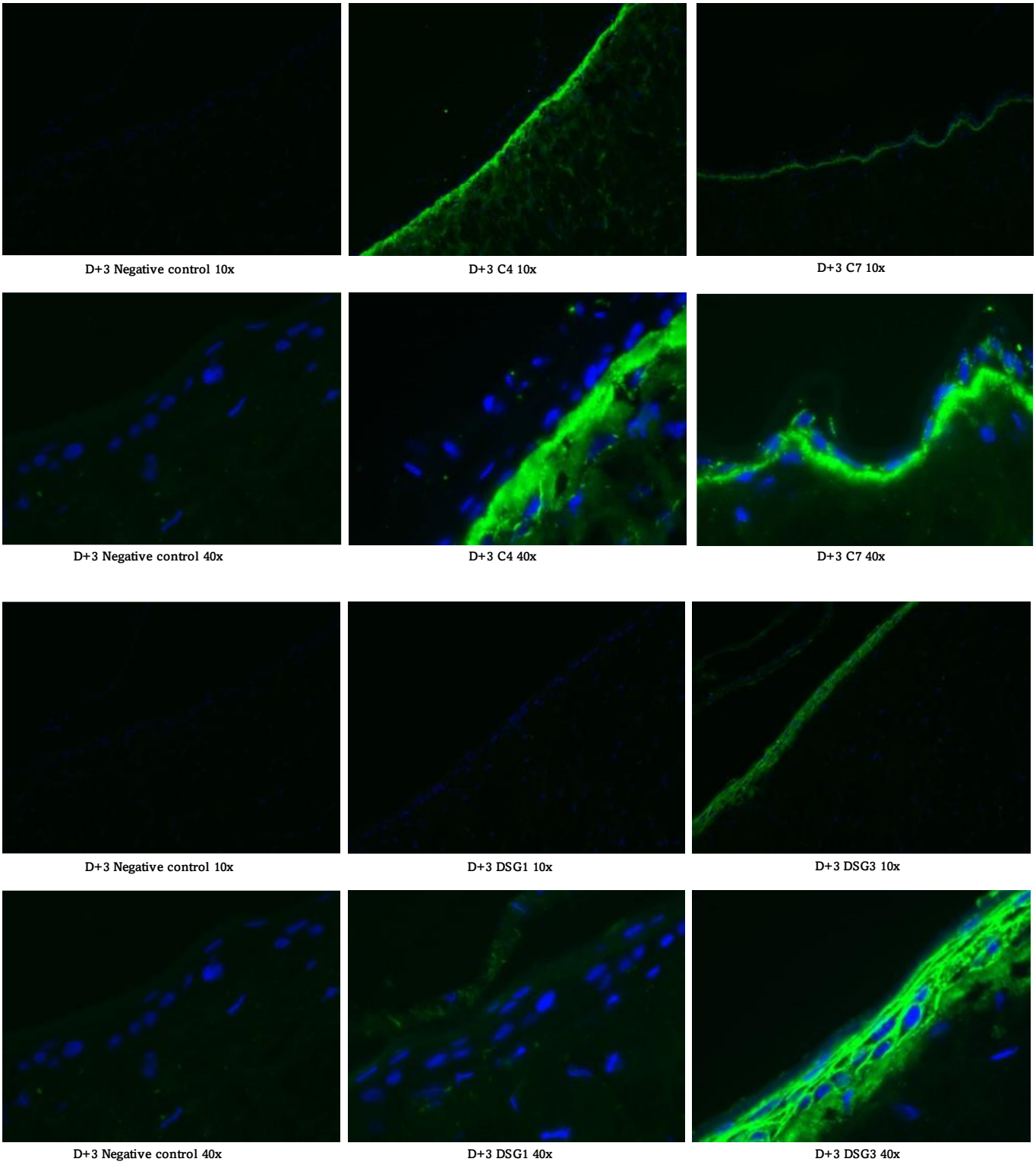

Figure 3.6D: Cryosections of standing skin model D + 3 stained for C7, C4, DSG-1 and DSG-3. 10x and 40x fluorescent microscopy images of skin model D + 3 cryosections stained for either C7, C4, DSG3 or DSG-1 (green), all containing a bisbenzimide (Hoechst) nuclei staining (Blue). The + 3 indicates how many days after adding the collagen mix containing fibroblasts, keratinocytes were added to the insert.

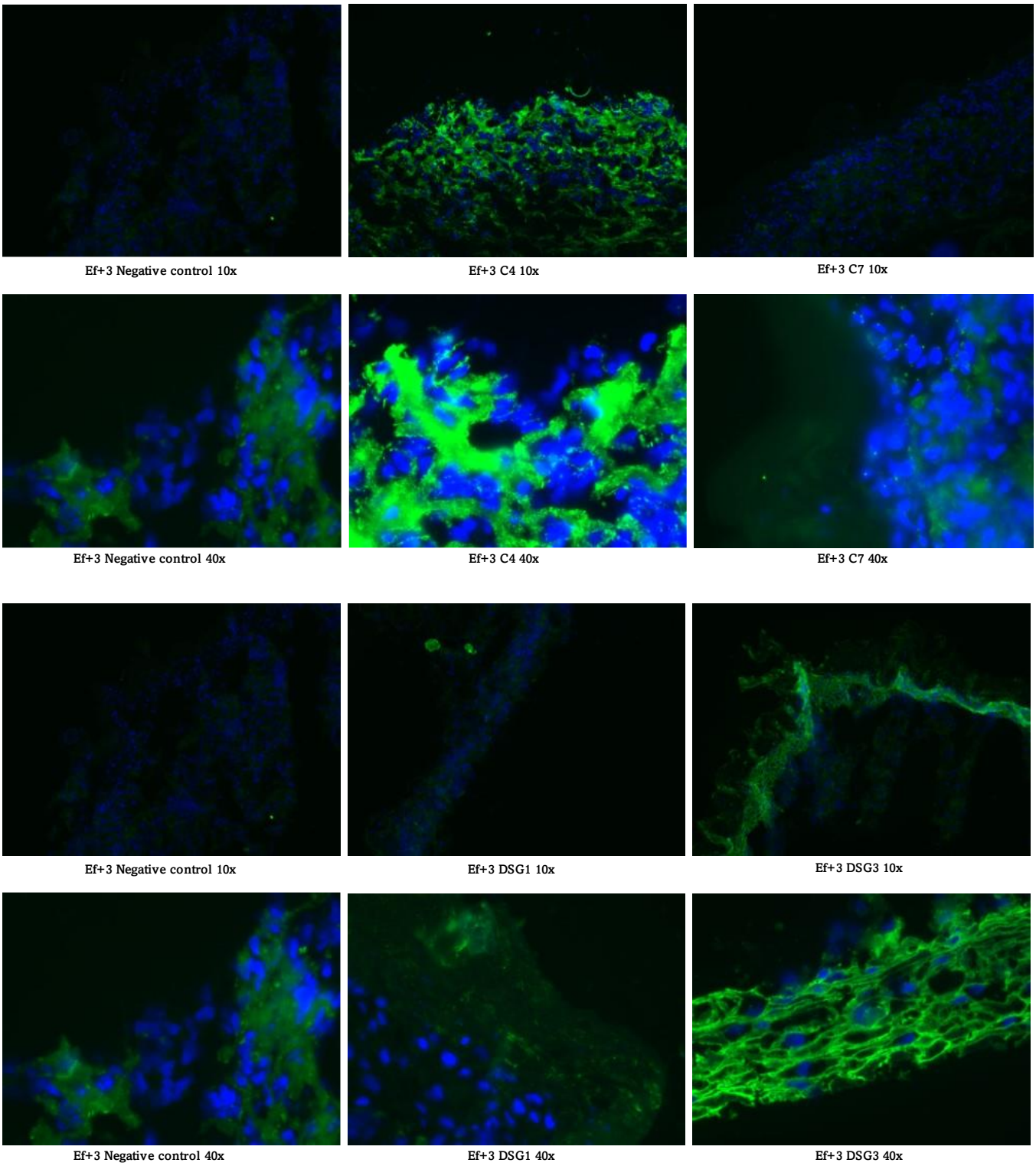

Figure 3.6E: Cryosections of hanging skin model Ef + 3 stained for C7, C4, DSG-1 and DSG-3. 10x and 40x fluorescent microscopy images of skin model Ef + 3 cryosections stained for either C7, C4, DSG3 or DSG-1 (green), all containing a bisbenzimide (Hoechst) nuclei staining (Blue). The f of Cf indicates that the medium used for culturing the model contained fungizone. The + 3 indicates how many days after adding the collagen mix containing fibroblasts, keratinocytes were added to the insert.

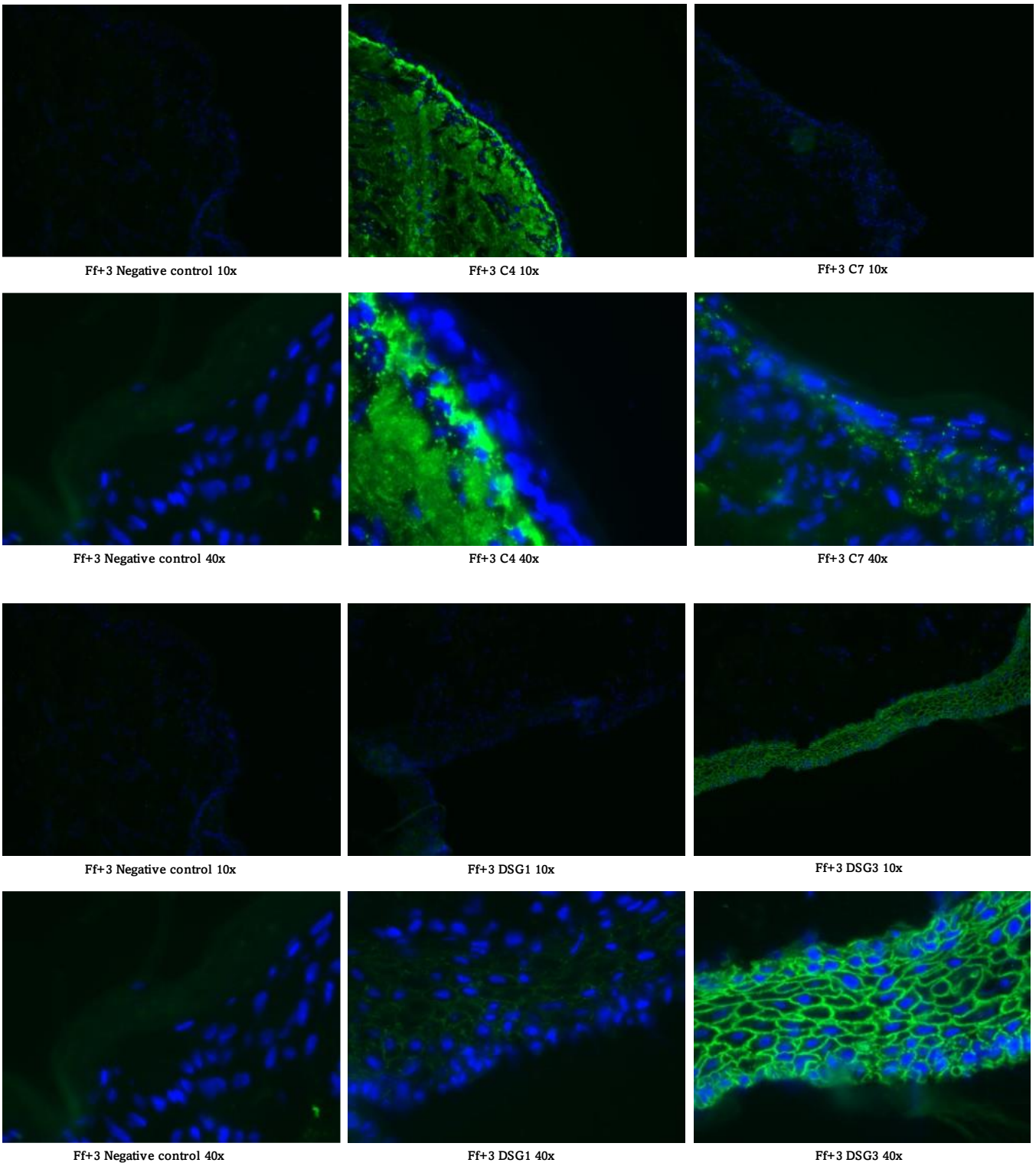

Figure 3.6F: Cryosections of hanging skin model Ff + 3 stained for C7, C4, DSG-1 and DSG-3. 10x and 40x fluorescent microscopy images of skin model Ff + 3 cryosections stained for either C7, C4, DSG3 or DSG-1 (green), all containing a bisbenzimide (Hoechst) nuclei staining (Blue). The f of Cf indicates that the medium used for culturing the model contained fungizone. The + 3 indicates how many days after adding the collagen mix containing fibroblasts, keratinocytes were added to the insert.

4. Discussion

Delivery of AONs *in vitro* is not generating a lot of issues, however, to get an AON *in vivo* to its target site at therapeutic window concentrations comes with many challenges. For AONs to reach the intercellular site of action they first have to make use of transcellular or paracellular transport to migrate across the capillary endothelium, migrate across the plasma membrane and escape the lysosomal machinery to not be degraded or exported via exocytosis. Additionally, naked AONs have a poor permeability at the plasma membrane and they lack stability in the extracellular environment (Gupta et al., 2023). Therefore, several chemical modifications have been developed as for instance modification of the ribose sugar moiety, as adding a phoshorothioate bond that is resistant to nuclease degradation, or modifying the base with a 2'-O-methoxyethyl-(2'-O-MOE) that improves binding affinity and resistance to enzymatic degradation, to improve bioavailability and delivery (Huang et al., 2022). Moreover, delivery of AONs is optimized by means of conjugation to several molecules including lipids, carbohydrates, aptamers, antibodies, peptides or using carrier-based systems as for instance lipid nanoparticles, liposomes, extracellular vesicles, exosomes, spherical nucleic acids and DNA nanostructures (Gupta et al., 2023; Huang et al., 2022). Here, our unique delivery method of AONs by means of conjugating AONs to a Fab fragment, created by pepsin digestion and subsequent reduction of an IgG molecule was investigated. Interestingly, antibody-AON conjugates in general have been studied before. Systemic administration of an AON conjugated to an antibody against murine transferrin receptor, 8D3130, in a spinal muscular atrophy mouse model, resulted in increased bioavailability of the AON in the brain. Moreover, it resulted in extended survival of a severely affected adult human survival motor neuron 2 (*SMN2*) transgenic mice by increasing the splicing of *SMN2* in their central nervous systems to therapeutic concentrations (Hammond et al., 2022). Furthermore, an AON conjugated to a CD22 antibody targeting MYC-associated factor X (*MAX*) dimerization protein 3 (*MXD3*), which appeared to be critical for precursor B-cell acute lymphoblastic leukemia (preB ALL) cell survival, resulted in protein knockdown and leukemic cell apoptosis *in vitro*. Additionally, the AON-antibody construct more than doubled survival time of xenograft Reh (median survival time 20.5 versus 42.5 d, $p < 0.001$) and primary preB ALL mouse model (median survival time 29.3 versus 63 d, $p < 0.001$) (Satake et al., 2016). Another AON conjugated to transferrin receptor 1 with an AON targeting myotonic dystrophy protein kinase (*DMPK*) was assessed for its activity in skeletal muscle of mice and compared to an unconjugated AON. The unconjugated AON required a 25x higher dose to achieve similar activity as the conjugated AON-construct (Malecova et al., 2023). These three examples show that antibody-AON conjugates can benefit delivery and bioavailability of AONs *in vivo* greatly, allowing lower concentrations of AONs to be administered, therefore lowering the chances at dose-related toxicity. Future *in vitro* experiments should optimize the concentration of our Fab-conjugated AON construct and it would be interesting to compare at an AON concentration of 250 nmol/l, transfection-based delivery of AONs with Fab-conjugated delivery of AONs.

This report can be divided into two separate sections; one being the optimization of delivery of therapeutic antisense oligonucleotides for exon skip therapy in EB and the second being the development of a human skin model to serve as a null-model or replacement model for human skin in EB research.

For the optimization of delivery of therapeutic AONs for exon skip therapy in EB, we have performed several experiments to optimize delivery of our flAON-Fab conjugate. These experiments included incubating differentiated primary keratinocytes and 6 mm biopsies with our conjugated AON construct. We have observed that the flAON-Fab conjugate binds, internalizes and becomes distributed intracellularly in differentiated primary keratinocytes when incubating them together for 24 hours. The concentration of the 2-MEA played an important role. The conjugated AON construct reduced at a 2-MEA concentration of 1 and 3 mM showed clear binding, internalization and intracellular distribution, whereas the conjugated AON construct of 10 mM did not. Although, we did not see any presumable exon skip band, when performing a gel electrophoresis. We hypothesized that the concentration of the conjugated AON construct was too low when compared to the transfected AONs or that the incubation time was not long enough. However, there is a slight possibility exon skipping was masked by heteroduplex formation between wildtype and skipped C7. Therefore, RT-qPCR should be performed to confirm our findings. For the 6 mm biopsies, we observed hardly any binding or internalization when incubating them with our conjugated AON construct for 48 hours. This is most likely caused by the same issue regarding the conjugated AON concentration. Following conjugations and incubation experiments should be performed using higher concentrations of the conjugated AONs.

Furthermore, we sought the most effective exon skipping 20 nucleotide long AON sequence for C7 exon 105, by optimizing lipofectamine2000 transfection of AONs in 96-well plates and performing an 'Oligowalk' in which we transfected 102 unique AON sequences targeting C7 exon 105. We found that several of the 102 unique AONs can induce exon skipping, verified by gel electrophoresis. However, also gel lanes showing no exon skipping band could contain skipped product masked by heteroduplex formation (Ogino et al., 2001). Therefore, a RT-qPCR will be performed to quantify exactly which AON sequence induces the highest level of exon skipping, in future experiments. It is highly likely that the AON sequences also producing the predicted exon skipping band are the most effective AON sequences. This already illustrates how important the AON sequence can be. Another study highlights this as well by showing that there is a difference in the number intracellular vesicles between N-acetyl galactosamine conjugated AONs only varying in sequence in treated renal proximal tubule epithelial cells. Interestingly, naked AONs and the N-acetyl galactosamine conjugated AONs co-localize in cytoplasmic vesicles of renal proximal tubule epithelial cells, suggesting similar intracellular processing paths (Sewing et al., 2019). It would be interesting to see whether this is also the case for Fab-conjugated constructs and whether the AON sequence could influence the number of intercellular vesicles and whether this correlates with the exon skipping efficiency. Currently, it is hypothesized that AONs are processed by two distinct endocytic routes. One is a non-productive route, where the AON accumulates and gets degraded in de lysozyme. The other is a productive route that results in nuclear trafficking and regulation of the targeted RNA. Interestingly, after treating differentiated myotubes with two different AONs, CAG7-OMePS and DMD23-OMePS, and adding chloroquine, a molecule that enhances endocytic release, it resulted in increased activity of both AONs, confirmed by a switch from a vesicular staining pattern to a nuclear staining pattern (González-Barriga et al., 2017). It would be interesting to investigate whether AON sequences that appear to be more effective at

inducing exon skipping, also increase in effectivity at a higher fold when adding a compound as chloroquine, compared to an AON that appears to be less effective at inducing exon skipping quantified by RT-qPCR. This might suggest that the specific AON sequence is of importance for endocytic release.

Lastly, we optimized our 3D skin equivalent culturing methods. We have cultured with a variety of variables like the type and size of the transmembrane insert (standing or hanging), the timing of adding the keratinocytes to the culture (1 or 3 days after adding the fibroblasts), the inclusion of anti-fungal products (with or without fungizone) and the type of membrane (standing: Millicel 0.4 µm and hanging: Brand 0.4 µm PC and 0.4 µm PET). We observed that the standing inserts did better at expressing C7 compared to the hanging inserts. C4 seemed to be similar between the standing and hanging models. However, the hanging inserts expressed DSG1 and DSG3 to a much greater extend compared to the standing inserts. Moreover, we observed that adding keratinocytes 3 days after adding the fibroblasts containing collagen mix resulted in skin models that resembled healthy human skin to a higher degree compared to skin models in which the keratinocytes were added 1 day after the fibroblast containing collagen mix. The number of days keratinocytes are seeded on the dermal scaffold still varies in literature. A recent review article, published as of March 2023, by Hoffman et al., states that keratinocytes are seeded after culturing the dermal scaffold a few days to a week (Hofmann et al., 2023). However, a recent article on *in vitro* 3D innervated skin models already adds keratinocytes after culturing the dermal scaffold for 24 hours (Rousi et al., 2022). This might indicate that there is still room for improvement regarding optimizing 3D skin models by tweaking culturing condition as indicated above. Furthermore, it seems that the standing skin models that skin models cultured without fungizone resembled healthy human skin to a higher degree when comparing them for C4, C7, DGS1 and DS3 staining. Interestingly, a paper by Nygaard et al., states that antibiotics should be omitted for culturing of conventional submerged cultures and 3D human epidermal equivalents (Nygaard et al., 2015). However, there is no data on the effects of fungizone (amphotericin B) on 3D skin models. It has been shown, however, that amphotericin B can affect proliferation and protein synthesis in human skin fibroblast cultures and that it can alter fibroblast lipid metabolism (Fujimoto et al., 1978; Levy et al., 1985). This could potentially explain some of the differences between our skin models cultured with or without fungizone. Lastly, amongst the hanging skin models, the morphology of the skin model containing a Brand 0.4 µm PET membrane (Ff + 3) resembled human skin to a much higher extend compared to the skin model containing a Brand 0.4 µm PC membrane (Ef + 3). However, making a cryosection of these skin models can be quite a challenge as the membrane deforms when cut, which might be the reason for skin model Ef + 3 not having a morphology representing healthy skin. Future skin models will also be subjected to electron microscopy to compare the ultrastructure of the basement membrane zone with healthy human skin similar as performed by Reijnders et al. (Reijnders et al., 2015).

5. Conclusions

The delivery of therapeutic AONs for exon skipping in EB depends on numerous factors. In this report we have optimized two of these factors being: (1) the method of delivery, by conjugating an AON to a Fab fragment and (2) the AON sequence for C7 exon 105. Additionally, we have cultured a variety of skin models varying based on the type of insert (hanging or standing), the medium composition (with or without fungizone), the number of days keratinocytes were added to the culture (after 1 or 3 days) and the type of membrane (Millicel 0.4 µm, Brand 0.4 µm PC and Brand 0.4 µm). From the experiments performed regarding these research objectives we can conclude that:

- Several of the 102 unique AON sequences have showed, in our 'Oligowalk', where we did a transfection analysis of 102 unique AONs in primary keratinocytes of 3 unique donors, clear exon skipping on agarose gel. Clear bands were mostly observed for keratinocytes transfected with AON 38, 39, 40, 41 and 42. AONs around 100 deserve to be noted as well.
- Our flAON-Fab conjugate showed clear cellular binding, internalization and distribution, confirmed by fluorescent microscopy.
- Lipofectamine2000 mediated transfection of naked AONs seems to be superior to PEI mediated transfection at inducing exon skipping in primary keratinocytes *in vitro*. Although, PEI mediated transfection was observed to be less harmful to the cells.
- Skin models cultured in standing inserts did better at expressing C7 compared to skin models cultured in hanging inserts. C4 seemed to be similar between the standing and hanging models. Hanging skin models did better at expressing DSG1 and DSG3 compared to standing skin models.
- Skin models in which keratinocytes were added 3 days after the fibroblasts containing collagen mix, resulted in skin models that resembled healthy human skin to a higher extend compared to skin models in which keratinocytes were added 1 day after the fibroblast containing collagen mix.
- Skin models cultured without fungizone resembled healthy human skin to a higher degree when comparing them for C4, C7, DGS1 and DSG3 staining.
- Amongst the hanging skin models, the morphology of the skin model containing a Brand 0.4 µm PET membrane (Ff + 3) resembled human skin to a much higher degree compared to the skin model containing a Brand 0.4 µm PC membrane.

6. Future perspectives

While the current data only provides confirmation that we accomplished exon skipping for several of the 102 unique AONs transfected, a future RT-qPCR should quantify exactly how much exon skipping has occurred, also considering exon skipping masked by heteroduplex formation. Additionally, to showing cellular binding, internalization and distribution of our Fab-conjugated AON construct, we will perform a functional assay to investigate if our Fab-conjugated AON construct can induce exon skipping and if so, quantify the amount of exon skipping by RT-qPCR. Lastly, we will improve our 3D human skin models by building on the data presented in this report and implement this model in future research.

7. References

1. Bardhan, A., Bruckner-Tuderman, L., Chapple, I. L. C., Fine, J., Harper, N., Has, C., Magin, T. M., Marinkovich, M. P., Marshall, J., McGrath, J. J., Mellerio, J. E., Polson, R., & Heagerty, A. (2020). Epidermolysis bullosa. Nature Reviews Disease Primers, 6(1). https://doi.org/10.1038/s41572-020-0210-0
2. Bornert, O., Kühl, T., Bremer, J., Van Den Akker, P. C., Pasmooij, A. M., & Nyström, A. (2016). Analysis of the functional consequences of targeted exon deletion in COL7A1 reveals prospects for dystrophic epidermolysis bullosa therapy. Molecular Therapy, 24(7), 1302–1311. https://doi.org/10.1038/mt.2016.92
3. Bremer, J., Bornert, O., Nyström, A., Gostyński, A., Jonkman, M. F., Aartsma-Rus, A., Van Den Akker, P. C., & Pasmooij, A. M. (2016). Antisense Oligonucleotide-mediated Exon Skipping as a Systemic Therapeutic Approach for Recessive Dystrophic Epidermolysis Bullosa. Molecular Therapy. Nucleic Acids, 5(10), e379. https://doi.org/10.1038/mtna.2016.87
4. Castle Creek Biosciences, Inc. (2022, June 29). Castle Creek Biosciences: D-Fi Gene Therapy. https://castlecreekbio.com/pipeline/gene-therapy-dystrophic-epidermolysis-bullosa/
5. Chen, M., Keene, D. R., Costa, F., Tahk, S., & Woodley, D. T. (2001). The Carboxyl Terminus of Type VII Collagen Mediates Antiparallel Dimer Formation and Constitutes a New Antigenic Epitope for Epidermolysis Bullosa Acquisita Autoantibodies. Journal of Biological Chemistry, 276(24), 21649–21655. https://doi.org/10.1074/jbc.m100180200
6. Chen, M., Marinkovich, M. P., Veis, A., Cai, X., Rao, C. N., O'Toole, E. A., & Woodley, D. T. (1997). Interactions of the Amino-terminal Noncollagenous (NC1) Domain of Type VII Collagen with Extracellular Matrix Components. Journal of Biological Chemistry, 272(23), 14516–14522. https://doi.org/10.1074/jbc.272.23.14516
7. Christiano, A. M., Hoffman, G., Chung-Honet, L. C., Lee, S., Cheng, W., Uitto, J., & Greenspan, D. S. (1994). Structural Organization of the Human Type VII Collagen Gene (COL7A1), Composed of More Exons Than Any Previously Characterized Gene. Genomics, 21(1), 169–179. https://doi.org/10.1006/geno.1994.1239
8. Colombo, M., Brittingham, R., Klement, J. D., Majsterek, I., Birk, D. E., Uitto, J., & Fertala, A. (2003). Procollagen VII Self-Assembly Depends on Site-Specific Interactions and Is Promoted by Cleavage of the NC2 Domain with Procollagen C-Proteinase. Biochemistry, 42(39), 11434–11442. https://doi.org/10.1021/bi034925d
9. Dieringer, H., Hollister, D. W., Glanville, R. W., Sakai, L. Y., & Kühn, K. (1985). Structural studies of human basement-membrane collagen with the use of a monoclonal antibody. Biochemical Journal, 227(1), 217–222. https://doi.org/10.1042/bj2270217
10. Dzierlega, K., & Yokota, T. (2020). Optimization of antisense-mediated exon skipping for Duchenne muscular dystrophy. Gene Therapy, 27(9), 407–416. https://doi.org/10.1038/s41434-020-0156-6
11. Egli, M., & Manoharan, M. (2023). Chemistry, structure and function of approved oligonucleotide therapeutics. Nucleic Acids Research, 51(6), 2529–2573. https://doi.org/10.1093/nar/gkad067
12. Fujimoto, W. Y., Starman, B. J., & Rowe, D. (1978). The effect of amphotericin b-deoxycholate on proliferation and protein synthesis in human skin fibroblast cultures. In Vitro, 14(12), 1003–1009. https://doi.org/10.1007/bf02616214
13. González-Barriga, A., Nillessen, B., Kranzen, J., Van Kessel, I. D., Croes, H., Aguilera, B., De Visser, P. C., Datson, N. A., Mulders, S. a. M., Van Deutekom, J. C., Wieringa, B., & Wansink, D. G. (2017). Intracellular Distribution and Nuclear Activity of Antisense Oligonucleotides

After Unassisted Uptake in Myoblasts and Differentiated MyotubesIn Vitro. Nucleic Acid Therapeutics, 27(3), 144–158. https://doi.org/10.1089/nat.2016.0641
14. Gupta, R., Salave, S., Rana, D., Karunakaran, B., Butreddy, A., Benival, D., & Kommineni, N. (2023). Versatility of Liposomes for Antisense Oligonucleotide Delivery: A Special Focus on Various Therapeutic Areas. PubMed, 15(5). https://doi.org/10.3390/pharmaceutics15051435
15. Hammond, S. M., Abendroth, F., Goli, L., Stoodley, J., Burrell, M., Thom, G., Gurrell, I., Ahlskog, N., Gait, M. J., Wood, M. J., & Webster, C. D. (2022). Antibody-oligonucleotide conjugate achieves CNS delivery in animal models for spinal muscular atrophy. JCI Insight, 7(24). https://doi.org/10.1172/jci.insight.154142
16. Has, C., Bauer, J. M., Bodemer, C., Bolling, M. C., Bruckner-Tuderman, L., Diem, A., Fine, J., Heagerty, A. M., Hovnanian, A., Marinkovich, M. P., Martinez, A. J., McGrath, J. J., Moss, C. W., Murrell, D. F., Palisson, F., Schwieger-Briel, A., Sprecher, E., Tamai, K., Uitto, J., . . . Mellerio, J. E. (2020). Consensus reclassification of inherited epidermolysis bullosa and other disorders with skin fragility. *British Journal of Dermatology*, *183*(4), 614–627. https://doi.org/10.1111/bjd.18921
17. Hofmann, E., Schwarz, A., Fink, J., Kamolz, L., & Kotzbeck, P. (2023). Modelling the Complexity of Human Skin In Vitro. Biomedicines, 11(3), 794. https://doi.org/10.3390/biomedicines11030794
18. Huang, S., Hao, X., Li, Y., Wu, J., Xiang, D., & Luo, S. (2022). Nonviral delivery systems for antisense oligonucleotide therapeutics. Biomaterials Research, 26(1). https://doi.org/10.1186/s40824-022-00292-4
19. Levy, R. H., Ostlund, R. E., & Brajtburg, J. (1985). The effects of amphotericin B on lipid metabolism in cultured human skin fibroblasts. In Vitro Cellular & Developmental Biology, 21(1), 26–31. https://doi.org/10.1007/bf02620910
20. Malecova, B., Burke, R. S., Cochran, M., Hood, M. D., Johns, R., Kovach, P. R., Doppalapudi, V. R., Erdogan, G., Arias, J. D., Darimont, B., Miller, C. D., Huang, H., Geall, A., Younis, H. S., & Levin, A. A. (2023). Targeted tissue delivery of RNA therapeutics using antibody–oligonucleotide conjugates (AOCs). Nucleic Acids Research. https://doi.org/10.1093/nar/gkad415
21. Niehues, H., Bouwstra, J. A., Ghalbzouri, A. E., Brandner, J. M., Zeeuwen, P. L., & Van Den Bogaard, E. H. (2018). 3D skin models for 3R research: The potential of 3D reconstructed skin models to study skin barrier function. Experimental Dermatology, 27(5), 501–511. https://doi.org/10.1111/exd.13531
22. Nygaard, U., Niehues, H., Rikken, G., Rodijk-Olthuis, D., Schalkwijk, J., & Van Den Bogaard, E. H. (2015). Antibiotics in cell culture: friend or foe? Suppression of keratinocyte growth and differentiation in monolayer cultures and 3D skin models. Experimental Dermatology, 24(12), 964–965. https://doi.org/10.1111/exd.12834
23. Ogino, S., Leonard, D. G., Rennert, H., Gao, S., & Wilson, R. (2001). Heteroduplex Formation in SMN Gene Dosage Analysis. The Journal of Molecular Diagnostics, 3(4), 150–157. https://doi.org/10.1016/s1525-1578(10)60666-6
24. Reijnders, C. M. A., Van Lier, A., Roffel, S., Kramer, D., Scheper, R. J., & Gibbs, S. (2015). Development of a Full-Thickness Human Skin Equivalent In Vitro Model Derived from TERT-Immortalized Keratinocytes and Fibroblasts. Tissue Engineering Part A, 21(17–18), 2448–2459. https://doi.org/10.1089/ten.tea.2015.0139
25. Rousi, E., Malheiro, A., Harichandan, A., Mohren, R., Lourenço, A., Mota, C. B., Cillero-Pastor, B., Wieringa, P., & Moroni, L. (2022). An innervated skin 3D in vitro model for dermatological research. *In Vitro Models*. https://doi.org/10.1007/s44164-022-00021-0

26. Rousselle, P., Keene, D. R., Ruggiero, F., Champliaud, M., Van Der Rest, M., & Burgeson, R. E. (1997). Laminin 5 Binds the NC-1 Domain of Type VII Collagen. Journal of Cell Biology, 138(3), 719–728. https://doi.org/10.1083/jcb.138.3.719
27. Satake, N., Duong, C. P., Yoshida, S., Oestergaard, M., Chen, C. W. S., Peralta, R., Guo, S., Seth, P. P., Li, Y., Beckett, L. A., Choi, S., Nolta, J. A., Nitin, N., & Tuscano, J. (2016). Novel Targeted Therapy for Precursor B-Cell Acute Lymphoblastic Leukemia: Anti-CD22 Antibody-MXD3 Antisense Oligonucleotide Conjugate. Molecular Medicine, 22(1), 632–642. https://doi.org/10.2119/molmed.2015.00210
28. Sewing, S., Gubler, M., Gérard, R., Avignon, B., Mueller, Y., Braendli-Baiocco, A., Odin, M., & Moisan, A. (2019). GalNAc Conjugation Attenuates the Cytotoxicity of Antisense Oligonucleotide Drugs in Renal Tubular Cells. Molecular Therapy Nucleic Acids, 14, 67–79. https://doi.org/10.1016/j.omtn.2018.11.005
29. Tang, J. Y., Marinkovich, M. P., Lucas, E., Gorell, E. S., Chiou, A. S., Lu, Y., Gillon, J., Takeno, M., & Rudin, D. (2021). A systematic literature review of the disease burden in patients with recessive dystrophic epidermolysis bullosa. *Orphanet Journal of Rare Diseases*, *16*(1). https://doi.org/10.1186/s13023-021-01811-7
30. Turczynski, S., Titeux, M., Tonasso, L., Décha, A., Ishida-Yamamoto, A., & Hovnanian, A. (2016). Targeted Exon Skipping Restores Type VII Collagen Expression and Anchoring Fibril Formation in an In Vivo RDEB Model. Journal of Investigative Dermatology, 136(12), 2387–2395. https://doi.org/10.1016/j.jid.2016.07.029
31. Vermeer, F. C., Bremer, J., Sietsma, R., Sandilands, A., Hickerson, R. P., Bolling, M. C., Pasmooij, A. M., Lemmink, H. H., Swertz, M. A., Knoers, N. V. a. M., Van Der Velde, K. J., & Van Den Akker, P. C. (2021). Therapeutic Prospects of Exon Skipping for Epidermolysis Bullosa. International Journal of Molecular Sciences, 22(22), 12222. https://doi.org/10.3390/ijms222212222
32. Watanabe, M., Natsuga, K., Shinkuma, S., & Shimizu, H. (2018). Epidermal aspects of type VII collagen: Implications for dystrophic epidermolysis bullosa and epidermolysis bullosa acquisita. Journal of Dermatology, 45(5), 515–521. https://doi.org/10.1111/1346-8138.14222

8. Supplementary

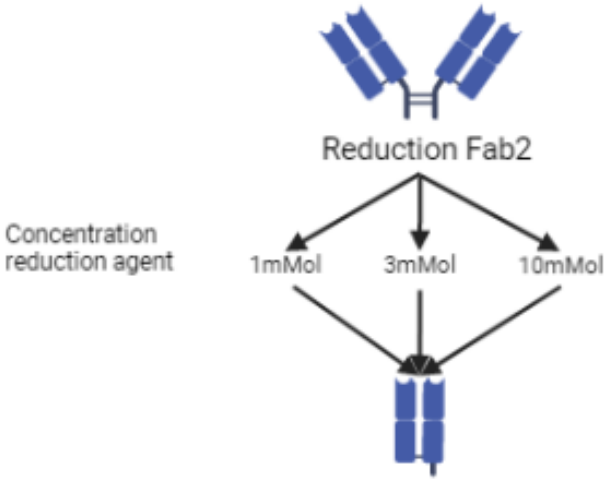

7.1 Example of Fab-2 reduction to Fab at varying reduction concentrations experiment 1.

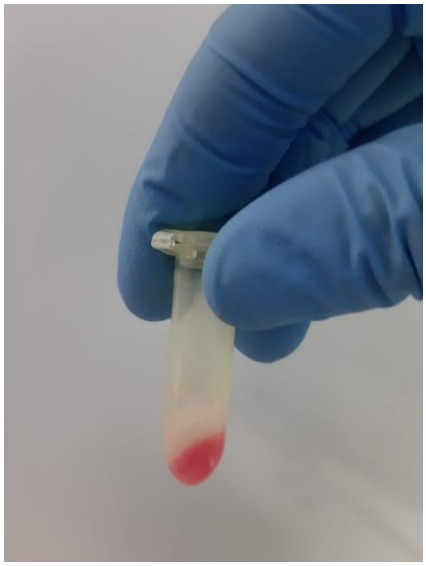

7.2 Example of separation of the aqueous phase from the organic phase by using a phasemaker tube.

Protocol Oligowalk 7-4-2023

Day 0

1. Culture keratinocytes in 4 T25 flasks. At least 3.0*10^6 cells are needed to test all AONs once. The procedure needs to be repeated for a duplicate and triplicate.
2. Harvest, count and resuspend the cells in the correct amount of CT-P. The seeding density should be 2.5*10^4 per well. To ensure there will be enough wells for transfection, the cell suspension should suffice for 120 wells. So, the cells need to be resuspended in 120*200ul = 24 ml of medium. This equals 3.0*10^6 cells at a seeding density of 2.5*10^4 cells per well

3. Make sure the cell suspension is resuspended every now and then when filling out the plate according to the scheme.
4. Incubate for 22 hrs. at 37 °C 5% CO_2.

Preparing the AON solutions.

1. Ensure the stocks of the 102 AONs selected for the Oligowalk are 100 uM.
2. Take two sterile 96 wells plate and add 35 µl of OptiMEM medium to the 102 AON wells according to the plating setup.
3. Add 5 µl of each AON to its corresponding well (resuspend well) and store at 4 °C.

Day 1

1. Remove the medium and wash the cells with 200 µl of HBSS. Use a multipippet
2. Add 75 µl Of OptiMEM to each well (make sure the cells do not dry out)
3. Dilute 70 µl of stock LF2000 in 6580 µl of OptiMEM and incubate 5 min at RT.
4. use a multipippet to add 47.5 µl of the LF dilution to a sterile 96 wells plate according to the scheme.
5. Add the 2.5 µl AON according to the scheme below and resuspend well
6. Incubate the transfection mix for 20-30 min RT.
7. Use the multipippet to transfer the 50 ul transfection mix dropwise to the corresponding wells with cells and 75ul of OptiMEM (total volume 125 µl).
8. Incubate 5 hrs. at 37 °C 5% CO_2
9. Remove the medium and wash 1x with HBSS (200ul)
10. Remove the HBSS and add 200 µl of CT-P

Day 2

11. Remove the medium and and lyse the cells with 200 µl trizol reagent. When lysing flush well and transfer to an RNAse free tube.
12. Store in -80 °C sto.

Images transfection optimization 1.

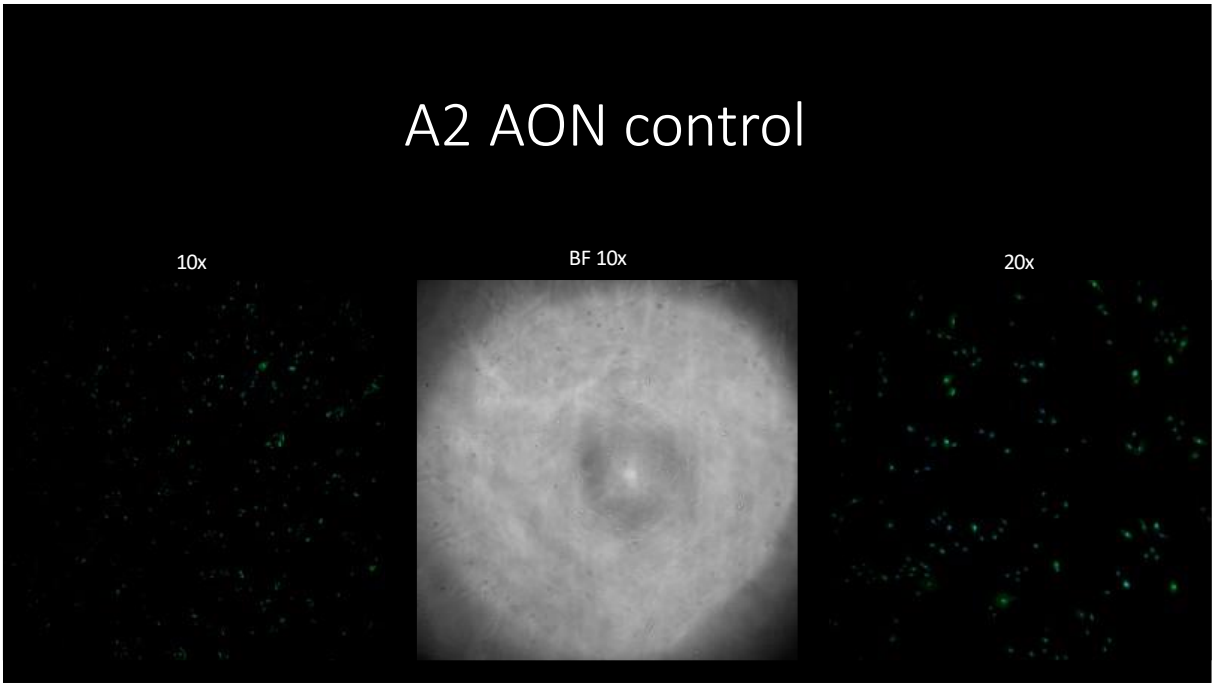
A2 AON control
10x
BF 10x
20x

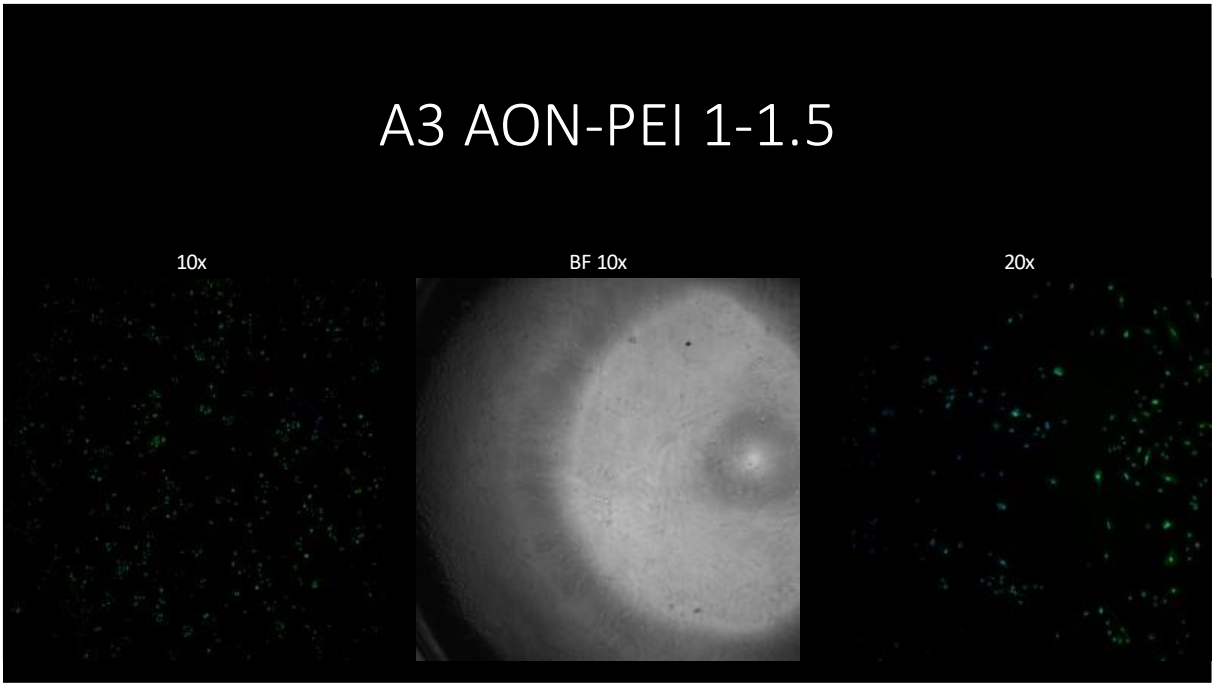
A3 AON-PEI 1-1.5
10x
BF 10x
20x

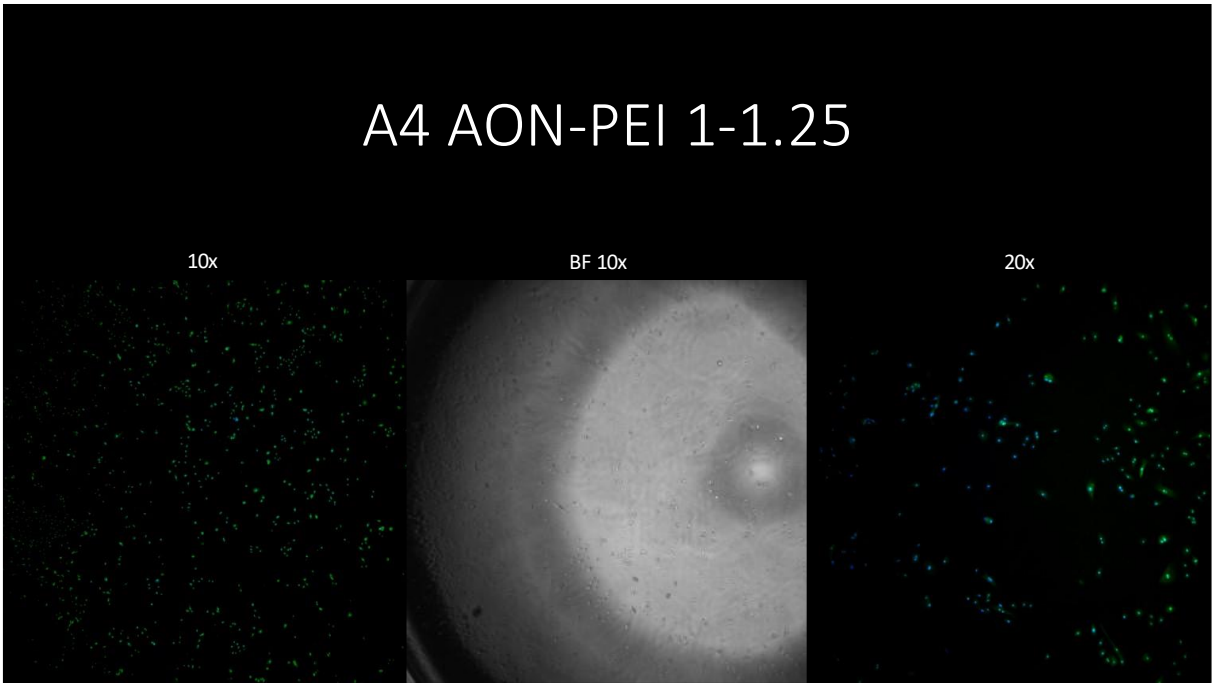
A4 AON-PEI 1-1.25
10x
BF 10x
20x

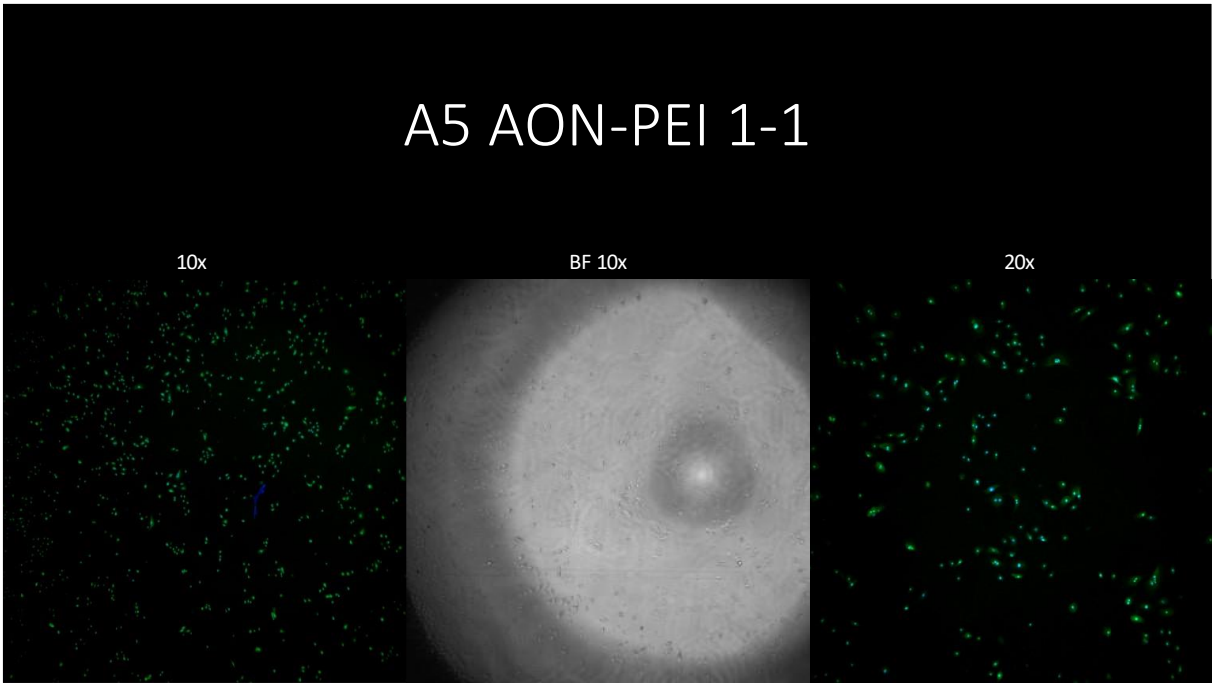
A5 AON-PEI 1-1
10x
BF 10x
20x

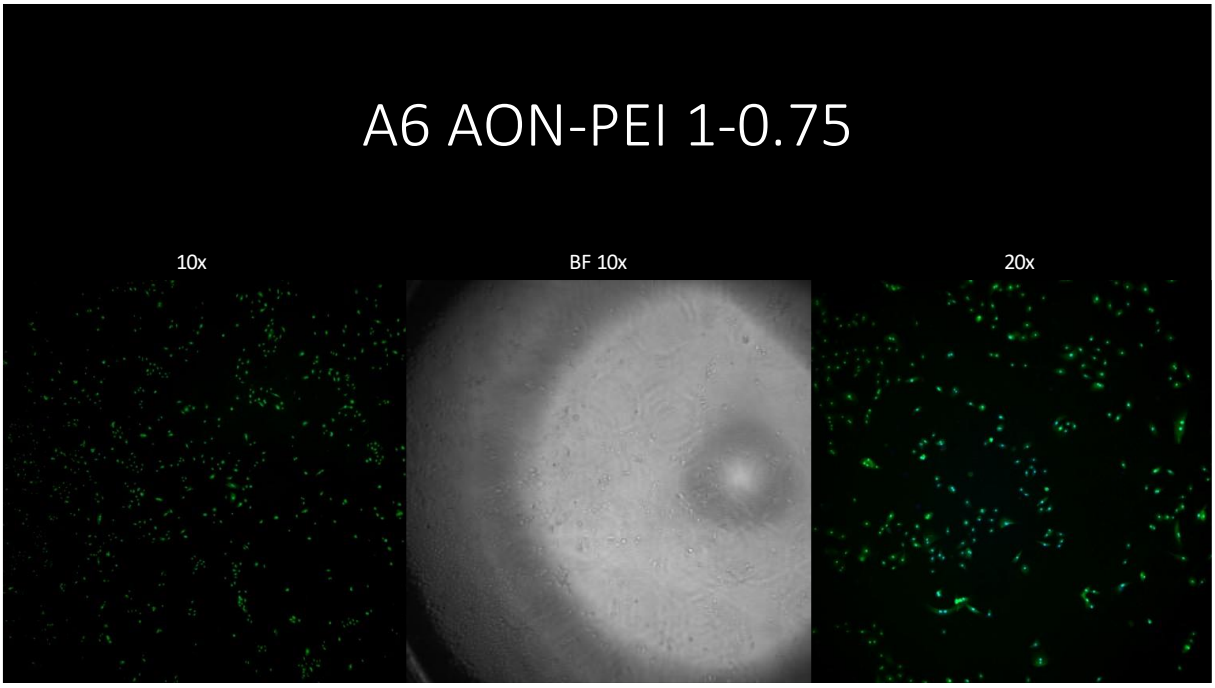
A6 AON-PEI 1-0.75
10x
BF 10x
20x

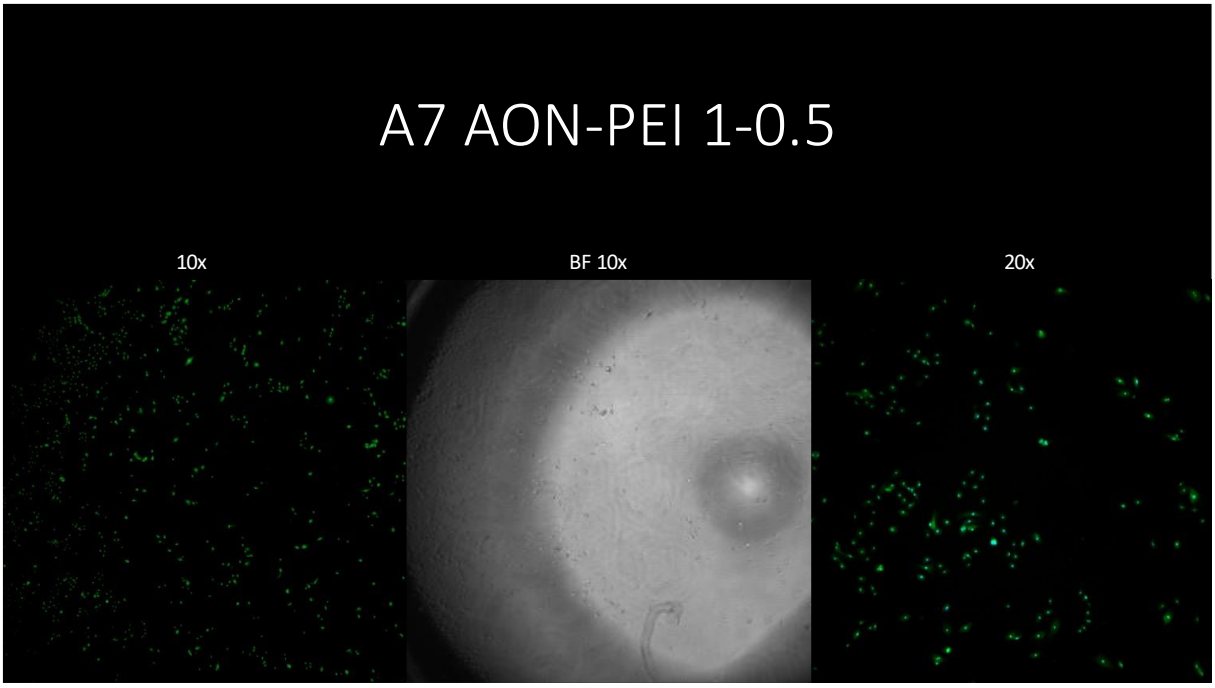
A7 AON-PEI 1-0.5
10x
BF 10x
20x

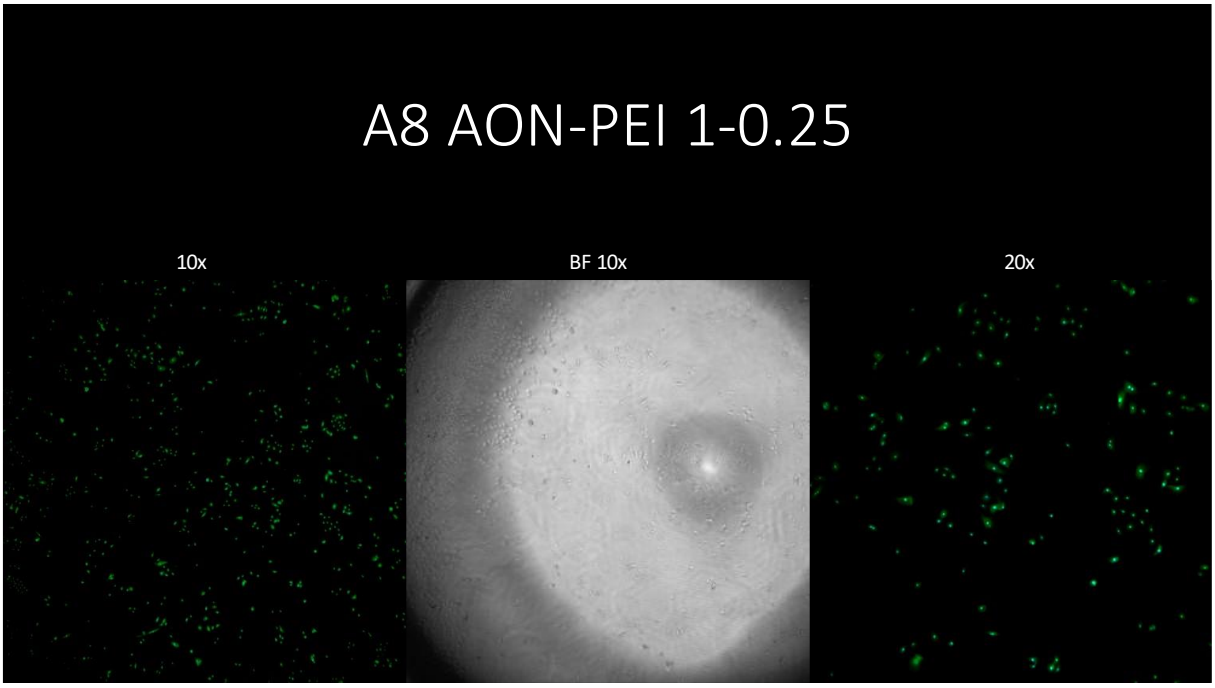
A8 AON-PEI 1-0.25
10x
BF 10x
20x

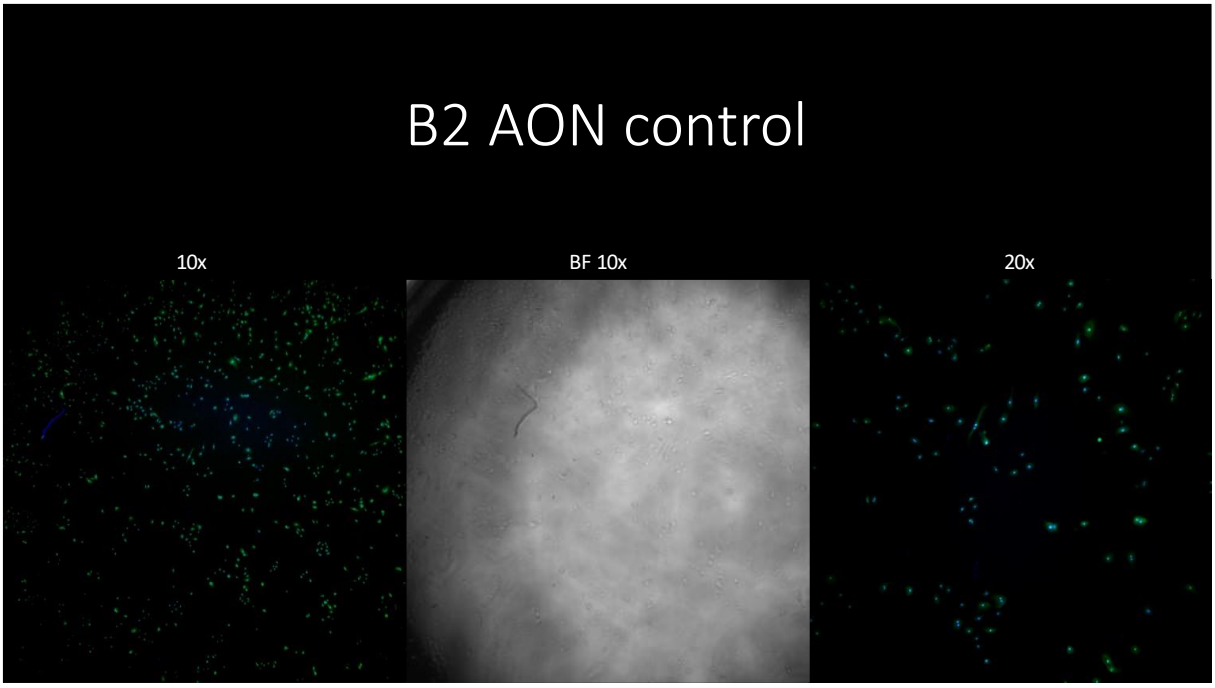
B2 AON control
10x
BF 10x
20x

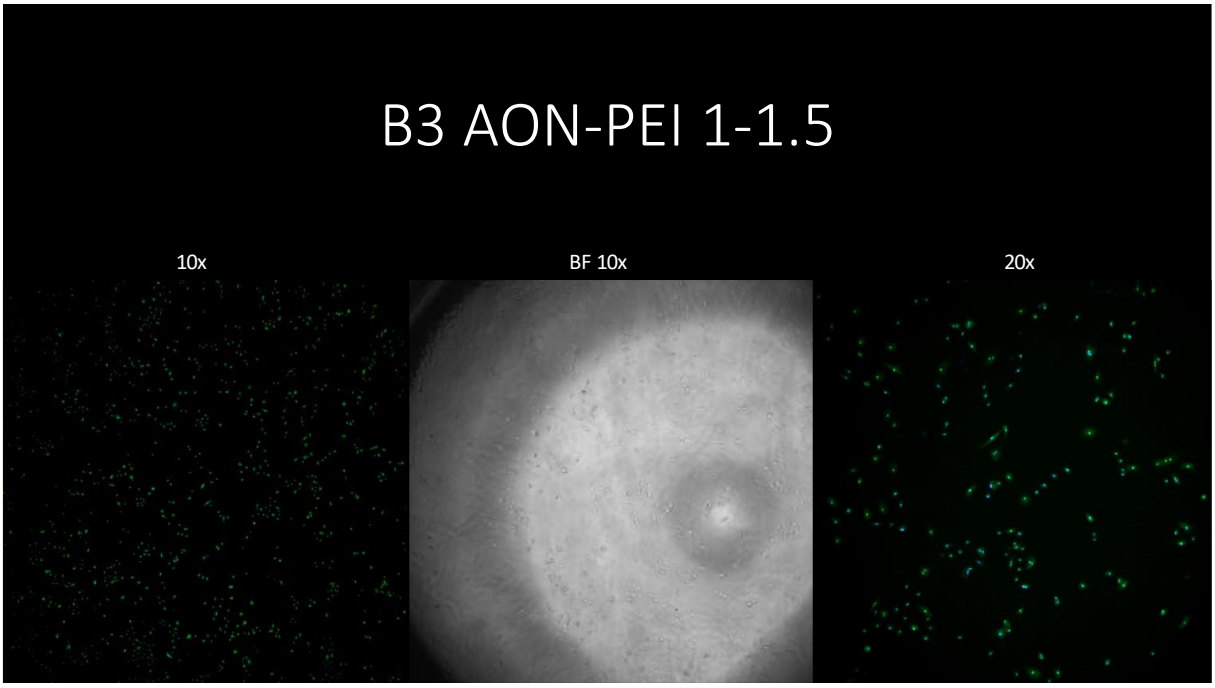
B3 AON-PEI 1-1.5
10x
BF 10x
20x

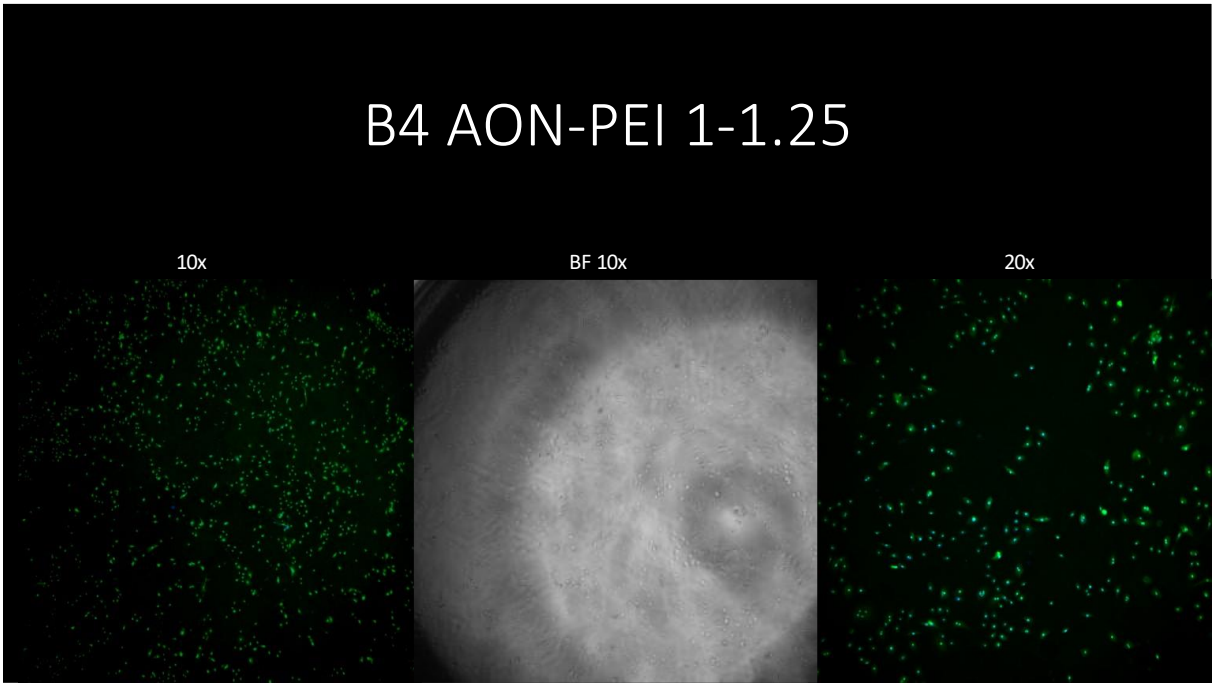
B4 AON-PEI 1-1.25
10x
BF 10x
20x

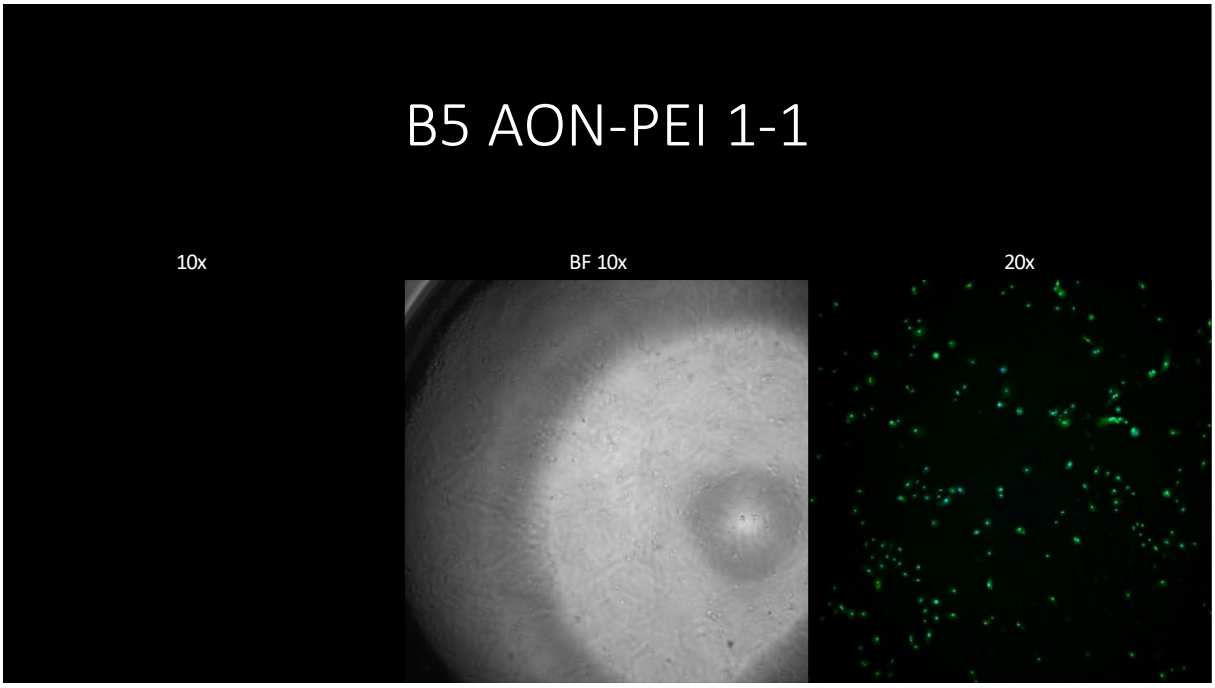
B5 AON-PEI 1-1
10x
BF 10x
20x

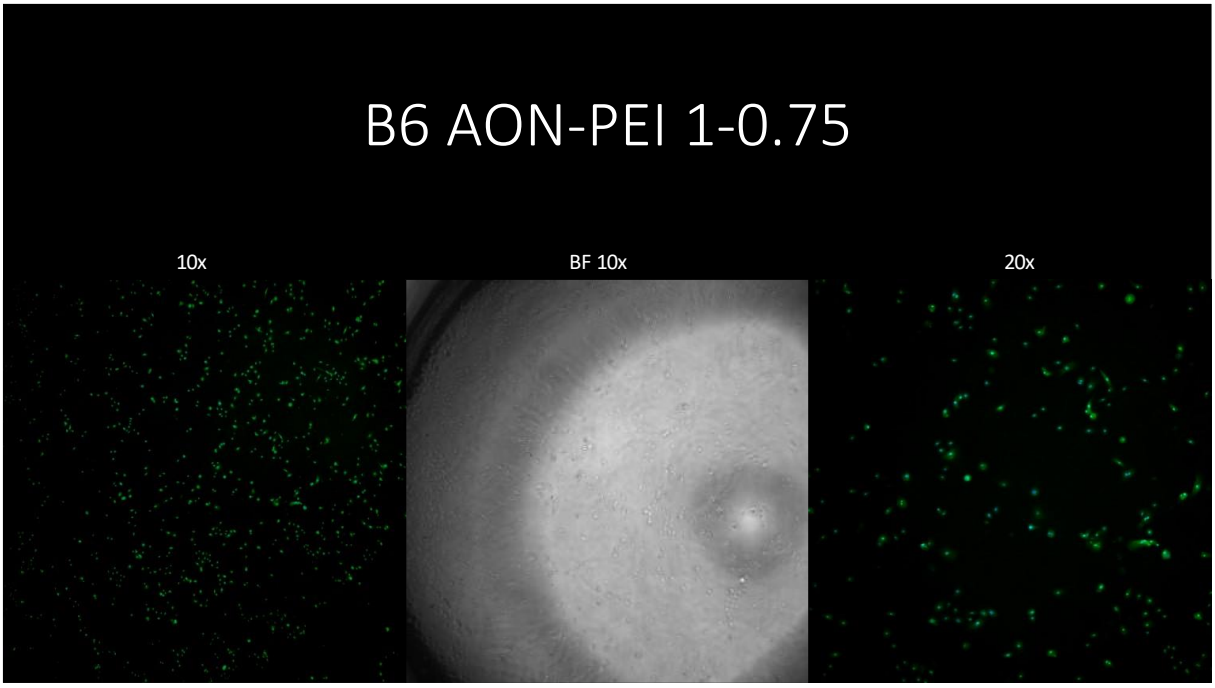
B6 AON-PEI 1-0.75
10x
BF 10x
20x

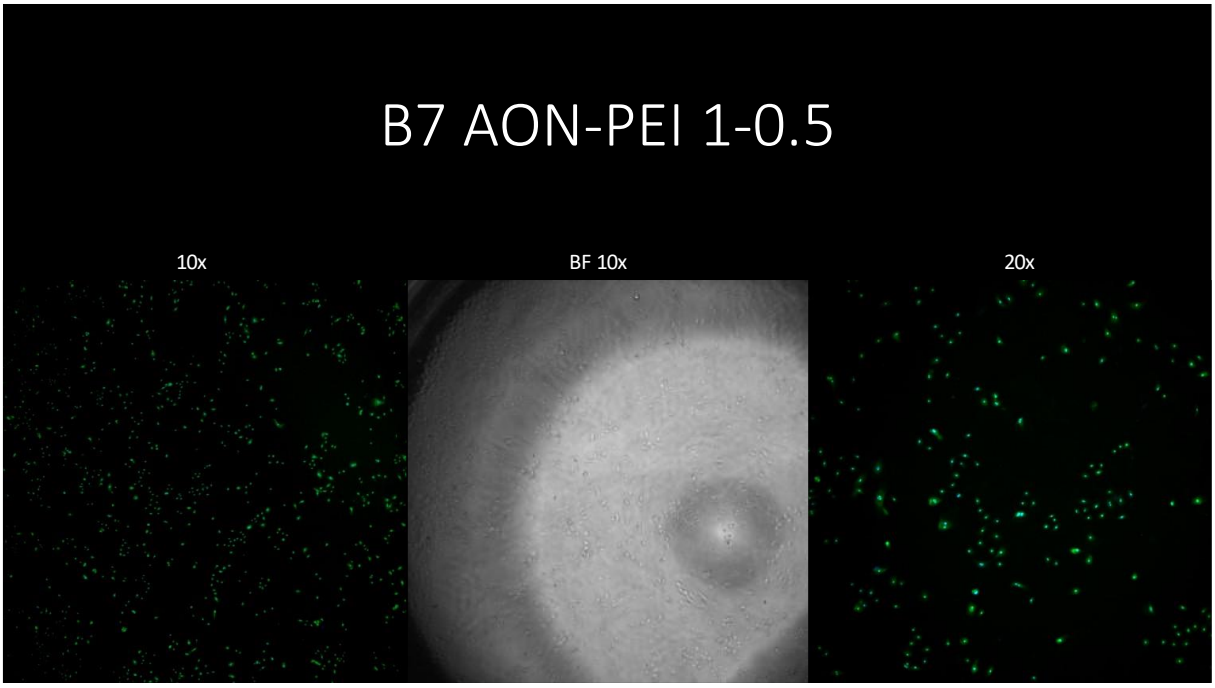
B7 AON-PEI 1-0.5
10x
BF 10x
20x

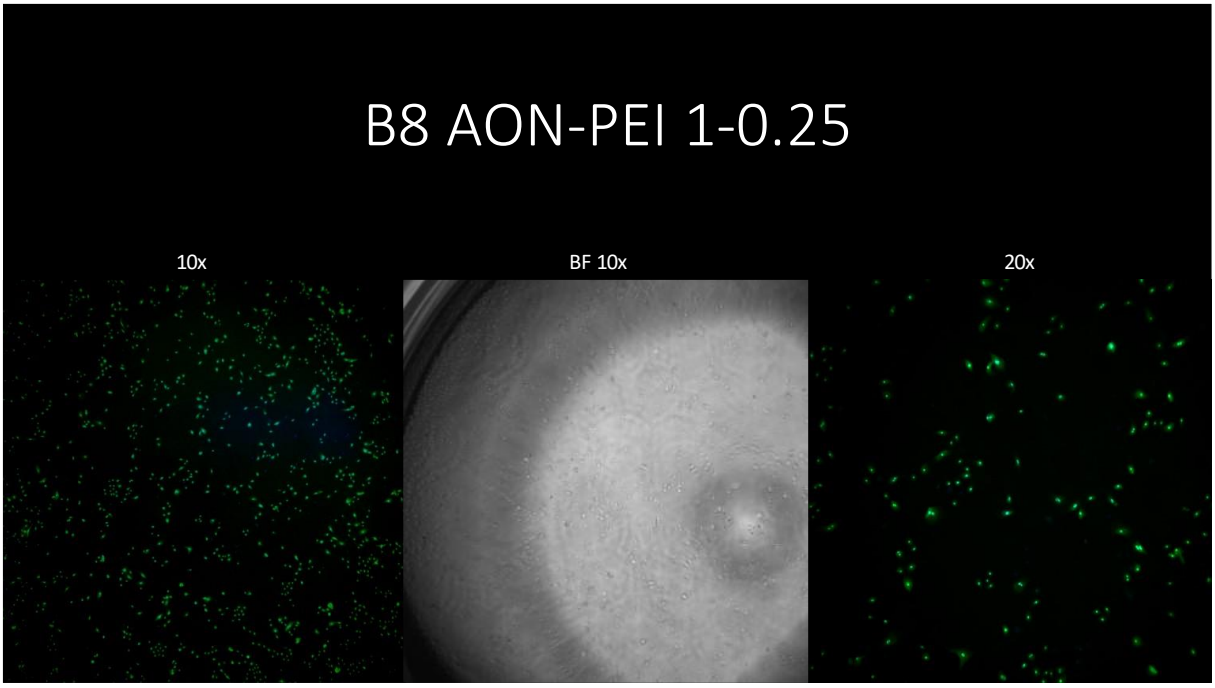
B8 AON-PEI 1-0.25
10x
BF 10x
20x

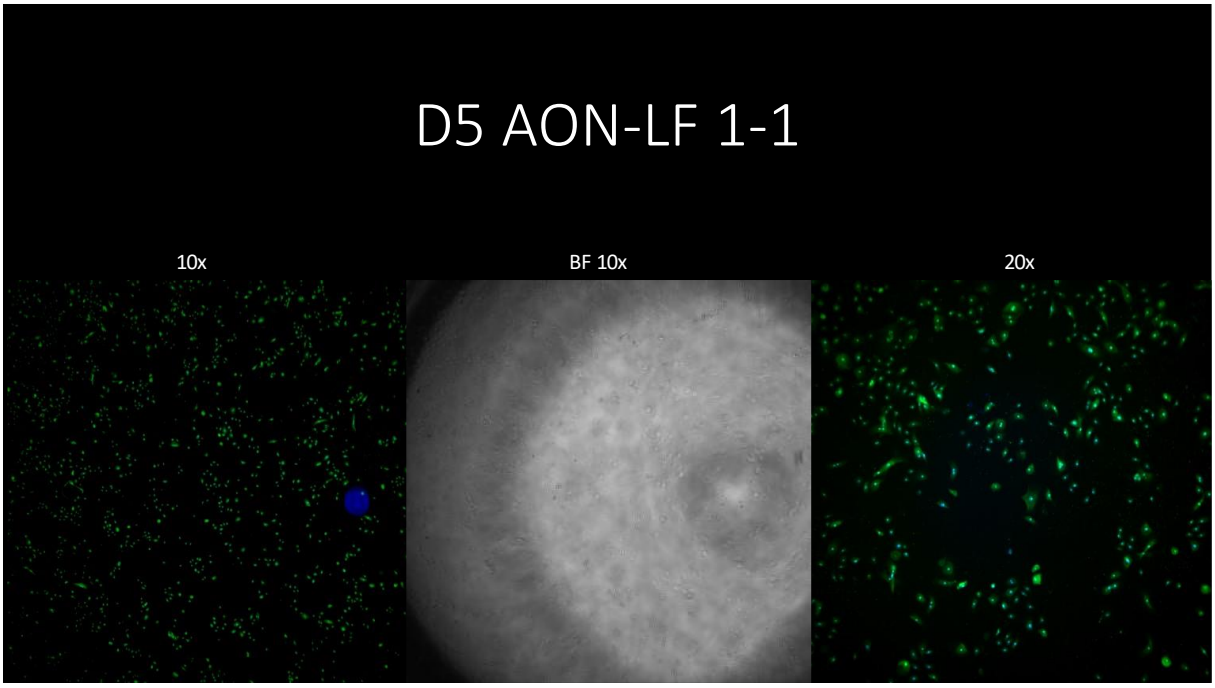
D5 AON-LF 1-1
10x
BF 10x
20x

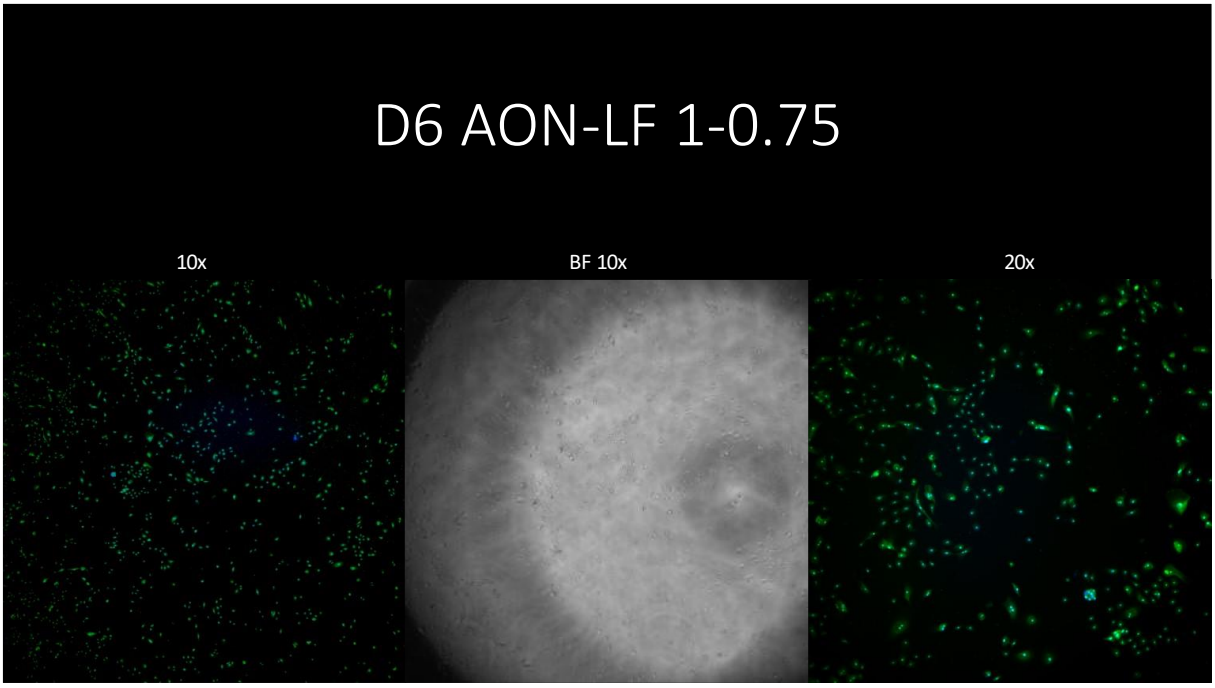
D6 AON-LF 1-0.75
10x
BF 10x
20x

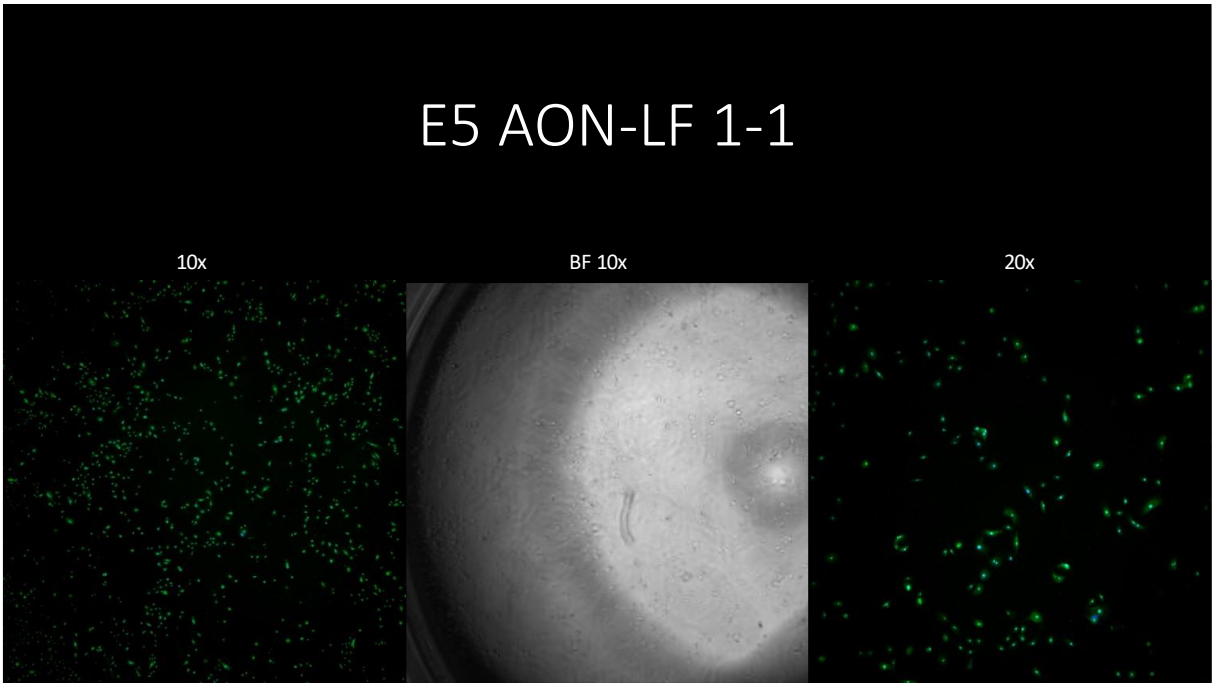
E5 AON-LF 1-1
10x
BF 10x
20x

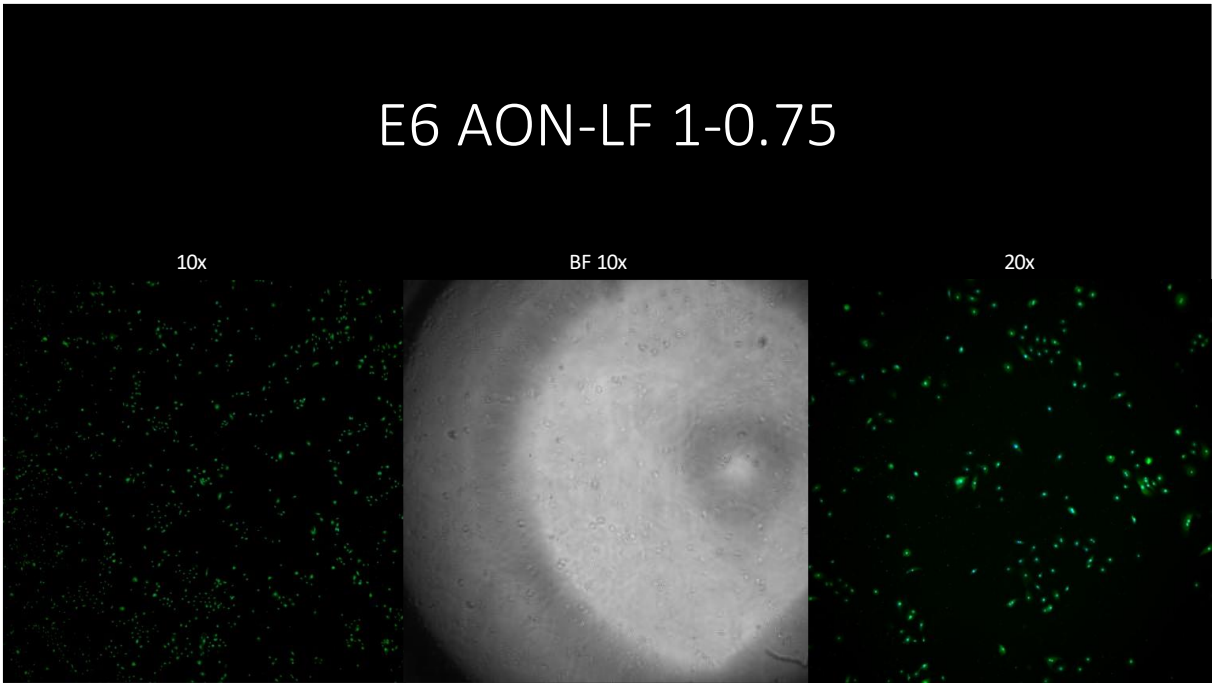
E6 AON-LF 1-0.75
10x
BF 10x
20x

Images transfection optimization 2.

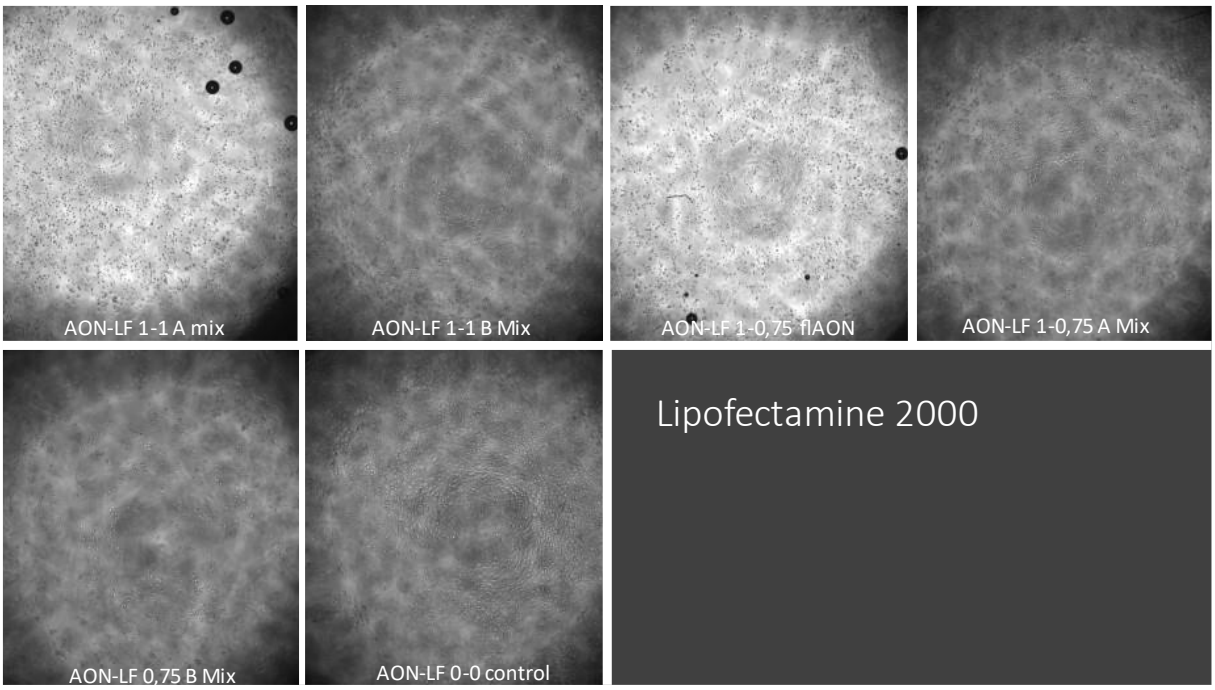

Figure 7. brightfield images 10x of transfection optimization 2 lipofectamine 2000

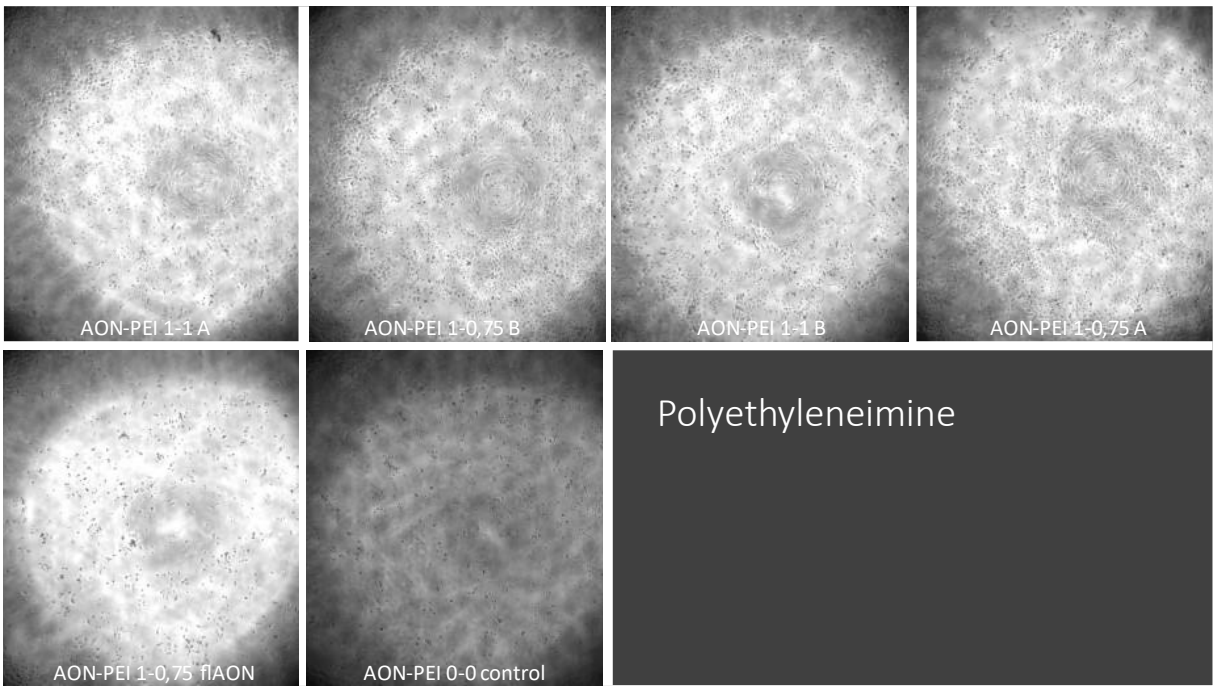

Figure 7. brightfield images 10x of transfection optimization 2 polyethyleneimine